

---

---

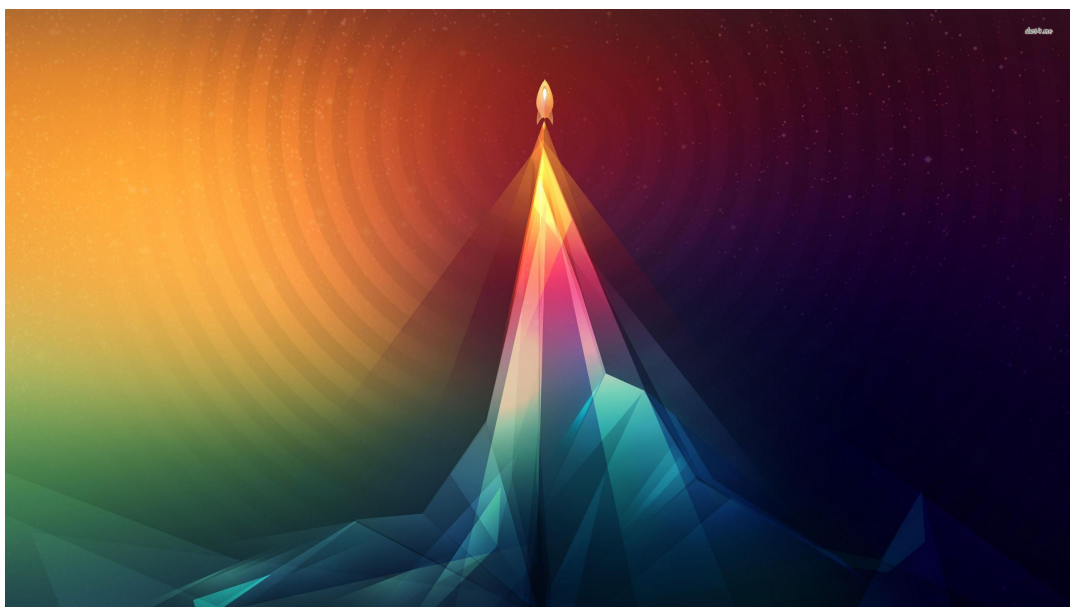
# Inverted Pendulum Balance and

# Rocket Trajectory Stability

- Compare and Control -

---

---



Project Report  
Group CE6-633  
Aalborg University  
Electronics and IT

Copyright © Group CE6-633, Electronics and IT, Aalborg University 2017

This report is compiled in L<sup>A</sup>T<sub>E</sub>X.





**AALBORG UNIVERSITY**  
STUDENT REPORT

**Electronics and IT**  
Aalborg University  
<http://www.aau.dk>

**Title:**  
Inverted Pendulum Balance  
and  
Rocket Trajectory Stability

**Theme:**  
Control Engineering

**Project Period:**  
Spring Semester 2017

**Project Group:**  
Group CE6-633

**Participants:**  
Geoffroy Sion  
Jacob Lassen  
Mathias Nielsen  
Maxime Remy  
Raphaël Casimir  
Romain Dieleman

**Supervisor:**  
Kirsten Nielsen  
Tom Pedersen

**Page Numbers:** 137

**Date of Completion:**  
30 May 2017

**Abstract:**

This report aims to investigate the inverted pendulum and a rocket launch, as balancing an inverted pendulum and following a flight path with a rocket are both unstable systems that are controlled by applying a torque on the bottom part of a long and narrow cylinder.

First, a brief overview is given as to why the two systems have similar stability problems before a mathematical model is derived. Both models are nonlinear and are linearized and reduced to two simple models. It is found that the simple mathematical models of each system are not identical. A single controller controlling both systems therefore cannot be made. A controller for each system is thus designed and implemented on the respective setups.

The controller designed for the inverted pendulum was implemented on an Arduino and uses two potentiometers and a tachometer as sensors. It is found that the controller balances the pendulum satisfactorily to the specifications made.

The controller designed for the rocket showed that it could follow the trajectory in a linear simulation based on the model. The rocket setup was built in its entirety by the group. The rocket controller was implemented but not tested due to time constraints.

In conclusion, while a rocket during flight and an inverted pendulum share similarities with instability, the models are not identical and a controller cannot be made to work with both systems. A controller showing satisfactory balancing of the inverted pendulum was made, but the rocket controller ultimately was not tested in flight.

*The content of this report is freely available, but publication may only be pursued with reference.*



# Preface

This report is composed by group CE6-633 during the 6th semester of the Bachelor of Electronics and IT at Aalborg University, 2017. The study of rocket stabilization and inverted pendulum balancing described in this report is part of the theme *Control Engineering*.

For citation the report employs IEEE style referencing. If citations are not present by figures or tables, these have been made by the authors of the report. Units are indicated according to the SI system.

The natural logarithm is denominated by  $\ln$  and  $\log_{10}$  is the base 10 logarithm.

A period is used as a decimal mark. Half a space is used as a 100 0 separator.

Aalborg University, May 29, 2017



---

Geoffroy Sion  
<gsion16@student.aau.dk>

Jacob Lassen  
<jlassie14@student.aau.dk>

Mathias Nielsen  
<mathni14@student.aau.dk>



---

Maxime Remy  
<mremy16@student.aau.dk>

Raphaël Casimir  
<rcasim16@student.aau.dk>

Romain Dieleman  
<rdiele16@student.aau.dk>

# Contents

<b>I Pre-analysis &amp; Requirements</b>	<b>1</b>
<b>1 Introduction</b>	<b>3</b>
<b>2 Initial Problem Statement</b>	<b>5</b>
<b>3 Inverted Pendulum Analysis</b>	<b>7</b>
3.1 Inverted Pendulum Description . . . . .	7
3.2 Modelling of the Arm and Stick . . . . .	12
3.3 Modeling of the Gear System . . . . .	17
3.4 Modeling of the DC-Motor . . . . .	22
3.5 Combining the Models for the Inverted Pendulum . . . . .	25
<b>4 Rocket Analysis</b>	<b>27</b>
4.1 Preliminary Analysis of a Rocket . . . . .	27
4.2 Rocket Modeling . . . . .	29
4.3 Modeling of the angle . . . . .	30
4.4 Comparison of the Inverted Pendulum and Rocket Models . . . . .	33
<b>5 Problem Statement &amp; Delimitation</b>	<b>35</b>
5.1 Problem Statement . . . . .	35
5.2 Delimitation . . . . .	35
<b>6 Requirements and Specifications</b>	<b>37</b>
6.1 Acceptance Test Specification . . . . .	40
<b>II Design &amp; Implementation</b>	<b>41</b>
<b>7 Design of the Inverted Pendulum Controller</b>	<b>43</b>
7.1 Design of Inner Loop Controller . . . . .	46
7.2 Design of Outer Loop Controller . . . . .	50
7.3 Verifying the Total Controller . . . . .	58
<b>8 Design of the Rocket and Gimbal Controller</b>	<b>61</b>
8.1 Rocket Design . . . . .	61
8.2 Rocket Controller Design . . . . .	65

<b>9 Inverted Pendulum Implementation</b>	<b>71</b>
9.1 Implementing Sensors . . . . .	71
9.2 Implementing ESCON Motor Controller . . . . .	74
9.3 Implementation Evaluation . . . . .	79
<b>10 Rocket Implementation</b>	<b>83</b>
10.1 Implementing Inertial Measurement Unit . . . . .	83
10.2 Implementing Sensors and Servomotors . . . . .	83
10.3 Rocket Software . . . . .	87
10.4 Flight test . . . . .	88
<b>III Test &amp; conclusion</b>	<b>89</b>
<b>11 Inverted Pendulum Acceptance Tests</b>	<b>91</b>
11.1 Acceptance Test 1 . . . . .	91
11.2 Acceptance Test 2 . . . . .	91
11.3 Acceptance Test 3 . . . . .	93
<b>12 Discussion</b>	<b>95</b>
12.1 Inverted Pendulum Possible Improvements . . . . .	95
12.2 Rocket . . . . .	95
12.3 Differences between the Rocket and the Inverted Pendulum . . . . .	96
<b>13 Conclusion</b>	<b>97</b>
<b>Bibliography</b>	<b>99</b>
<b>A Test Journal: Gear Train System</b>	<b>101</b>
A.1 Electronics characteristics . . . . .	101
A.2 Mechanical Characteristics . . . . .	111
<b>B Linearization of the Arm and Stick Model</b>	<b>117</b>
<b>C Test Journal: Tachometer</b>	<b>119</b>
<b>D Test Journal: Potentiometer</b>	<b>123</b>
<b>E Test Journal: rocket motor test</b>	<b>129</b>
<b>F Test Journal: Servomotors</b>	<b>133</b>



## **Part I**

# **Pre-analysis & Requirements**



# **Chapter 1**

## **Introduction**

The stabilization of an inverted pendulum is one of the well-known example used in education to explain classical mechanics and physics. It started to appear in the 1960's with Roberge's bachelor thesis "The Mechanical Seal" [6]. It is now one of the main benchmark for testing nonlinear control techniques. Its principle is to balance a stick in an upright position by controlling a mechanical system.

The project aims to model and control an unstable inverted pendulum system to prove that its fundamental principle is applicable to a real life system. The flight control of a rocket during the initial stage of its launch presents similarities [6]. These similarities can already be intuitively seen as both aims to stabilize a stick by applying a force lower than its center of gravity. Therefore a comparison between the model and control of the inverted pendulum and the rocket will be drawn in the report. An initial problem statement will be determined to set the project research focus.



## Chapter 2

# Initial Problem Statement

In order to compare the inverted pendulum a rocket the following thesis questions are set:

*To what degree is the stabilization of the inverted pendulum similar to the flight control of a rocket?*

- Is the model of the inverted pendulum similar to the rocket's flight control?
- Can the inverted pendulum and the rocket be stabilized using similar control methods?

These questions lead to a preliminary analysis of both systems models in order to examine their similarities.



## Chapter 3

# Inverted Pendulum Analysis

### 3.1 Inverted Pendulum Description

For this project an inverted pendulum setup is given. It consists of:

- A DC motor
- A gear system
- An arm
- A stick connected to the end of the arm.

A diagram of the setup when fully assembled is seen on Figure 3.1.

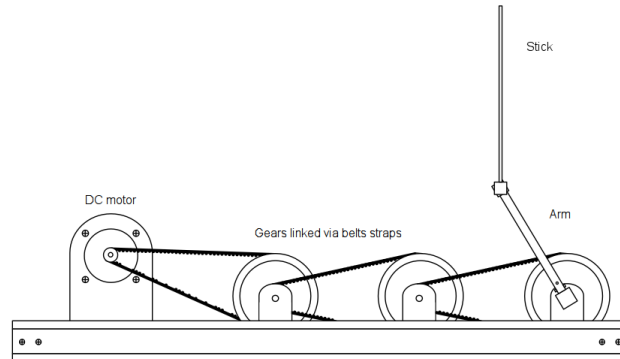


**Figure 3.1:** Diagram of the mechanical system[1].

Each part will be described with its specifications and use in the setup. The input and output relations of each block are illustrated on Figure 3.2, where the goal throughout the chapter will be to determine the transfer functions describing these relations.

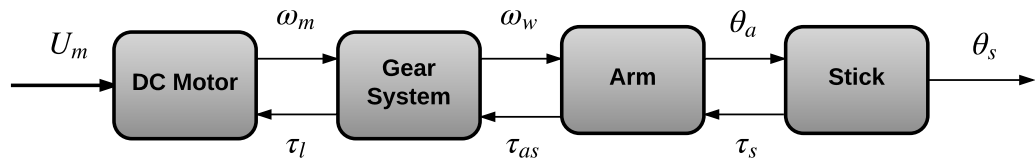


**Figure 3.2:** Block diagram of the input/output relations of the system.

Where:

$U_m$	is the motor input voltage	[V]
$\omega_m$	is the angular velocity of the motor	[rad s <sup>-1</sup> ]
$\omega_w$	is the angular velocity of the gear connected to the arm	[rad s <sup>-1</sup> ]
$\tau_l$	is the total load of the gears, arm and stick	[N m]
$\tau_{as}$	is the load of the arm and the stick	[N m]
$\tau_s$	is the load of the stick	[N m]
$\theta_a$	is the angle from the arm to the y-axis	[rad]
$\theta_s$	is the angle from the stick to the y-axis	[rad]

## DC Motor

An Axem DC servo motor model F9M2 is attached to the gears to create an angular velocity in the system. The integrated tachometer of the motor is used as feedback to ensure control precision. Which is done to give the possibility to sample the velocity and direction of the motor and relate it to the position of the arm. Using the DC motor also means implementing a motor controller. Already implemented in the setup is a Maxon Escon 50/5 Servocontroller, which can be controlled through PWM [7]. The servocontroller is supplied through a 230 V regulator that can supply the servocontroller with up to 56 V and 15 A depending the power supply. The regulator in itself will be considered a blackbox, because of user limitations when working with 230 V at the university. The DC motor and servo controller will, in system diagrams, be evaluated as one unit, but further considered when implementing a system controller.

## Gear System

Between the DC motor and arm is the gear system. The goal of the gear system is to reduce the ratio between the rotation of the motor versus the arm. The gear system is series of six gear, three small and three big connected with belts. The setup is seen on Figure 3.1, where the number of gear is illustrated. The parameters of the gear system is listed in Table 3.1.

**Table 3.1:** Parameters of gear system.

Piece	Parameter	Value	Unit
Gear <sub>big</sub>	Teeth	40	[1]
Gear <sub>big</sub>	Diameter	0.12	[m]
Gear <sub>small</sub>	Teeth	12	[1]
Gear <sub>small</sub>	Diameter	0.04	[m]
Belt	Length	0.6	[m]

## Stick and Arm

The goal is for the arm to apply force on their common joint, which would affect the stick's orientation around its center of gravity. The physical parameters for the stick and arm are listed in Table 3.2.

**Table 3.2:** Physical parameters of the arm and sticks.

Piece	Parameter	Value	Unit
Stick <sub>long</sub>	Length	0.8	[m]
Stick <sub>long</sub>	Weight	0.344	[kg]
Stick <sub>short</sub>	Length	0.4	[m]
Stick <sub>short</sub>	Weight	0.170	[kg]
Arm	Length	0.33	[m]
Arm	Weight	0.288	[kg]

Feedback is needed to be able to control the stick through the arm and gears. The sensors used are an integrated part of the setup, and the choice of these will not be further discussed.

A necessary feedback to take in account is the angle between the stick and arm. The angle between the stick and arm is detected and sampled from a potentiometers rotational position. Equally the position of the arm is needed to detect its angle. The position of each potentiometer is shown with boxes on Figure 3.3.

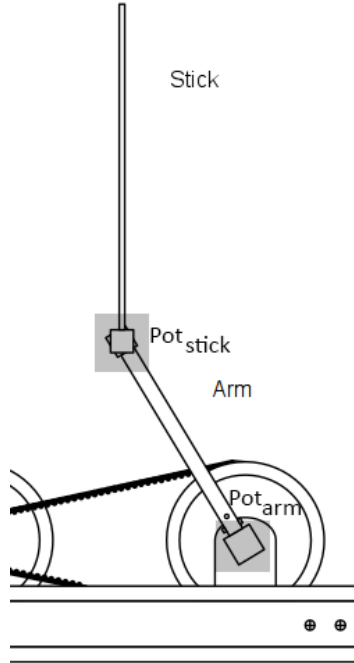


**Figure 3.3:** Diagram of the arm and stick with sensors illustrated.

The block diagram for the standard feedback control system with the known system plant is seen on Figure 3.4.

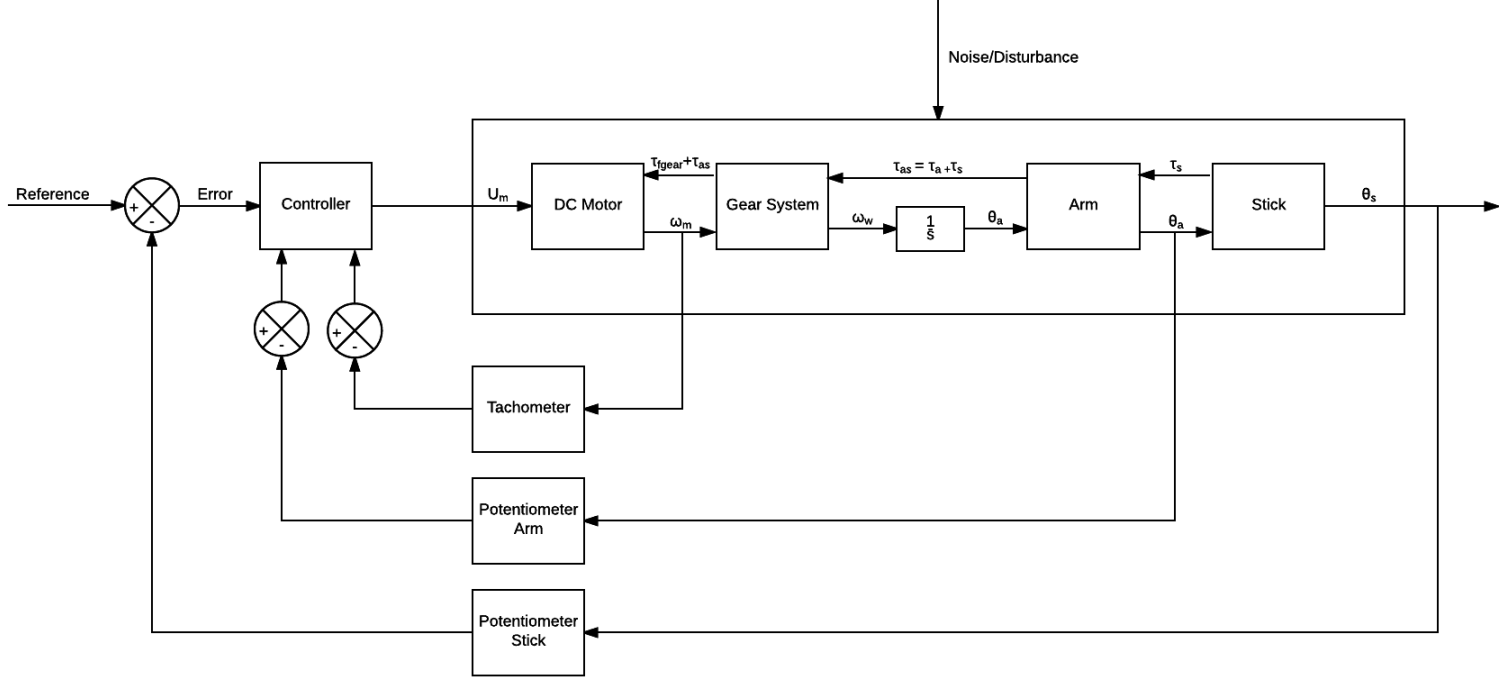


**Figure 3.4:** Block diagram of the setup's feedback loop.

The basics of each system in the inverted pendulum is now described with its specifications, and the dynamics of the system can be modelled. Each section will be modelled from the output to the input as the sections generate a torque that affects the previous sections of the system.

## 3.2 Modelling of the Arm and Stick

The goal of this section is to have a mathematical model for the behaviour of the angle of the stick in relation to the angle of the arm. The inputs and outputs of this system can be seen by the block diagram in Figure 3.5.

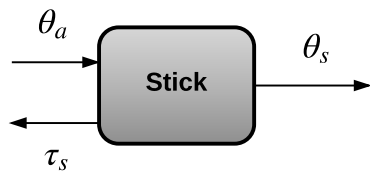


**Figure 3.5:** Block diagram of the inputs and outputs of the stick section of the inverted pendulum setup.

The angles, constants and forces used to describe the system are seen on Figure 3.6.

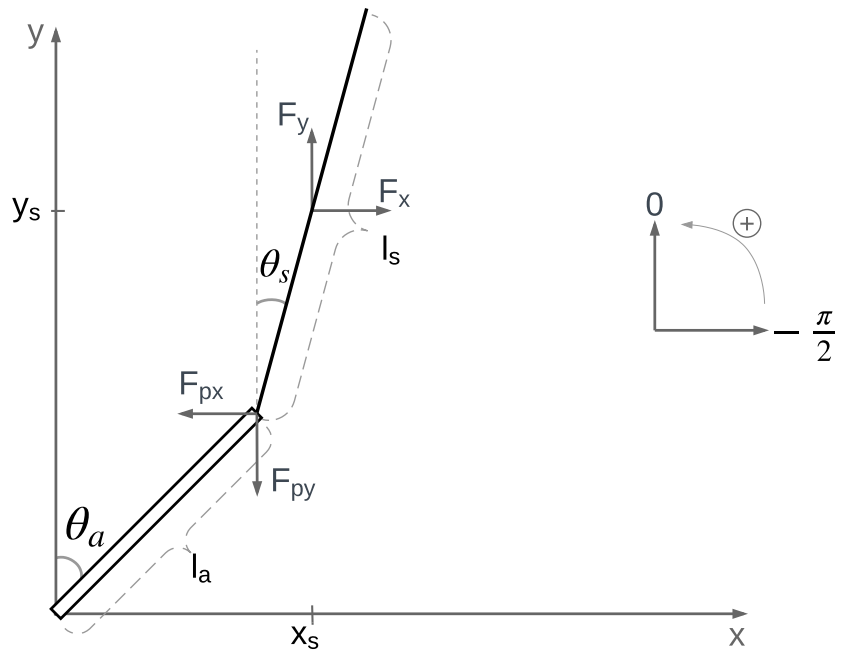


**Figure 3.6:** Diagram of the angles and forces acting on the arm and the stick.

Where:

$F_x$ is the force in the x direction	[N]
$F_y$ is the force in the y direction	[N]
$F_{px}$ is the x direction's reaction force for the arm and stick connection	[N]
$F_{py}$ is the y direction's reaction force for the arm and stick connection	[N]
$x_s$ is the position of the center of mass of the stick in the x direction	[m]
$y_s$ is the position of the center of mass of the stick in the y direction	[m]
$l_a$ is the length of the arm	[m]
$l_s$ is the length of the stick	[m]
$\theta_a$ is the angle from the arm to the y-axis	[rad]
$\theta_s$ is the angle from the stick to the y-axis	[rad]

All forces, constants and variables that relates to the arm and stick are denoted by a subscripted  $a$  and  $s$  respectively.

The behaviour of the stick can be fully described by three movements; two translatory and one rotary. It can move in the x and y direction and rotate around its center of gravity. To fully describe the system two geometric equations are also needed.

The two translatory forces acting on the stick in the x and y directions are found by Equation (3.1) using Newton's 2nd law of motion.

$$\ddot{x}_s M_s = F_x \quad (3.1a)$$

$$\ddot{y}_s M_s = F_y - g M_s \quad (3.1b)$$

$$F_y = (\ddot{y}_s + g) M_s \quad (3.1c)$$

Where:

$g$ is the standard gravitational acceleration near the surface of the earth	[ $m\ s^{-2}$ ]
$M_s$ is the mass of the stick	[kg]

The rotational movement of the stick is described by Equation (3.2).

$$J_s \ddot{\theta}_s = \frac{l_s}{2} (F_x \cos(\theta_s) + F_y \sin(\theta_s)) - b_{as} \dot{\theta}_{as} \quad (3.2)$$

Finally the position of the center of mass of the stick in the x and y direction is found by Equation (3.3) using geometry.

$$x_s = l_a \sin(-\theta_a) + \frac{l_s}{2} \sin(-\theta_s) \quad (3.3a)$$

$$x_s = -l_a \sin(\theta_a) - \frac{l_s}{2} \sin(\theta_s) \quad (3.3b)$$

$$y_s = l_a \cos(-\theta_a) + \frac{l_s}{2} \cos(-\theta_s) \quad (3.3c)$$

$$y_s = l_a \cos(\theta_a) + \frac{l_s}{2} \cos(\theta_s) \quad (3.3d)$$

Equation (3.1a), Equation (3.1c), Equation (3.2), Equation (3.3b) and Equation (3.3d) are all the equations necessary to fully describe the behaviour of the system. The goal of the modeling is to determine a transfer function that relates the angle of the stick to the angle of the arm. There are six unknown variables in the five equations:  $F_x$ ,  $F_y$ ,  $x_s$ ,  $y_s$ ,  $\theta_a$  and  $\theta_s$ . It should therefore be possible to end with one equation with the two unknowns  $\theta_a$  and  $\theta_s$  i.e. the transfer function.

The derivatives of  $x_s$  and  $y_s$  are found in Equation (3.4).

$$\dot{x}_s = -l_a \dot{\theta}_a \cos(\theta_a) - \frac{l_s}{2} \dot{\theta}_s \cos(\theta_s) \quad [\text{m s}^{-1}] \quad (3.4a)$$

$$\ddot{x}_s = -l_a \ddot{\theta}_a \cos(\theta_a) + l_a \dot{\theta}_a^2 \sin(\theta_a) - \frac{l_s}{2} \ddot{\theta}_s \cos(\theta_s) + \frac{l_s}{2} \dot{\theta}_s^2 \sin(\theta_s) \quad [\text{m s}^{-2}] \quad (3.4b)$$

$$\dot{y}_s = -l_a \dot{\theta}_a \sin(\theta_a) - \frac{l_s}{2} \dot{\theta}_s \sin(\theta_s) \quad [\text{m s}^{-1}] \quad (3.4c)$$

$$\ddot{y}_s = -l_a \ddot{\theta}_a \sin(\theta_a) - l_a \dot{\theta}_a^2 \cos(\theta_a) - \frac{l_s}{2} \ddot{\theta}_s \sin(\theta_s) - \frac{l_s}{2} \dot{\theta}_s^2 \cos(\theta_s) \quad [\text{m s}^{-2}] \quad (3.4d)$$

The forces  $F_x$  and  $F_y$  have an equal and opposite force at the point where the arm and stick connect. These can be decomposed into perpendicular and parallel forces. The parallel forces are negligible when assuming the stick is perfectly solid and unable to stretch or compress. The perpendicular forces are found by using geometry and show up in Equation (3.2) for the rotary force and are seen on Figure 3.6.

The derivatives of the two geometric equations are inserted into Equation (3.1a) and Equation (3.1c) which are then inserted into Equation (3.2) in Equation (3.5b).

$$J_s \ddot{\theta}_s = \frac{l_s}{2} (\ddot{x}_s M_s \cos(\theta_s) + (\ddot{y}_s + g) M_s \sin(\theta_s)) - b_{as} \dot{\theta}_{as} \quad (3.5a)$$

$$\begin{aligned} J_s \ddot{\theta}_s &= \frac{l_s}{2} M_s \left( -l_a \ddot{\theta}_a (\cos(\theta_a) \cos(\theta_s) + \sin(\theta_a) \sin(\theta_s)) \right. \\ &\quad + l_a \dot{\theta}_a^2 (\sin(\theta_a) \cos(\theta_s) - \cos(\theta_a) \sin(\theta_s)) \\ &\quad - \frac{l_s}{2} \ddot{\theta}_s (\cos(\theta_s) \cos(\theta_s) + \sin(\theta_s) \sin(\theta_s)) \\ &\quad \left. + \frac{l_s}{2} \dot{\theta}_s^2 (\sin(\theta_s) \cos(\theta_s) - \cos(\theta_s) \sin(\theta_s)) \right. \\ &\quad \left. + g \sin(\theta_s) \right) - b_{as} \dot{\theta}_{as} \end{aligned} \quad (3.5b)$$

Using the trigonometric properties in Equation (3.6), Equation (3.5b) is reduced to Equation (3.7).

$$\cos(\theta_a) \cos(\theta_s) \pm \sin(\theta_a) \sin(\theta_s) = \cos(\theta_a \mp \theta_s) \quad (3.6a)$$

$$\sin(\theta_a) \cos(\theta_s) \pm \cos(\theta_a) \sin(\theta_s) = \sin(\theta_a \pm \theta_s) \quad (3.6b)$$

$$\cos(\theta_s)^2 + \sin(\theta_s)^2 = 1 \quad (3.6c)$$

$$\begin{aligned} J_s \ddot{\theta}_s &= \frac{l_s}{2} M_s \left( -l_a \ddot{\theta}_a \cos(\theta_a - \theta_s) + l_a \dot{\theta}_a^2 \sin(\theta_a - \theta_s) \right. \\ &\quad \left. - \frac{l_s}{2} \ddot{\theta}_s + g \sin(\theta_s) \right) - b_{as} \dot{\theta}_{as} \end{aligned} \quad (3.7)$$

This is the nonlinear mathematical model for the system. This will be linearized in order to perform a Laplace transformation. The linearization can be seen cf. Appendix B.

The linearized model is Equation (3.8).

$$J_s \ddot{\theta}_s = \frac{l_s}{2} M_s \left( -l_a \ddot{\theta}_a - \frac{l_s}{2} \ddot{\theta}_s + g \theta_s \right) - b_{as} \dot{\theta}_{as} \quad (3.8)$$

Inserting the moment of inertia for a rotating stick,  $J_s = \frac{1}{12}M_s l_s^2$ , the linearized model becomes (3.9d) [9].

$$\frac{1}{12}M_s l_s^2 \ddot{\theta}_s = \frac{l_s}{2} M_s \left( -l_a \ddot{\theta}_a - \frac{l_s}{2} \ddot{\theta}_s + g \theta_s \right) - b_{as} \dot{\theta}_{as} \quad (3.9a)$$

$$\frac{1}{12}M_s l_s^2 \ddot{\theta}_s + \frac{1}{4}M_s l_s^2 \ddot{\theta}_s = \frac{l_s}{2} M_s \left( -l_a \ddot{\theta}_a + g \theta_s \right) - b_{as} \dot{\theta}_{as} \quad (3.9b)$$

$$\frac{1}{3}M_s l_s^2 \ddot{\theta}_s = \frac{l_s}{2} M_s \left( -l_a \ddot{\theta}_a + g \theta_s \right) - b_{as} \dot{\theta}_{as} \quad (3.9c)$$

$$\ddot{\theta}_s = \frac{3}{2l_s} \left( -l_a \ddot{\theta}_a + g \theta_s \right) - \frac{3b_{as} (\dot{\theta}_s - \dot{\theta}_a)}{M_s l_s^2} \quad (3.9d)$$

The linearized model is now Laplace transformed in Equation (3.10c) in order to find the transfer function.

$$s^2 \Theta_s = \frac{3}{2l_s} \left( -s^2 l_a \Theta_a + g \Theta_s \right) - s \frac{3b_{as}}{M_s l_s^2} \Theta_s + s \frac{3b_{as}}{M_s l_s^2} \Theta_a \quad (3.10a)$$

$$\Theta_s \left( s^2 + \frac{3b_{as}}{M_s l_s^2} s - \frac{3g}{2l_s} \right) = \Theta_a \left( -\frac{3l_a}{2l_s} s^2 + \frac{3b_{as}}{M_s l_s^2} s \right) \quad (3.10b)$$

$$\frac{\Theta_s}{\Theta_a} = \frac{-\frac{3l_a}{2l_s} s^2 + \frac{3b_{as}}{M_s l_s^2} s}{s^2 + \frac{3b_{as}}{M_s l_s^2} s - \frac{3g}{2l_s}} \quad (3.10c)$$

The system has a zero in 0 (two if the friction is considered negligible) which gives a 0 dB DC gain. This makes sense as the stick should not move if the angle of the arm is constant. The poles show that the natural frequency of the system depends only on the gravity and length of the stick. This is similar to Equation (3.11) for the frequency of a simple pendulum [10].

$$\omega_n = \sqrt{\frac{g}{L}} \quad (3.11)$$

A linearized model in the Laplace domain for the arm and the stick has been derived and the model for the motor and gears is now derived. The load torque generated by the arm and stick is significantly smaller than the torque of the gear system, at the DC motor, and is therefore assumed negligible. Equally the friction between the arm and the stick is assumed to be zero as the joint consists of a ball bearing.

### 3.3 Modeling of the Gear System

This section aims to describe the behaviour of the gear system.

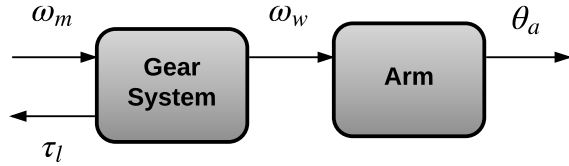


**Figure 3.7:** Block diagram of the inputs and outputs of the gear system.

Where:

$\tau_l$	is the torque of the motor's load	[N m]
$\omega_m$	is the motor's angular velocity	[m s <sup>-1</sup> ]
$\omega_{w_3}$	is the third wheel's angular velocity	[m s <sup>-1</sup> ]

Two transfer functions are going to be determined in this section:

- The relation between the motor velocity,  $\omega_m$ , and the angle of the arm,  $\theta_a$ .
- The load torque,  $\tau_l$ , generated by the gears.

#### 3.3.1 Relation between Motor Velocity and Angle of the Arm

The motor is connected to the first wheel of the gear system by a belt as shown on Figure 3.9. The first wheel has a smaller wheel rigidly attached on its axis. Both gears are turning in the same direction. The smallest wheel on the wheel 1 is connected to a second wheel with a belt. Wheel 2 has the same small wheel attached to its axis. The relation between Wheel 2 and 3 are the same as wheel 1 and 2.

The entire system shown on Figure 3.8 can thus be described by Figure 3.9 translated to each small to large wheel connection.

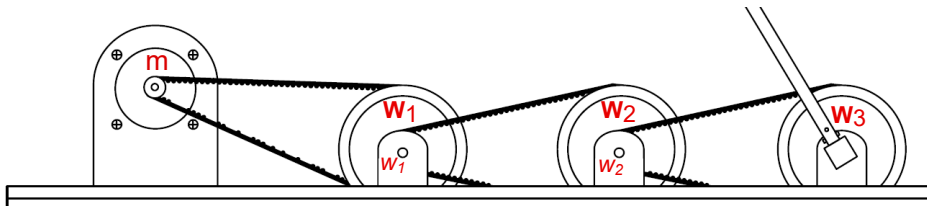


**Figure 3.8:** Diagram of the gear train.

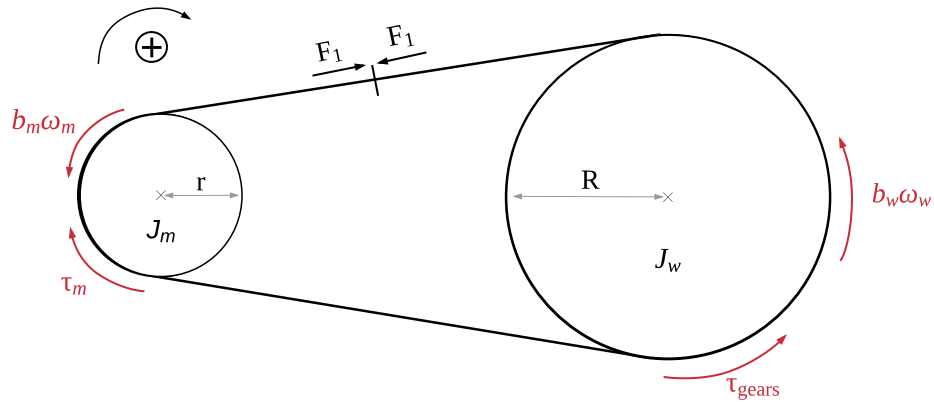


**Figure 3.9:** Free body diagram of the motor wheel system.

Where:

$J_m$ is the moment of inertia of the motor	$[\text{kg m}^2]$
$J_w$ is the moment of inertia of the wheel	$[\text{kg m}^2]$
$\omega_m$ is the motor's angular velocity	$[\text{m s}^{-1}]$
$\omega_w$ is the wheel's angular velocity	$[\text{m s}^{-1}]$
$F_1$ is the force transferred from the motor to the wheel	[N]
$r$ is the radius of the motor's wheel	[m]
$R$ is the radius of the wheel	[m]
$\tau_m$ is the torque of the motor	[N m]
$\tau_{gears}$ is the torque of the wheel's load	[N m]
$b_m$ is the viscous friction coefficient of the motor	$[\text{N m s}]$
$b_w$ is the viscous friction coefficient of the wheel	$[\text{N m s}]$

If the motor shaft turns, the belt joining the small and the big wheel will make them turn the same distance, giving the relation in Equation (3.12).

$$\theta_m r = \theta_w R \quad (3.12)$$

This expression is then differentiated to find the relation with the angular velocities in Equation (3.13).

$$\omega_m r = \omega_w R \quad (3.13)$$

The gear ratio can then be defined by Equation (3.14).

$$N = \frac{r}{R} \quad (3.14)$$

As the gear system is composed by three similar connected wheels structures like Figure 3.9, the ratio between one of the small wheels,  $r_x$ , and the big wheel connected by the belt,  $R_x$ , is the same and is seen in Equation (3.15).

$$\frac{r_x}{R_x} = \frac{r_{\text{motor}}}{R_{w_1}} = \frac{r_{w_1}}{R_{w_2}} = \frac{r_{w_2}}{R_{w_3}} = N \quad (3.15)$$

Knowing this and since  $\omega_m$  is transferred through three gears reductions, the relation between the angular velocity of the motor  $\omega_m$  and the angle of the arm  $\theta_a$  is found following the principle of Equation (3.13).

$$\omega_a(t) = N^3 \omega_m(t) \quad (3.16a)$$

$$\theta_a(t) = N^3 \int_0^t \omega_m(v) dv \quad (3.16b)$$

$$\mathcal{L}\{\theta_a(t)\} = \Theta_a(s) = N^3 \cdot \frac{1}{s} \Omega_m(s) \quad (3.16c)$$

The transfer function from the motor's angle velocity to the angle of the arm becomes Equation (3.17).

$$\frac{\Theta_a(s)}{\Omega_m(s)} = \frac{N^3}{s} \quad (3.17)$$

### 3.3.2 Determining the Load Torque Produced by the Gears

The torque of the load put on the motor is the sum of the torque produced by the gears and the torque produced by the arm and stick. As the torque from the arm and stick are considered negligible c.f. Section 3.2, only the torque of the gears needs to be described.

The torque on the motor shaft can be described by Equation (3.19).

$$J_m \dot{\omega}_m = \tau_m - \tau_l - \tau_{fm} \quad (3.18)$$

$$J_m \dot{\omega}_m = \tau_m + F_1 r - b_m \omega_m \quad (3.19)$$

Where:

$J_m$  is the moment of inertia of the motor [kg m<sup>2</sup>]

$\tau_m$  is the torque of the DC-motor [N m]

$\tau_l$  is the torque of the load [N m]

$\tau_{fm}$  is the torque of the friction of the motor [N m]

This means that the torque of the load produced by the gears is equal to  $-F_1 r$ . To find  $F_1$  the torque on the wheel is examined and seen in Equation (3.20).

$$J_w \dot{\omega}_w = -F_1 R - \tau_{\text{gears}} - b_w \omega_w \quad (3.20)$$

Here  $\tau_L$  is the load on wheel 1 that comes from the rest of the wheels connected to it. Wheel 2 is connected to wheel 1 similar to how wheel 1 is connected to the motor. This means that the load torque on wheel 1 is related to  $F_2$  and the load torque on wheel 2 is related to  $F_3$ . Substituting the load torque for the forces, the torques for each wheel is Equation (3.21).

$$J_{w1}\dot{\omega}_{w1} = -F_1R + F_2r - b_{w1}\omega_{w1} \quad (3.21a)$$

$$J_{w2}\dot{\omega}_{w2} = -F_2R + F_3r - b_{w2}\omega_{w2} \quad (3.21b)$$

$$J_{w3}\dot{\omega}_{w3} = -F_3R - b_{w3}\omega_{w3} \quad (3.21c)$$

Using the relation in Equation (3.13), the angular velocity of each wheel can be found to be Equation (3.22).

$$\omega_{w1} = N\omega_m \quad (3.22a)$$

$$\omega_{w2} = N\omega_{w1} = N^2\omega_m \quad (3.22b)$$

$$\omega_{w3} = N\omega_{w2} = N^3\omega_m \quad (3.22c)$$

The same equations are valid with angular accelerations and are inserted in Equation (3.21) giving Equation (3.23).

$$J_{w1}N\dot{\omega}_m = -F_1R + F_2r - b_{w1}N\omega_m \quad (3.23a)$$

$$J_{w2}N^2\dot{\omega}_m = -F_2R + F_3r - b_{w2}N^2\omega_m \quad (3.23b)$$

$$J_{w3}N^3\dot{\omega}_m = -F_3R - b_{w3}N^3\omega_m \quad (3.23c)$$

The forces  $F_1$ ,  $F_2$  and  $F_3$  are isolated giving Equation (3.24).

$$F_1 = -\frac{1}{R}N \left( b_{w1}\omega_m + J_{w1}\dot{\omega}_m - \frac{F_2r}{N} \right) \quad (3.24a)$$

$$F_2 = -\frac{1}{R}N^2 \left( b_{w2}\omega_m + J_{w2}\dot{\omega}_m - \frac{F_3r}{N^2} \right) \quad (3.24b)$$

$$F_3 = -\frac{1}{R}N^3 (b_{w3}\omega_m + J_{w3}\dot{\omega}_m) \quad (3.24c)$$

Inserting Equation (3.24c) in Equation (3.24b) gives Equation (3.25).

$$F_2 = -\frac{1}{R}N^2 \left( b_{w2}\omega_m + J_{w2}\dot{\omega}_m + \frac{r}{R} \frac{N^3}{N^2} (b_{w3}\omega_m + J_{w3}\dot{\omega}_m) \right) \quad (3.25)$$

Where simplification gives that.

$$\frac{r}{R} \frac{N^3}{N^2} = N^2 \quad (3.26)$$

Equation (3.25) is then inserted in Equation (3.24a) giving Equation (3.27) while remembering that the gear ratio is defined by Equation (3.14).

$$\begin{aligned} F_1 = & -\frac{1}{R} N \left( b_{w_1} \omega_m + J_{w_1} \dot{\omega}_m \right. \\ & \left. + N^2 \left( b_{w_2} \omega_m + J_{w_2} \dot{\omega}_m \right. \right. \\ & \left. \left. + N^2 \left( b_{w_3} \omega_m + J_{w_3} \dot{\omega}_m \right) \right) \right) \end{aligned} \quad (3.27)$$

Since  $\tau_{\text{gears}} = -F_1 r$  and the torque of the load on the motor is the torque of the gears,  $\tau_{\text{gear}}$  can be expressed by Equation (3.28).

$$\begin{aligned} \tau_{\text{gear}} = & N^2 \left( b_{w_1} \omega_m + J_{w_1} \dot{\omega}_m \right. \\ & \left. + N^2 \left( b_{w_2} \omega_m + J_{w_2} \dot{\omega}_m \right. \right. \\ & \left. \left. + N^2 \left( b_{w_3} \omega_m + J_{w_3} \dot{\omega}_m \right) \right) \right) \end{aligned} \quad (3.28)$$

Equation (3.28) is Laplace-transformed and reorganized giving Equation (3.29b).

$$\begin{aligned} \mathcal{L}\{\tau_{\text{gear}}(t)\} = \tau_{\text{gear}}(s) = & N^2 \left( B_{w_1} \Omega_m + s J_{w_1} \Omega_m \right. \\ & \left. + N^2 \left( B_{w_2} \Omega_m + s J_{w_2} \Omega_m \right. \right. \\ & \left. \left. + N^2 \left( B_{w_3} \Omega_m + s J_{w_3} \Omega_m \right) \right) \right) \end{aligned} \quad (3.29a)$$

$$\tau_{\text{gear}} = \left( \left( N^2 J_{w_1} + N^4 J_{w_2} + N^6 J_{w_3} \right) s + \left( N^2 B_{w_1} + N^4 B_{w_2} + N^6 B_{w_3} \right) \right) \Omega_m \quad (3.29b)$$

The moments of inertia and the frictions for each wheel are grouped into two variables  $J_{\text{gear}}$  and  $B_{\text{gear}}$  respectively giving the torque for the gears in Equation (3.30).

$$\tau_{\text{gear}} = \left( J_{\text{gear}} s + B_{\text{gear}} \right) \Omega_m \quad (3.30)$$

### 3.4 Modeling of the DC-Motor

The purpose of this section is to establish a dynamic model of the DC-motor. The inputs and outputs of the model can be seen on the block diagram on Figure 3.10.

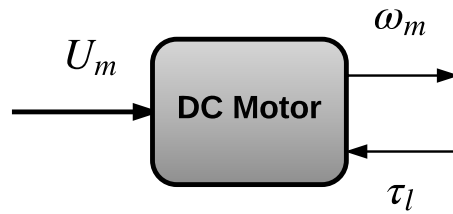


**Figure 3.10:** Block diagram showing the inputs and outputs of a DC motor.

Only the transfer function from the voltage input,  $U_m$ , to the angular velocity output,  $\omega_m$ , needs to be found. It will be done by modeling the electrical and the mechanical part of the motor in that order before combining them.

#### 3.4.1 Electrical Model of the Motor

The electrical circuit of the motor is presented in Figure 3.11.

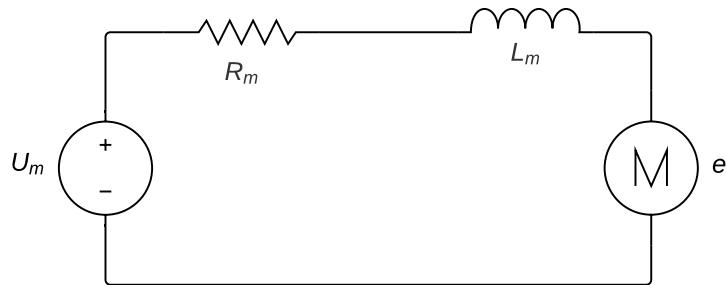


**Figure 3.11:** Circuit diagram of a DC-motor.

Using Kirchhoff's voltage law, the electric model of the DC-motor is Equation (3.31).

$$U_m = R_m i + L_m \frac{di}{dt} + e \quad (3.31a)$$

$$e = K_e \omega_m \quad (3.31b)$$

Where:

$U_m$ is the voltage output of the generator	[V]
$R_m$ is the resistance of the DC-motor	[ $\Omega$ ]
$L_m$ is the inductance of the DC-motor	[H]
$i$ is the current in the DC-motor	[A]
$e$ is the electromotive force	[V]
$K_e$ is the motor velocity constant	[ $V \cdot s \cdot rad^{-1}$ ]
$\omega_m$ is the angular velocity of the motor	[ $rad \cdot s^{-1}$ ]

This is all that is needed for the electrical part to find the model of the motor.

### 3.4.2 Mechanical Model of the Motor

The mechanical free body diagram of the motor is presented in Figure 3.12.

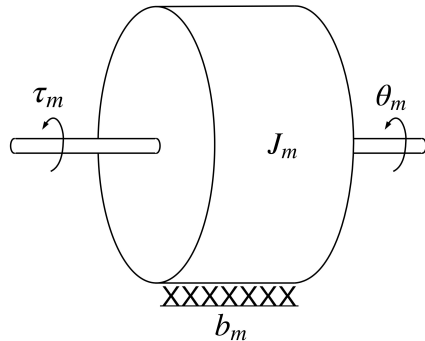


**Figure 3.12:** Free body diagram of a DC-motor.

From Figure 3.12, the sum of the torques for the mechanical part of the motor is described in Equation (3.32).

$$J_m \ddot{\theta}_m = \tau_m - \tau_l - \tau_{fm} \quad (3.32)$$

Where:

$J_m$ is the moment of inertia of the motor	[ $kg \cdot m^2$ ]
$\tau_m$ is the torque of the DC-motor	[N m]
$\tau_l$ is the torque of the load	[N m]
$\tau_{fm}$ is the torque of the friction of the motor	[N m]

The motor's torque and the friction's torque, respectively  $\tau_m$  and  $\tau_f$ , are defined by Equation (3.33) while  $\tau_l$  is the torque of the gears,  $\tau_{gear}$ , found in Section 3.3.2.

$$\tau_m = K_t \cdot i \quad (3.33a)$$

$$\tau_{\text{fm}} = b_m \cdot \omega_m \quad (3.33b)$$

Where:

$$\begin{aligned} K_t &\text{ is the motor torque constant} & [\text{N m A}^{-1}] \\ b_m &\text{ is the viscous friction coefficient} & [\text{N m s rad}^{-1}] \end{aligned}$$

Inserting Equation (3.33) into Equation (3.32) gives Equation (3.34).

$$J_m \dot{\omega}_m = K_t i - \tau_{\text{gear}} - b_m \omega_m \quad (3.34)$$

The mechanical and electrical model of the motor can now be combined.

### 3.4.3 Combined Model of the Motor

First the electrical and mechanical equations of the motor are Laplace-transformed in Equation (3.35)

$$U_m(s) = R_m I(s) + sL_m I(s) + K_e \Omega_m(s) \quad (3.35a)$$

$$sJ_m \Omega_m(s) = K_t I(s) - \tau_{\text{gear}} - B_m \Omega_m(s) \quad (3.35b)$$

The current,  $I(s)$ , is isolated and inserted in Equation (3.35b) giving Equation (3.36).

$$sJ_m \Omega_m(s) = K_t \frac{U_m(s) - K_e \Omega_m(s)}{R_m + sL_m} - \tau_{\text{gear}} - B_m \Omega_m(s) \quad (3.36)$$

Equation (3.30) is inserted in Equation (3.36) and rearranged giving Equation (3.37c). The equation is simplified by setting  $J_t = J_m + J_{\text{gear}}$  and  $B_t = B_m + B_{\text{gear}}$ .

$$\Omega_m(s) \left( (J_m + J_{\text{gear}}) s + (B_m + B_{\text{gear}}) \right) = K_t \frac{U_m(s) - K_e \Omega_m(s)}{R_m + sL_m} \quad (3.37a)$$

$$\Omega_m(s) \left( J_t L_m s^2 + (R_m + B_t L_m) s + B_t R_m + K_t K_e \right) = K_t U_m(s) \quad (3.37b)$$

$$\frac{\Omega_m(s)}{U_m(s)} = \frac{K_t}{J_t L_m s^2 + (J_t R_m + B_t L_m) s + B_t R_m + K_t K_e} \quad (3.37c)$$

As  $L_m$  is significantly smaller than  $R_m$  it is assumed to be 0. This assumption is made to simplify the motor model and is fair as a small  $L_m$  would have almost no influence on the system as seen in Equation (3.36). This gives Equation (3.38) which is the final transfer function for the DC motor model.

$$\frac{\Omega_m(s)}{U_m(s)} = \frac{K_t}{J_t R_m s + B_t R_m + K_t K_e} \quad (3.38)$$

### 3.5 Combining the Models for the Inverted Pendulum

With a model for each individual part of the inverted pendulum derived, a combined model for the entire system can be made. This model will have voltage,  $U_m(s)$ , as input and the angle of the stick,  $\Theta_s(s)$ , as the output. This is done by multiplying all transfer functions together as seen in Equation (3.39).

$$\frac{\Omega_m(s)}{U_m(s)} \cdot \frac{\Theta_a(s)}{\Omega_m(s)} \cdot \frac{\Theta_s(s)}{\Theta_a(s)} = \frac{\Theta_s(s)}{U_m(s)} \quad (3.39)$$

By combining Equation (3.38), Equation (3.17) and Equation (3.10c) the model for the inverted pendulum becomes Equation (3.40).

$$\frac{\Theta_s(s)}{U_m(s)} = \frac{K_t}{J_t R_m s + B_t R_m + K_t K_e} \cdot \frac{N^3}{s} \cdot \frac{-\frac{3l_a}{2l_s}s^2 + \frac{3b_{as}}{M_s l_s^2}s}{s^2 + \frac{3b_{as}}{M_s l_s^2}s - \frac{3g}{2l_s}} \quad (3.40)$$

The values for all constants of the inverted pendulum along with their origin is shown in Table 3.3. The friction between the arm and the stick is assumed to be zero as the joint consists of a ball bearing.

**Table 3.3:** Parameters for the inverted pendulum and their origin.

Variable	Value	Parameter	Unit	Origin
$K_t$	$29.3 \cdot 10^{-3}$	Mechanical motor constant	N m A <sup>-1</sup>	Section A.1.4
$K_e$	$35.5 \cdot 10^{-3}$	Electrical motor constant	V/(rad/s)	Section A.1.3
$J_m$	$29.0 \cdot 10^{-6}$	Moment of inertia of motor	kg m <sup>2</sup>	[14]
$J_{gear}$	$0.153 \cdot 10^{-3}$	Moment of inertia of gear	kg m <sup>2</sup>	Section A.2.2
$R_m$	0.8	Resistance	$\Omega$	Section A.1.1
$B_m$	$0.159 \cdot 10^{-3}$	Friction in motor	N/(rad/s)	Section A.2.1
$B_{gear}$	$1.11 \cdot 10^{-3}$	Friction in the gears	N/(rad/s)	[1]
$N$	0.3	Gear ratio	1	Table 3.1
$l_a$	0.33	Length of arm	m	Table 3.2
$l_s$	0.8	Length of stick	m	Table 3.2
$M_a$	0.288	Mass of arm	kg	Table 3.2
$M_s$	0.344	Mass of stick	kg	Table 3.2
$b_{as}$	0	Friction in arm and stick	N/(rad/s)	Assumption
$g$	9.8	Standard gravity	$\text{m s}^{-2}$	[13]

The inverted pendulum model is determined. The rocket model will then be found to make the comparison between them, and conclude if the models share similarities.



# Chapter 4

## Rocket Analysis

### 4.1 Preliminary Analysis of a Rocket

The following chapter describes the functionality and structure behind a rocket. The goal is to determine which factors lead to instability in flight and launch of a rocket.

#### 4.1.1 Stability of a Rocket

A rocket often has a target, either if it is space travelling or just collecting orbit data on earth, but in order to succeed it has to be stable [2]. The flight direction of a rocket can change due to disturbances like wind and thrust instabilities.

Stability can be defined within many categories. In the case of a rocket the stability is considered as the directional and flight stability.

Center of gravity and pressure are related to the forces acting on a rocket. Figure 4.1 describes the different situations a rocket encounters during its flight and describes the forces applied in these cases.

In Figure 4.1 two points can be seen on the rockets. One is CP the Center of Pressure where the lift and the drag force apply to a rocket. The other one is CG the Center of Gravity, which is the point which the rocket rotates around. Due to this characteristics the torque applied by the lift and the drag is dependent of the relative positioning between the CG and the CP. Since a rocket tilts due to a torque applied by external forces such as the wind, then lift and the drag has to be oriented so it counters these forces. In order to do so the CG has to be above the CP. This means depending of the position of the CP compared to the CG the rocket flight

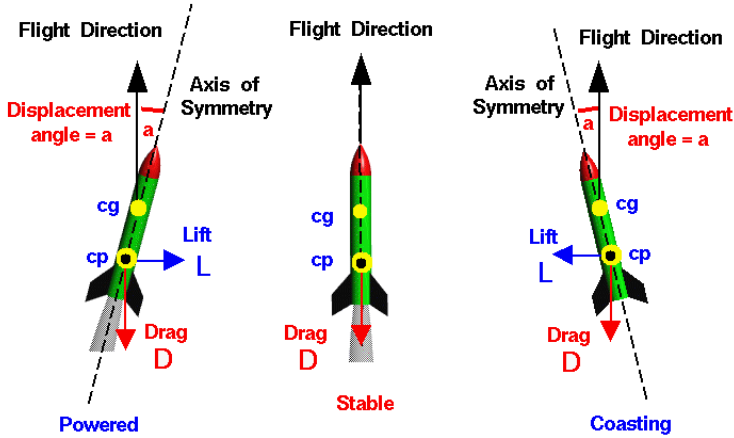


**Figure 4.1:** Summary of forces applied to a rocket during its flight [2].

will be either stable or unstable. That is why in simpler rockets without any control system, its design is made so that CP is indeed above CG [2].

This preliminary analysis gives the possibility to further examine on how to control the stability of a rocket.

#### 4.1.2 Controlling a Rocket's Stability

The design method for placing the CP and GP does not always provide a perfectly stable attitude control. Indeed to have such precision an active control system is necessary. Full scale rockets use the thrusting force to achieve alike control. In order to do so most of them operate with the gimbaled thrust method. It consists of steering the engine's nozzle to get the thrusting force in right incidence. An example is seen cf. figure Figure 4.2.

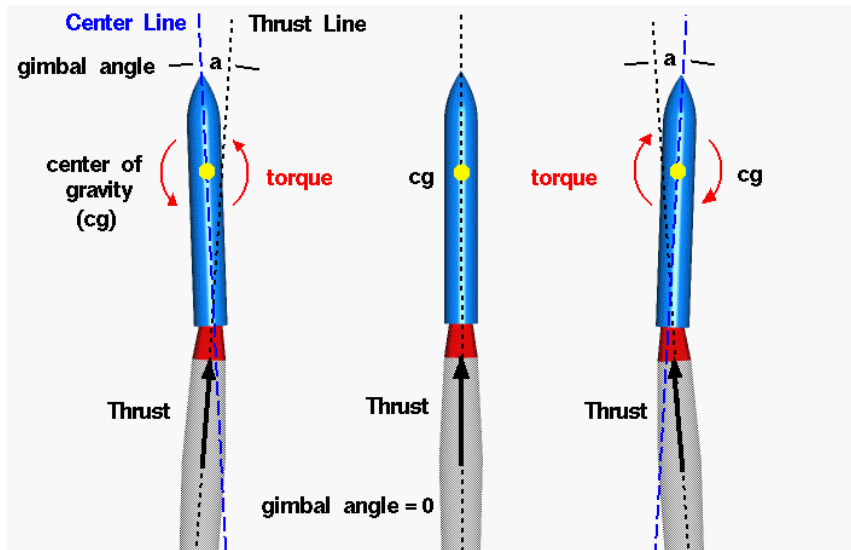


Figure 4.2: Example of gimballing a rocket nozzle [2].

Where a torque is applied to create a rotation around the rocket's center of gravity. The thrust direction is relative to the position of the center of gravity. This should compensate for direction deviations from the rocket's center line or trajectory, and keep the rocket stable. The described gimbal method will be the control method focused on in this project. The rocket will be designed with a control system depending on vectoring the thruster in relation to the attitude position of the rocket.

## 4.2 Rocket Modeling

A rocket model needs to be done in order to compare the rocket with the inverted pendulum. It also adds one degree of freedom compared to the inverted pendulum, since it can be controlled in two horizontal directions. A model of the rocket is made to be able to compare the two systems' dynamics. In order to keep the rocket project as close as possible of the inverted pendulum, the goal of the rocket model is to control the angle of the body  $\theta_b$  by changing the angle of the thruster  $\theta_t$ .

All the forces applied to the rocket body can be decomposed into two forces: one parallel to the rocket body and another perpendicular to it. It is considered that the rocket body is incompressible as well as unstretchable, therefore the parallel forces are null.

Since the project is about controlling a rocket in its initial stage of flight, the speed is considered low enough to neglect the drag force produced by it. The gravity is also neglected as it is mainly canceled by the thrust. These approximation results

of having the thruster force as the only acting force on the rocket as showed in Figure 4.3.

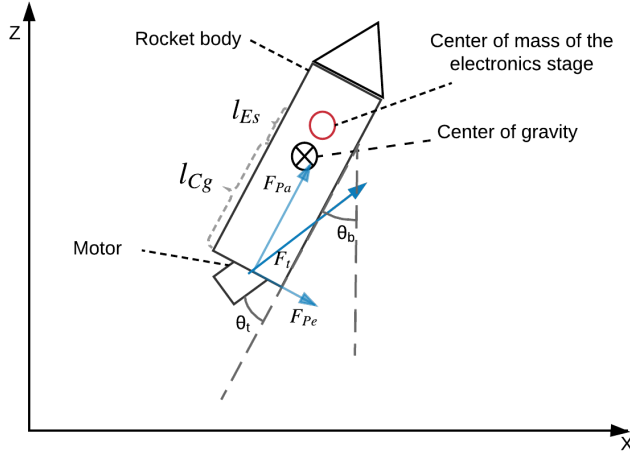


**Figure 4.3:** Simplified sum of forces on the rocket.

Where:

$\theta_t$ is the thruster angle compared to the body	[rad]
$\theta_b$ is the body angle compared to vertical	[rad]
$l_{Es}$ is the distance from the electronics stage to the center of gravity	[m]
$l_{Cg}$ is the distance from the thruster end to the center of gravity	[m]
$F_t$ is the thruster force	[N]
$F_{pa}$ is the thruster force	[N]
$F_{pe}$ is the thruster force	[N]
$\tau_t$ is the torque created by the thruster on the rocket	[N m]

### 4.3 Modeling of the angle

Using Newton's second law the Equation (4.1) can be derived.

$$J_r \ddot{\theta}_b = \tau_t \quad [\text{N m}] \quad (4.1)$$

Where:

$J_r$ is the moment of inertia of the rocket	$[\text{kg m}^2]$
$\tau_t$ is the torque exerted by the thrust of the rocket	$[\text{N m}]$

By using geometry,  $\tau_t$  is found in Equation (4.4).

$$\tau_t = F_t \sin(\theta_t) l_{Cg} \quad [\text{N m}] \quad (4.2)$$

70 % of the weight is in fact concentrated on the electronic's stage (rocket is about 0.300 kg and the electronics stage is around 0.210 kg). Therefore it is assumed, that apart from this stage everything is weightless. Consequently the rocket can be approximated as a pendulum where the electronics stage is mass rotating around the gravity center. The center of gravity position is determined by simply balancing the rocket on a finger [8]. The moment of inertia is then found in Equation (4.5) [11].

$$I_r = m_{Es} l_{Es}^2 \quad [\text{kg m}^2] \quad (4.3)$$

Where:

$m_{Es}$  is the mass of the electronics stage [kg]

By using geometry,  $\tau_t$  is found in Equation (4.4).

$$\tau_t = F_t \cdot \sin(\theta_t) \cdot l_{Cg} \quad [\text{N m}] \quad (4.4)$$

70 % of the weight is in fact concentrated on the electronic's stage (the rocket is about 0.300 kg and the electronics stage is around 0.210 kg). Therefore it is assumed, that apart from this stage everything is weightless. Consequently the rocket can be approximated as a pendulum where the electronics stage is mass rotating around the gravity center. The center of gravity position is determined by simply balancing the rocket on a finger [8]. The moment of inertia is then found in Equation (4.5) [11].

$$J_r = m_{Es} \cdot l_{Es}^2 \quad [\text{kg m}^2] \quad (4.5)$$

Where:

$m_{Es}$  is the mass of the electronics stage [kg]

By combining Equation (4.1) with Equation (4.4) and Equation (4.5), Equation (4.11) is obtained.

$$m_{Es} l_{Es}^2 \ddot{\theta}_b = F_t \sin(\theta_t) l_{Cg} \quad [\text{N m}] \quad (4.6)$$

The thruster force  $F_t$  will be considered as constant. See the rocket motor test experiment for details in Appendix E.

Equation (4.11) needs to be linearized in order to go into to Laplace domain. To do so a first order Taylor approximation around the null angle is done in Equation (4.12).

$$m_{\text{Es}} l_{\text{Es}}^2 \ddot{\theta}_b = F_t \theta_t l_{\text{Cg}} \quad [\text{N m}] \quad (4.7)$$

By going to the Laplace domain and grouping elements the transfer function of the rocket is found in Equation (4.13).

$$s^2 m_{\text{Es}} l_{\text{Es}}^2 \Theta_b(s) = F_t l_{\text{Cg}} \Theta_t(s) \quad [1] \quad (4.8a)$$

$$\frac{\Theta_b(s)}{\Theta_t(s)} = \frac{F_t l_{\text{Cg}}}{s^2 m_{\text{Es}} l_{\text{Es}}^2} \quad [1] \quad (4.8b)$$

The servomotors introduce a delay between the controller output and the rocket system. This delay is modeled in Equation (4.14).

$$\frac{\Theta_b(s)}{\Theta_{\text{b}_{\text{in}}}(s)} = \frac{1}{\tau s + 1} \quad [1] \quad (4.9)$$

Where:

$$\begin{aligned} \Theta_{\text{b}_{\text{in}}(s)} &\text{ is the angle sent to the servo by the controller} & [1] \\ \tau &\text{ is the time constant} & [1] \end{aligned}$$

The time constant of the servomotors is determined in Appendix F, while the final transfer function of the rocket model is found to be Equation (4.15).

$$\frac{\Theta_b(s)}{\Theta_t(s)} = \frac{1}{\tau s + 1} \frac{F_t l_{\text{Cg}}}{s^2 m_{\text{Es}} l_{\text{Es}}^2} \quad (4.10)$$

Now that the model of the rocket is done a comparison is done with the model of the inverted pendulum.

By combining Equation (4.1) with Equation (4.4) and Equation (4.5), Equation (4.11) is obtained.

$$m_{\text{Es}} \cdot l_{\text{Es}}^2 \cdot \ddot{\theta}_b = F_t \cdot \sin(\theta_t) \cdot l_{\text{Cg}} \quad [\text{N m}] \quad (4.11)$$

The thruster force  $F_t$  will be considered as constant. See the rocket motor test experiment for details in Appendix E.

Equation (4.11) needs to be linearized in order to go into to Laplace domain. To do so a first order Taylor approximation around the null angle is done in Equation (4.12).

$$m_{Es} \cdot l_{Es}^2 \cdot \ddot{\theta}_b = F_t \cdot \theta_t \cdot l_{Cg} \quad [\text{N m}] \quad (4.12)$$

By going to the Laplace domain and grouping elements the transfer function of the rocket is found in Equation (4.13).

$$s^2 \cdot m_{Es} \cdot l_{Es}^2 \cdot \Theta_b(s) = F_t \cdot l_{Cg} \cdot \Theta_t(s) \quad [1] \quad (4.13a)$$

$$\frac{\Theta_b(s)}{\Theta_t(s)} = \frac{F_t \cdot l_{Cg}}{s^2 \cdot m_{Es} \cdot l_{Es}^2} \quad [1] \quad (4.13b)$$

The servomotors introduce a delay between the controller output and the rocket system. This delay is modeled in Equation (4.14).

$$\frac{\Theta_b(s)}{\Theta_{bin}(s)} = \frac{1}{\tau \cdot s + 1} \quad [1] \quad (4.14)$$

Where:

$$\begin{aligned} \Theta_{bin}(s) &\text{ is the angle sent to the servo by the controller} & [1] \\ \tau &\text{ is the time constant} & [1] \end{aligned}$$

The time constant of the servomotors is determined in Appendix F, while the final transfer function of the rocket model is found to be Equation (4.15).

$$\frac{\Theta_b(s)}{\Theta_t(s)} = \frac{1}{\tau \cdot s + 1} \cdot \frac{F_t \cdot l_{Cg}}{s^2 \cdot m_{Es} \cdot l_{Es}^2} \quad (4.15)$$

Now that the model of the rocket is done a comparison is done with the model of the inverted pendulum.

## 4.4 Comparison of the Inverted Pendulum and Rocket Models

From Chapter 3 and Section 4.2 it is found, that the models are slightly different. First of all, opposite angles were chosen in the beginning of the modeling process. Moreover, the inverted pendulum is fixed to the gears and motor, while the rocket is floating in the air, and thus canceling the gravity. The inverted pendulum has

two more zeros in 0 and two real poles equidistant from zero, whereas the rocket has two poles in 0. The difference in poles is due to the absence of gravity into the rocket modeling, while the difference in zeros might be due to the fact that the arm is rigidly attached compared to the thruster.

Due to this difference a different controller needs to be designed for each model.

# Chapter 5

## Problem Statement & Delimitation

This chapter will include the problem statement and delimitations in the project.

### 5.1 Problem Statement

It is chosen to separate the design of controller into two separate persons, considering that the model of the inverted pendulum and the rocket do not share an overall similarity. A problem statement for each part is introduced.

*How can a control system be designed for implementation in the inverted pendulum system? And would this system be capable of balancing the stick?*

*How can a control system be designed for implementation on the rocket? And is it possible to stabilize the rockets trough thrust vectoring with this system?*

### 5.2 Delimitation

In the project some limits have to be set for the use of models and materials. The objective of the control system is to find the similarities of using a electronic stabilization system for rockets and inverted pendulums. The system is developed as a proof-of-concept solution. The models in the project can only be approximations of reality, and it is therefore observable that the transfer to a larger scale project will not be linear.

**Physical delimitation:** The inverted pendulum setup used in the project is pre-fabricated and made available by the university. The choice of motor, gears, and other components will therefore not be further considered. The setup is a inverted pendulum, and contains therefore of both an arm and a stick. The inverted pendulum setup will from here on be called "inverted pendulum". The setup is shown cf. figure 5.1.

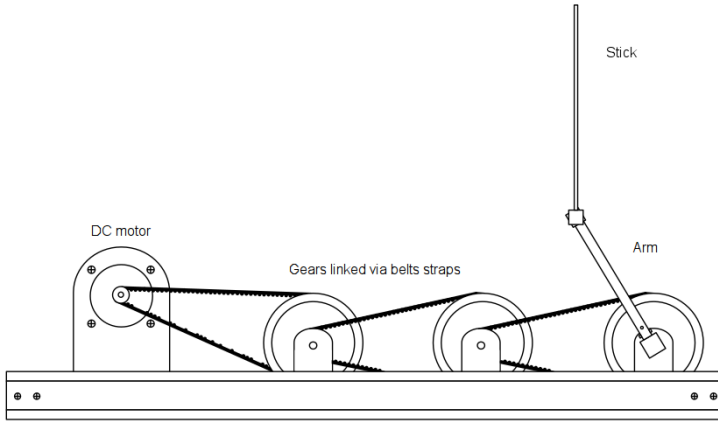


**Figure 5.1:** Diagram of the inverted pendulum setup[1].

Construction and modeling of the rocket will be limited to a minor-scale rocket. The rocket will be designed around a solid propellant thruster, and will therefore not contain any liquid fuel. This is to limit the constraints from laws and keep the cost low. Furthermore weight and dimension limits are set before designing the rocket.

**Control delimitation:** A choice is made that the starting point for controlling the stick is as illustrated cf. figure 5.1 in upwards vertical position. Therefore the controller will not be able to balance the stick, if its vertical balance limits is surpassed. The delimitation is made to simplify the controlling, and make it as similar as possible to controlling a rocket.

**Test delimitation:** Launching and flight of a rocket for testing a controller is a high cost procedure because of the chance of damaging the rocket and the cost of thrusters per launch. The testing of the rockets stabilization will be a ground based test setup, where the controller can be tested without the risk of damaging the rocket. If, and only if the control system proves stable and safe, a launch and flight of the rocket will be conducted under circumstances fulfilling given laws.

The delimitation now gives the possibility to set requirements and specifications for the established models for both systems.

# Chapter 6

## Requirements and Specifications

The following chapter describes requirements and specifications determined for controlling both the rocket and the inverted pendulum. The requirements are set to obtain a system which fulfils the problem statement.

As described previously the goal of both systems is to react to deviations from its stable position. The goal of the rocket is the launch and a stable flight, versus the inverted pendulum where the goal is to balance the stick in vertical upwards position.

Both systems will be described with physical and control requirements in separate sections. The physical requirements will be set based on the limits of the models.

### 6.0.1 Requirements for the Inverted Pendulum

The requirements are based on figure 3.1, and the modeling behind where the angle relations and positions is described between the gears, arm and stick. It is yet decided that the main requirement is to balance the stick. But requirements have to be set considering when the stick is balanced and when not.

- 1. The control position of the arm must not exceed  $\pm \frac{\pi}{4}$  radians from the 0 radians vertical position.**

A choice made to limit the arm's movements around vertical upwards position which will act as the initial position. The arm should not exceeded the limit because

the control of the stick will become more vertical than horizontal. It is therefore considered that the arm is not able to control the stick in a stable manor.

**2. The angle of the stick must not exceed  $\pm \frac{\pi}{18}$  radians from vertical position.**

An assumption made to simplify and limit the sticks movement, which would relate it to the control of a rocket. Assuming that the arm can not move to more than  $\frac{\pi}{4}$ , gives that the overshoot of the arm can be at maximum:

$$\frac{\pi}{4} - \frac{\pi}{18} = \frac{7\pi}{36} \quad (6.1)$$

$$\frac{\frac{7\pi}{36}}{\frac{\pi}{18}} = 350 \% \quad (6.2)$$

This only apply when considering the worst case position of the stick when the arm is still in vertical position. It means that arm should be able to catch the stick without overshooting more than 350%. The overshoot is limited, because 350% is considered unstable when the goal is to balance the stick. The maximum overshoot is limited to a tenth of the sticks angular position  $\frac{\pi}{180}$ . And may therefore not exceed:

$$\frac{\frac{\pi}{180}}{\frac{\pi}{18}} = 10 \% \quad (6.3)$$

**3. Deviation from the upright position of the stick must not exceed  $\pm \frac{\pi}{36}$  radians when considered balanced.**

A choice made to ensure stability and avoid oscillation around the equilibrium position. This means that if the angle is exceeded the controller needs to react. The requirement is mainly set to ensure that the stick balancing precision is within the sampling precision of the sensors. The controller will be designed based on a steady state error of zero, which means that errors from balanced position are from disturbance and not from the controller's steady state error.

- 4. The system should be able to regain balance if an impulse of  $\frac{\pi}{18}$  radians is applied, in form of a push on the stick.**

If an impulse from the external disturbance is acting on the stick then the control should be able to counteract the stick back into equilibrium position.

### 6.0.2 Requirements for the Rocket

Some limits has to be set based on the capability of building and using a rocket. The controller requirements will be the same as with the inverted pendulum. The physical dimensions of the rocket can not exceed:

Parameter	Value	Unit
Length	0.25	[m]
Width	0.25	[m]
Height	0.5	[m]
Total volume	0.03	[m <sup>3</sup> ]
Weight	0.2	[kg]

**Table 6.1:** Maximum size and weight of the rocket.

As tested in Appendix E, the thruster force is approximatively 3 Newtons. 0.2 Kg corresponds to approximately 2 N towards the ground.

- 5. Deviation from the rockets initial trajectory must not exceed  $\pm \frac{\pi}{18}$  radians.**

A choice made to limit the movement of the rocket during flight. If the limit is exceeded the rocket controller will not guarantee stability, but might stabilize the rocket none the less.

- 6. The system should be able to regain its stability and direction if an external disturbance impulse of  $\frac{\pi}{36}$  radians is applied on the rocket.**

A choice made to ensure flight stability even if the rocket is influenced by a external disturbance.

## 7. Settling time of the rocket should be less than $\frac{1}{3}$ of the flight time.

A choice made to ensure the stabilisation of the rocket during the short duration of flight. The rise time should be as fast as permitted without influencing greatly the overshoot.

### 6.1 Acceptance Test Specification

The following section describes how the requirements can be tested. This verification is made to ensure that the system fulfils the set requirements.

#### Acceptance Test 1.

Verification of requirement 1 will not be proceeded, but simply implemented in the software based on feedback from the arm potentiometer. The software will, if the angle exceeds  $\pm \frac{\pi}{4}$  radians, no longer react on feedback from the stick and shut off.

#### Acceptance Test 2.

Requirement 2 and 3 is tested based on placing the stick and arm in vertical balanced position. The controller is engaged and the system is ran for one minute. The feedback data of the sensors will be collected to determine if the sticks angle have exceeded the requirement. As well is the sampled data from the motor used to compare with the position changes of the stick and see if the controller consider the stick balanced when the angle of the stick is within  $\pm \frac{\pi}{36}$  of 0 radians.

#### Acceptance Test 3.

Requirement 4 are tested from holding the stick in  $\pm \frac{\pi}{18}$  radians when the arm is at 0 radians vertical position. The control system is activated and the stick is released. Sensor data is sampled and saved.

#### Acceptance tests for the Rocket.

The acceptance test will only be proceeded if the rocket implementation proves successful. The specification will be set prior of testing.

## **Part II**

# **Design & Implementation**



## Chapter 7

# Design of the Inverted Pendulum Controller

The goal of the controller is to balance the stick in an upright position. The system is seen as a block diagram on Figure 7.1. Inserting all the constants from Table 3.3 gives the transfer function seen in Equation (7.1).

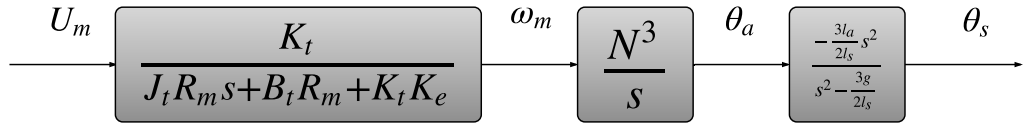


**Figure 7.1:** Block diagram of the inverted pendulum system.

$$\frac{\Theta_s}{U_m} = \frac{-3.36s^2}{s(14.1088 + s)(-4.2874 + s)(4.2885 + s)} \quad (7.1)$$

The system is inherently unstable as it is evident by the pole in the right half plane of the pole-zero plot in Figure 7.2.

In order to achieve a stable system, the right half plane pole needs to be moved to the left half plane.

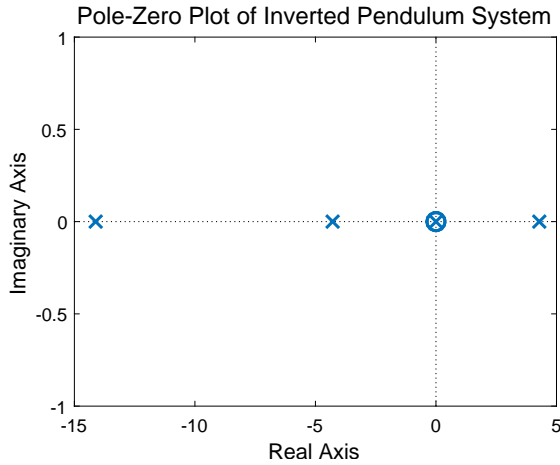


**Figure 7.2:** Pole-zero plot for the inverted pendulums transfer function.

There is a plethora of different options for the controller to use; the simplest being a proportional controller. A simple way to check whether the proportional controller is feasible is by examining the root locus of the transfer function in Figure 7.3a. The pole in the right half plane moving towards infinity is caused by the transfer function being negative and can be fixed with a negative gain as shown on figure Figure 7.3b.

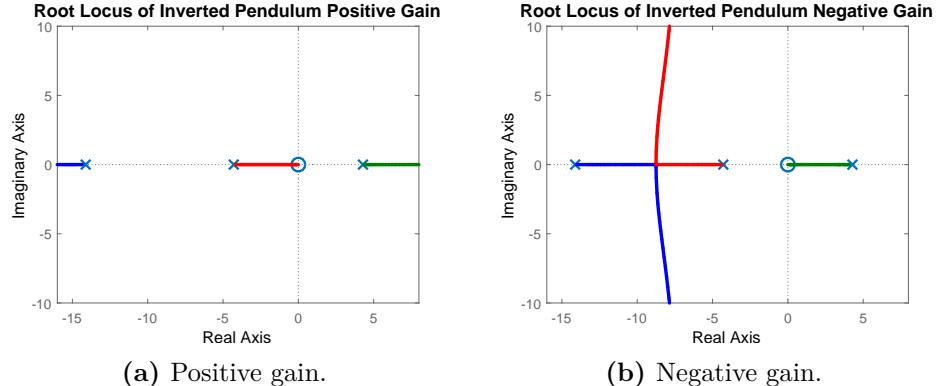


**Figure 7.3:** Root locus of the inverted pendulums transfer function.

The proportional controller is not feasible as the pole in the right half plane never enters the stable region even with a negative gain. This is because the pole will always end at a zero if available. The zero in 0 blocks the unstable pole from moving into the stable region.

The controller can be simplified by using cascade control. This means two controllers should be designed; one that controls the angle of the arm and one that controls the angle of the stick. The cascade control system can be seen on Figure 7.4.

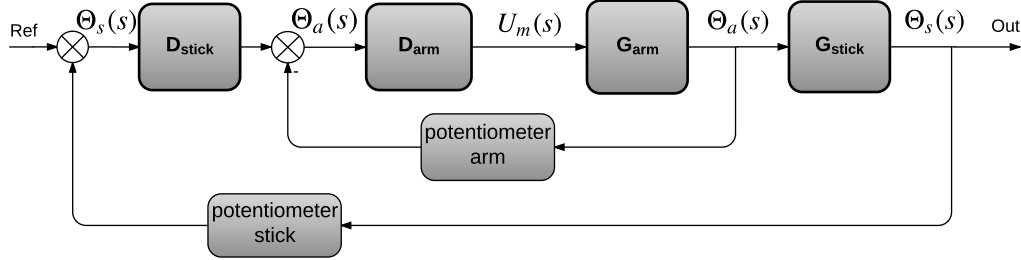


**Figure 7.4:** Block diagram of the inverted pendulum system with cascade control.

If the inner loop is fast enough compared to the outer loop, it is negligible to the outer loop controller. This means the root locus can be split into two separate systems with a respective controller that needs to be designed. The two new loops will be referred to as the inner loop and outer loop and their transfer function is seen in Equation (7.2).

$$\frac{\Theta_a}{U_m} = \frac{5.43}{s^2 + 14.11s} \quad (7.2a)$$

$$\frac{\Theta_s}{\Theta_a} = \frac{-0.62s^2}{s^2 - 18.38} \quad (7.2b)$$

The root locus of the two subsystems is seen on Figure 7.5.

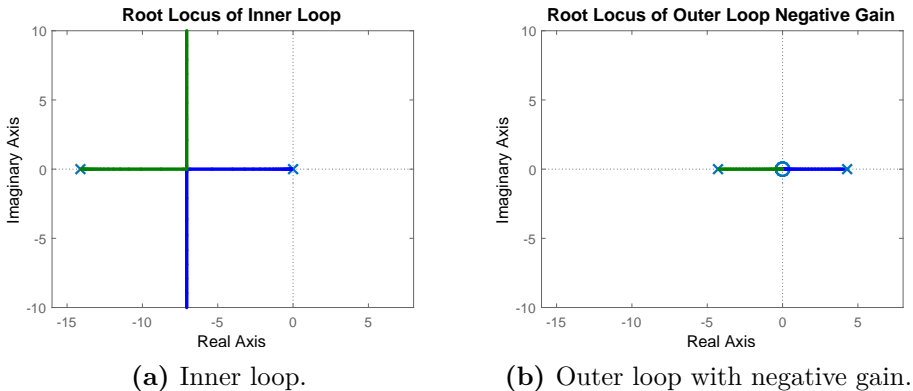


**Figure 7.5:** Root locus of the inverted pendulum with cascade control.

With this split it is simpler to design a controller that can move the unstable pole to the stable region. The inner loop controller will be designed first as it is essential

to this split that the inner loop is faster than the outer loop. The inner loop controller will be designed to be as fast as possible before the outer loop controller is designed.

## 7.1 Design of Inner Loop Controller

For the design of the inner loop controller, it is important that it settles faster than the outer loop controller without any overshoot. This means the natural frequency of the system with the controller needs to be larger and the poles close to the real axis. With the help of Figure 7.6 a gain of 9.17 is chosen as it is the maximum gain obtainable without having any overshoot.

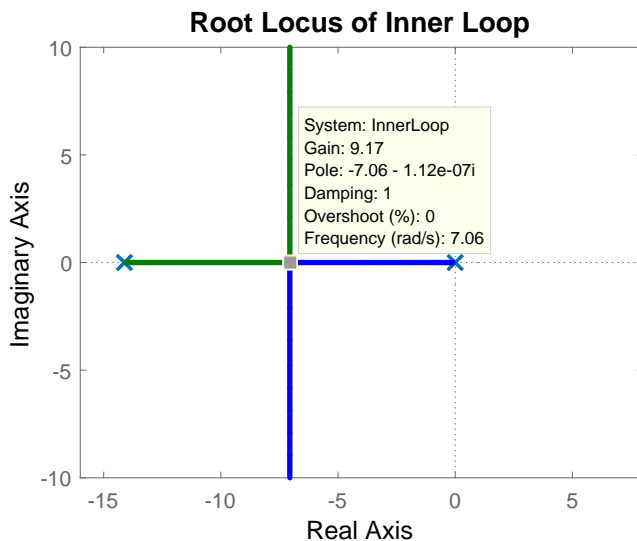


**Figure 7.6:** Root locus of the inner loop showing the gain required for the poles to meet.

However in this system the two poles are still very close to the outer loop system.

In order to speed up the inner loop, two options are available. The first one is to use a more elaborate controller than the P controller such as a PD- or a lead controller. The second one is to once again divide the inner loop into two loops. The second method is preferred as the integrated tachometer in the motor can be used to control the velocity. Furthermore when testing for the motor parameters, the driver did not deliver a constant speed for a constant voltage. A feedback loop of the velocity would be able to reduce the inconsistencies generated by the driver.

The two new loops will thus control the motor velocity and angle of the arm and will be called motor loop and arm loop respectively.

The first loop to be designed will be the motor loop as it is the most inner loop. The new control loop is added to Figure 7.4 to form the final block diagram presented in Figure 7.7.

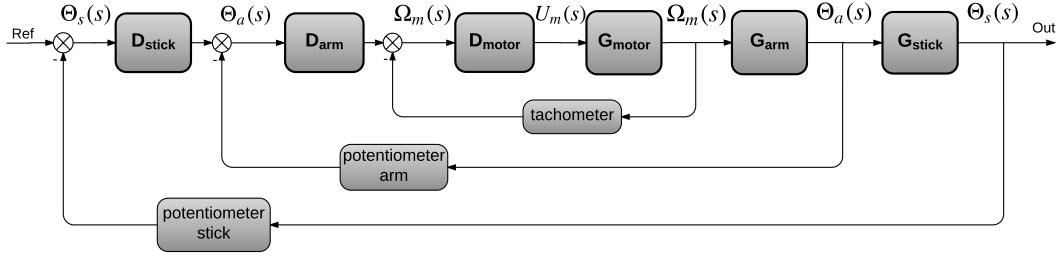


**Figure 7.7:** New block diagram of the inverted pendulum system with cascade control.

### 7.1.1 Design of the Motor Loop Controller

The first loop controller is the one adjusting the motor velocity,  $\omega_m$ , according to the voltage. The transfer function from  $U_m$  to  $\omega_m$  is determined in Section 3.4. The values for the variables in Equation (3.38) is inserted giving Equation (7.3b).

$$\frac{\Omega_m(s)}{U_m(s)} = \frac{K_t}{J_t R_m s + B_t R_m + K_t K_e} \quad (7.3a)$$

$$\frac{\Omega_m(s)}{U_m(s)} = \frac{201.24}{s + 14.11} \quad (7.3b)$$

As it is the most inner loop of the system, the step response has to be faster than the outer loops controlling the arm and the stick. The transfer function has a negative pole making the system stable. It also has a large gain already, so closing the loop is enough to get a faster response. The step response of the closed motor loop is seen on Figure 7.8.

There is a small steady state error that will be corrected slightly by increasing the gain. The gain is increased until the steady state error is less than 5%. The gain required is 1.35. The step response of the closed motor loop with a gain of 1.35 can be seen on Figure 7.9, and gives a settling time of 0.0137 seconds.

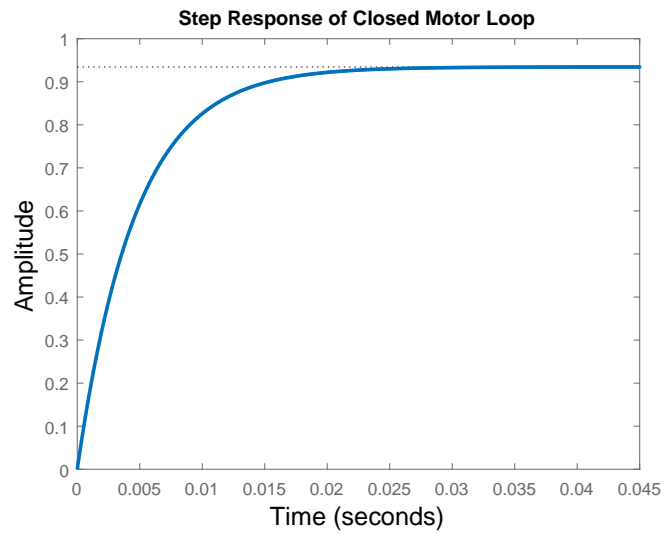


**Figure 7.8:** Step response of the closed motor loop with a gain of 1.

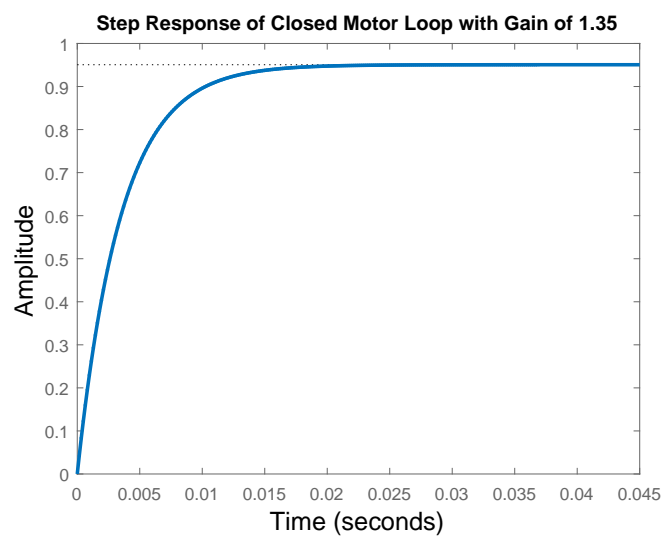


**Figure 7.9:** Step response of the closed motor loop with a gain of 1.35.

The controller for the motor loop thus becomes Equation (7.4).

$$D_{\text{motor}} = 1.35 \quad (7.4)$$

### 7.1.2 Design of the Arm Loop Controller

The motor loop has a settling time of 0.0137 s, so the settling time of the arm loop has to be slower than 0.137 s in order to make the assumption that the motor loop transfer function is equal to 1 for the arm loop. The transfer function for the arm loop is found by inserting the values in Equation (3.17) giving Equation (7.5).

$$\frac{\Theta_a}{\Omega_m} = \frac{0.027}{s} \quad (7.5)$$

The root locus of Equation (7.5), in Figure 7.10, shows that there is theoretically no gain limitation for the arm as the pole moves to the left side plan making the system stable, as long as the gain is high enough. The pole is also always on the real axis which means there will be no overshoot no matter the gain.

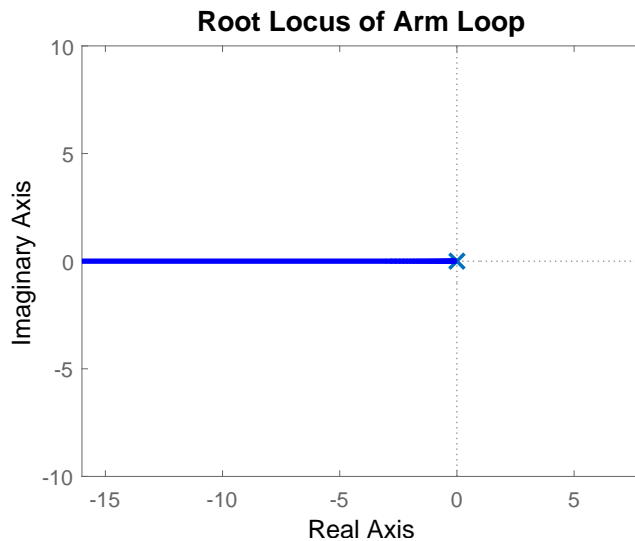


**Figure 7.10:** Velocity as input and Arm's angle as the output

The gain for the closed loop will be chosen to give a settling time slower than 0.137. A gain of 900 is satisfactory as it gives a settling time of 0.16 seconds as seen on the step response on Figure 7.11.

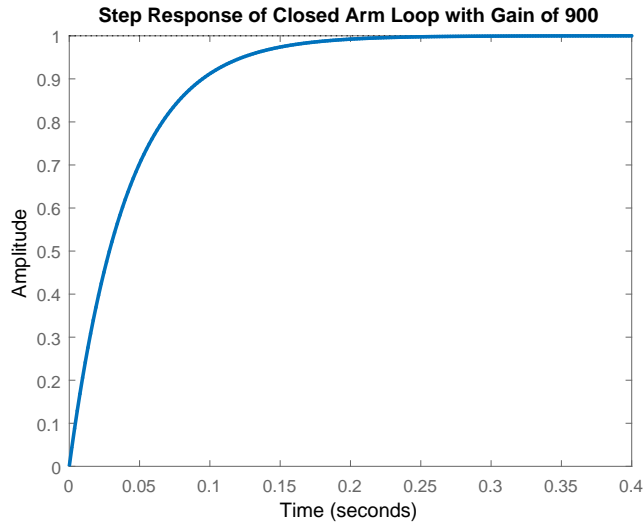


**Figure 7.11:** Step response of the closed arm loop with a gain of 900.

The arm loop controller then becomes Equation (7.6).

$$D_{\text{arm}} = 900 \quad (7.6)$$

## 7.2 Design of Outer Loop Controller

As the poles will eventually end up at the zeros with a large enough gain when the loop is closed, there are two options to bring the unstable pole into the stable region: Remove all zeros in 0 so the pole can cross the into the stable region along the real axis or add another unstable open loop pole to force the poles off the real axis and then try to circumvent the zeros in 0.

Removing the zeros in 0 can not be done by adding poles as  $\infty \cdot 0$  is not defined. Instead it is better to try and redefine the model output to something with a DC gain but at the same time requires the stick to be balanced to achieve the new output. This could be done by attempting to control the position of a point on the stick. The stick would need to be balanced in order to always have the point in the correct position.

### 7.2.1 Redefining the Inverted Pendulums Output

The inverted pendulum model will be redefined so the output is the distance from a point on the stick to the vertical axis instead of the angle of the stick. The point,  $\alpha$ , and the distance to the vertical axis,  $x_\alpha$ , are seen on Figure 7.12.

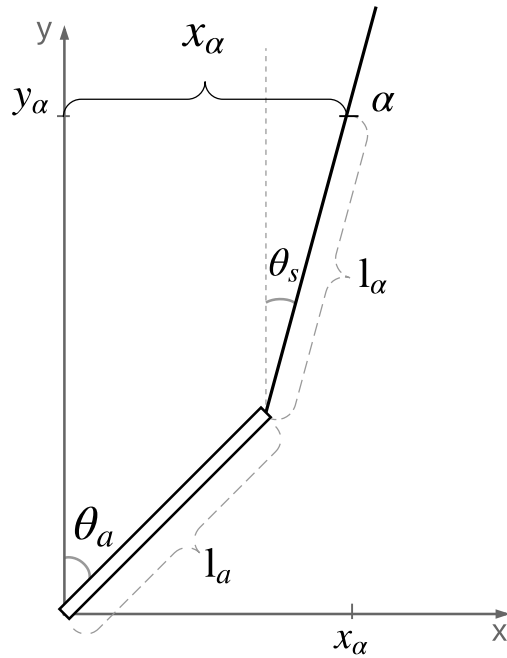


**Figure 7.12:** Diagram of the distance that will be controlled instead of the angle of the stick.

The distance to the point can be described by Equation (7.7).

$$x_\alpha(t) = l_a \sin(\theta_a(t)) + l_\alpha \sin(\theta_s(t)) \quad (7.7)$$

This is not a linear equation and needs to be linearized in order to Laplace transform it. This is done with a 1st order Taylor approximation around the equilibrium where  $\theta_a = \theta_s = 0$  in Equation (7.8)

$$x_\alpha(t) \approx l_a \sin(0) + l_a \cos(0)\theta_a(t) + l_\alpha \sin(0) + l_\alpha \cos(0)\theta_s(t) \quad (7.8a)$$

$$x_\alpha(t) \approx l_a \theta_a(t) + l_\alpha \theta_s(t) \quad (7.8b)$$

This will then be Laplace transformed in Equation (7.9).

$$X_\alpha(s) = l_a \Theta_a(s) + l_\alpha \Theta_s(s) \quad (7.9)$$

By isolating  $\Theta_s(s)$  in Equation (3.10c) and inserting it into Equation (7.9), the transfer function in (7.10c) is found. The friction part is removed according to Table 3.3.

$$X_\alpha(s) = l_a \Theta_a(s) + l_\alpha \frac{-\frac{3l_a}{2l_s} s^2}{s^2 - \frac{3g}{2l_s}} \Theta_a(s) \quad (7.10a)$$

$$X_\alpha(s) = \frac{l_a \left( s^2 - \frac{3g}{2l_s} \right) + l_\alpha \left( -\frac{3l_a}{2l_s} s^2 \right)}{s^2 - \frac{3g}{2l_s}} \Theta_a(s) \quad (7.10b)$$

$$\frac{X_\alpha(s)}{\Theta_a(s)} = \frac{s^2 \left( l_a - l_\alpha \frac{3l_a}{2l_s} \right) - l_a \frac{3g}{2l_s}}{s^2 - \frac{3g}{2l_s}} \quad (7.10c)$$

The transfer function still ends up with 2 zeros but it is possible to remove them by selecting the point  $\alpha$  so  $l_\alpha = \frac{2l_s}{3}$ . Inserting this into Equation (7.10c) the transfer function becomes Equation (7.11).

$$\frac{X_\alpha(s)}{\Theta_a(s)} = \frac{-l_a \frac{3g}{2l_s}}{s^2 - \frac{3g}{2l_s}} \quad (7.11)$$

The zeros in 0 has been removed but the distance,  $x_\alpha$ , now needs to be measured for the feedback. This can be done by measuring the angles, which was also necessary before, but now use Equation (7.7) to calculate the distance instead of using the angle directly. The controller for the transfer function in Equation (7.11) can now be designed.

### 7.2.2 Controlling the Distance from the Stick to Vertical

The new block diagram for the controllers can be seen on Figure 7.13.

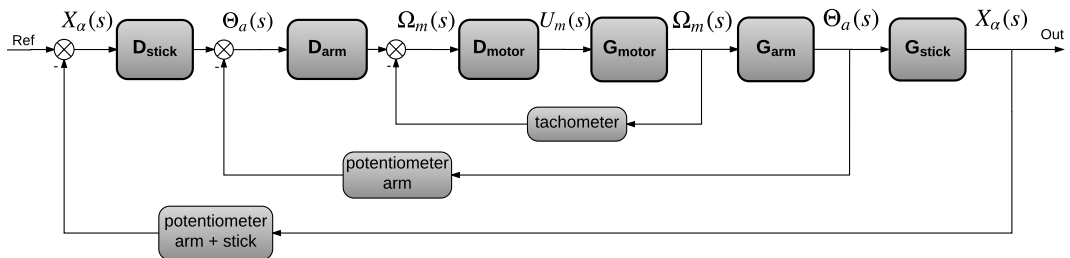


**Figure 7.13:** Block diagram of the inverted pendulum system with inner and outer loop controllers.

With the redefined transfer function the outer loop will control the transfer function in Equation (7.11). From the root locus in Figure 7.14 it can be seen that a zero

needs to be added on the real axis in the left half plane in order to move the pole in the right half plane to the stable region.

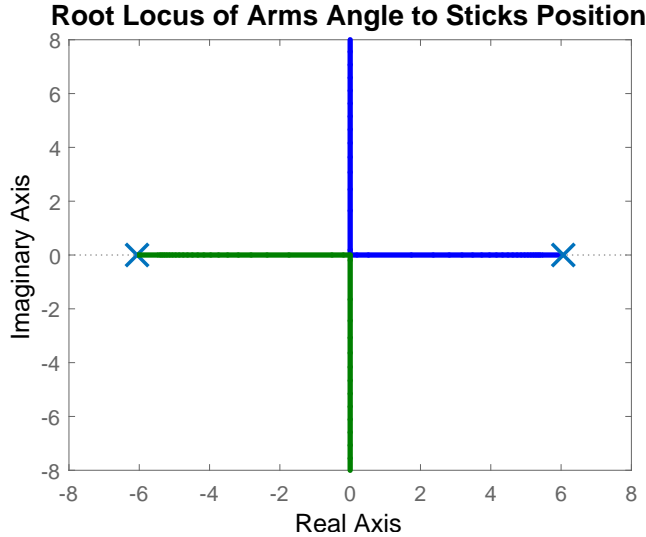


**Figure 7.14:** Root locus of the transfer function from the angle of the arm to the position of a point on the stick.

If the zero is positioned between the two poles, the rightmost will move towards the zero while the leftmost moves towards infinity; both along the real axis. Positioning the zero close to the origin does not allow for the pole to move far into the left half plane. If it is put far to the left of the stable pole the poles will move off the real axis and to the left of the zero with higher gain. This can move them far into the left half plane before they return to the real axis which could cause issues for making the inner loop faster than the outer loop. This is because the further away the poles are from origin, the higher the natural frequency which means a low settling time. If the poles are off the real axis it will introduce overshoot which needs to be under 10% per Section 6.0.1.

Placing the zero close to the leftmost pole would allow for the unstable pole to move further into the left half plane without an overly fast response or any overshoot.

The zero could theoretically be placed on the pole to cancel it and allow the pole to move further into the left half plane along the real axis. This would be ideal but the true location of the pole of the real system is difficult to find as small variations in measurements of the system could move the pole slightly.

The zero will initially be placed on the pole as it does not change the system drastically whether it is slightly off to either side. The pole is then placed at  $-\sqrt{\frac{3g}{2l_s}}$ . This can be seen in Figure 7.15.

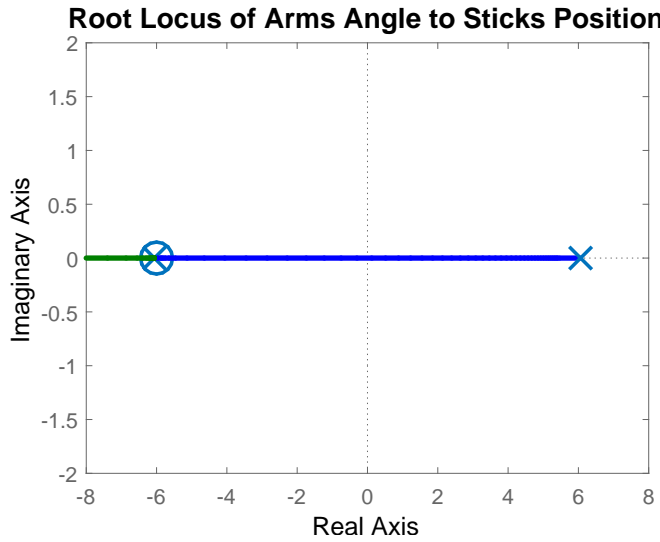


**Figure 7.15:** Root locus of the outer loop system with a zero cancelling the left pole.

The unstable pole can now enter the stable region by selecting a gain large enough. Simply adding a zero to the system will however amplify high frequencies. This can be avoided by adding a pole further into the left half plane. This effectively makes the controller a lead controller. The position of the pole and the gain will determine the settling time and overshoot of the system. The settling time for the outer loop controller should be more than 10 times slower so the assumption, that the inner loop controller is much faster than the outer loop controller, holds true. As the gain increases the two poles move closer to each other before meeting and moving into the imaginary plane. The gain will be selected to be as high as necessary for the poles to meet. The pole can then be selected such that the place where the poles meet will give a settling time 10 times slower than the inner loop.

As the settling time of the inner loop is 0.16 seconds, the natural frequency of the outer loop can be approximated by Equation (7.12).

$$T_{s_{\text{outer}}}(2\%) = -\frac{\ln(0.02)}{\zeta \cdot \omega_n} \quad (7.12a)$$

$$\omega_n = -\frac{\ln(0.02)}{\zeta \cdot T_{s_{\text{inner}}} \cdot 10} \quad (7.12b)$$

$$\omega_n = -\frac{\ln(0.02)}{1 \cdot 0.16 \cdot 10} \quad (7.12c)$$

$$\omega_n = 2.45 \quad (7.12d)$$

This approximation only holds true for 2nd order systems without zeros which is only the case if the zero placed exactly on the pole removes both. This is not the

case however it is still a good place to start. To achieve a natural frequency of 2.45, the lead controller pole needs to be placed so the halfway point between it and the unstable pole is -2.45. The pole location is then found by Equation (7.13).

$$-2.45 = \frac{p_{\text{unstable}} + p_{\text{lead}}}{2} \quad (7.13\text{a})$$

$$p_{\text{lead}} = -2.45 \cdot 2 - \sqrt{\frac{3g}{2l_s}} \quad (7.13\text{b})$$

$$p_{\text{lead}} = -9.19 \quad (7.13\text{c})$$

This can be seen on Figure 7.16.

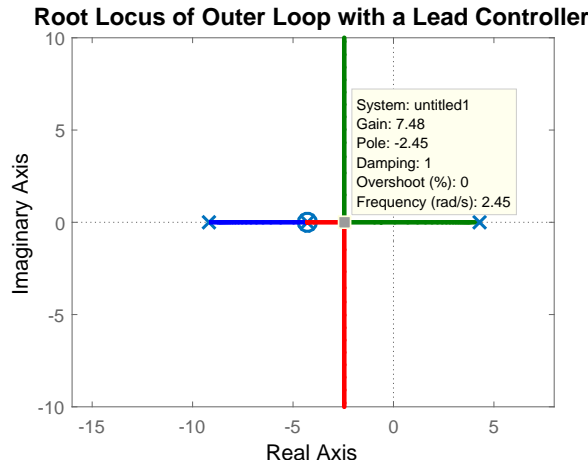


**Figure 7.16:** Root locus of the outer loop with the lead controller.

To make the two poles meet, a gain of 7.48 is needed. This gives a lead controller of Equation (7.14).

$$D_x = 7.48 \frac{s + \sqrt{\frac{3g}{2l_s}}}{s + 9.19} \quad (7.14)$$

The settling time is determined by looking at the impulse response on Figure 7.17.

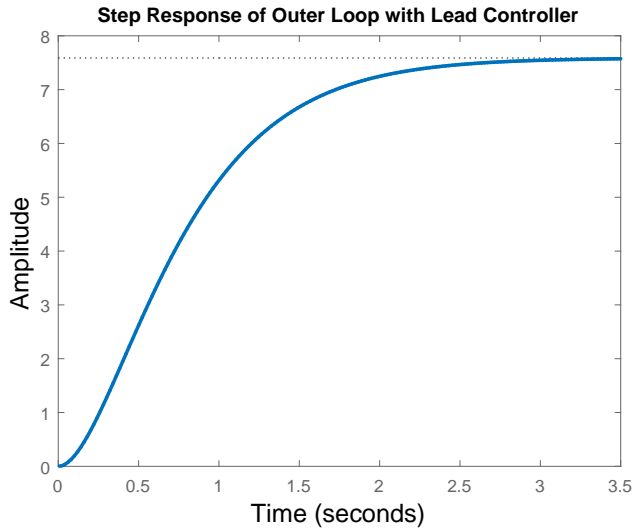


**Figure 7.17:** Step response showing the settling time of the outer loop with a lead controller.

The settling time is slower than the 1.6 seconds that was expected and this is because the zero placed on the pole still has an influence on the system. A bit of overshoot can also be added in this system to get a faster rise time but a similar settling time. This is acceptable as the specifications are only for overshoot of the angle of the stick. It is uncertain how an overshoot when controlling the distance to a point on the stick will affect the angle of the stick. A maximum overshoot for the distance is therefore arbitrarily chosen to be the same as the overshoot for the angle. To get a settling time of 1.6 seconds a new gain needs to be found to give a faster settling time but no more than 10% overshoot. If it is not possible without more than 10% overshoot the controller pole has to be moved further to the left.

The lead controller then becomes Equation (7.15b).

$$D_x = 8.8 \frac{s + \sqrt{\frac{3g}{2l_s}}}{s + 2\frac{\ln(0.02)}{1.6} + \sqrt{\frac{3g}{2l_s}}} \quad (7.15a)$$

$$D_x = 8.8 \frac{s + 4.29}{s + 9.19} \quad (7.15b)$$

This controller gives a fast rise time, a settling time of 1.61 seconds and overshoot of less than 10%. This can be seen on the step response on Figure 7.18.

The steady state error is not an issue as the reference is never changed and all disturbances will be impulses. The impulse response gives no overshoot as seen on Figure 7.19. The impulse is applied on the output as it corresponds to a push on the stick.

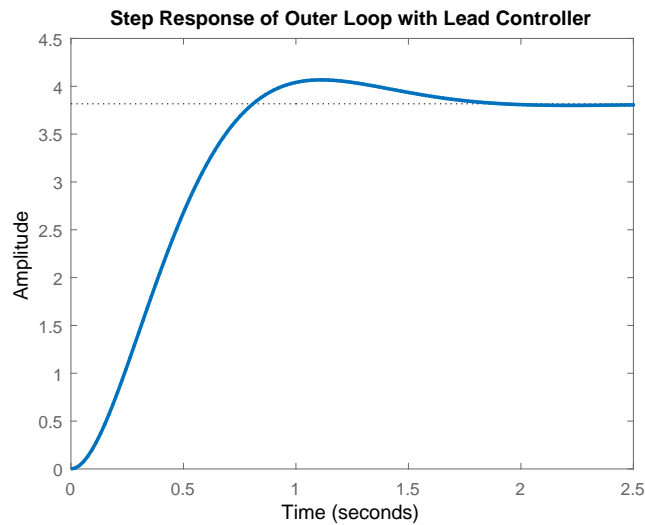


**Figure 7.18:** Step response of the outer loop with the lead controller that gives less than 10% of overshoot.

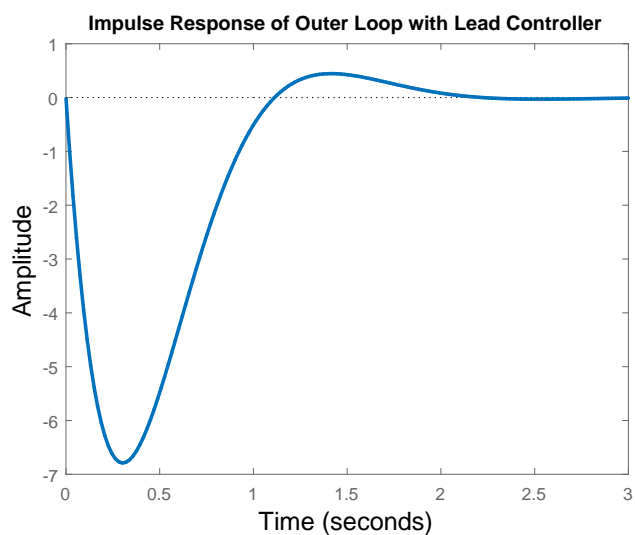


**Figure 7.19:** Impulse response of the outer loop controller with the impulse applied on the output.

### 7.3 Verifying the Total Controller

The final controller consists of the motor loop controller, the arm loop controller and the outer loop controller and are seen in Equation (7.16).

$$D_{\text{motor}} = 1.35 \quad (7.16a)$$

$$D_{\text{arm}} = 900 \quad (7.16b)$$

$$D_x = 8.8 \frac{s + 4.29}{s + 9.19} \quad (7.16c)$$

These are implemented as shown on Figure 7.13 and the entire system has the pole-zero plot on Figure 7.20 which shows it should be stable as all poles are in the left half plane.

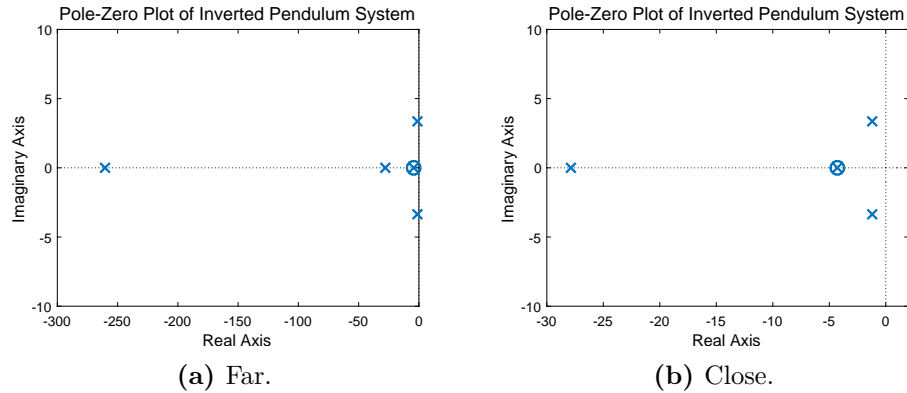


**Figure 7.20:** Pole-zero plot of the final inverted pendulum system.

The impulse response for the inverted pendulum with the final controller is seen on Figure 7.21.

The controller has a settling time of 3.15 seconds and shows it can balance a point on the stick sufficiently. The final block diagram can be seen on Figure 7.22.

The controller is deemed satisfactory and will be implemented.

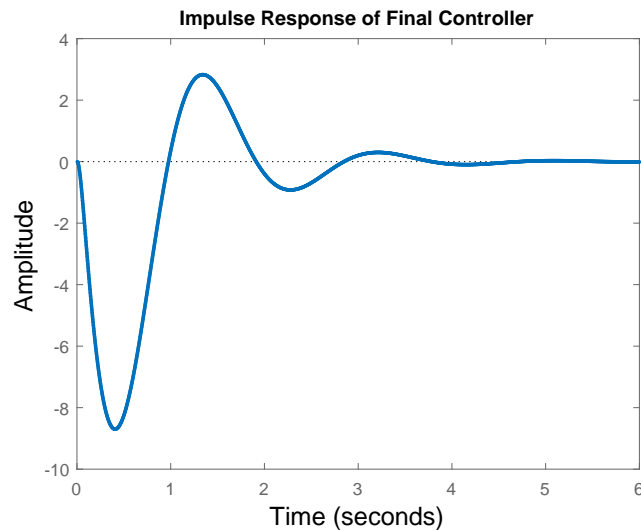


**Figure 7.21:** Impulse response of the final controller with the impulse applied on the output.

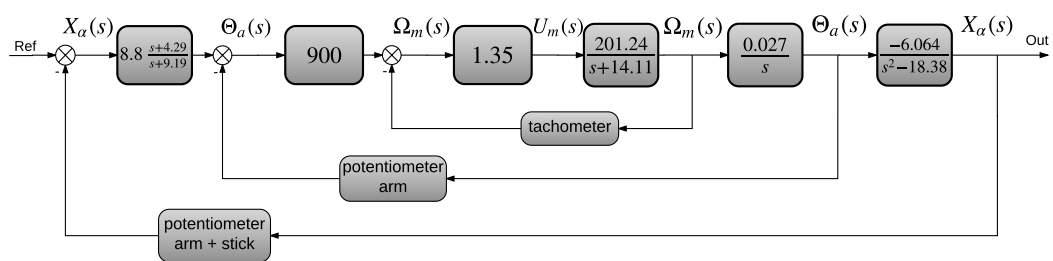


**Figure 7.22:** Block diagram of the final system with all controllers.



# Chapter 8

## Design of the Rocket and Gimbal Controller

The following chapter describes the design of the rocket and its control system. The main objective is not to design the rocket, but to implement a control system that can stabilize it during launch and flight.

### 8.1 Rocket Design

For the purpose of studying the problem of the rocket control, a model rocket was designed and built. Since mechanical design is out of this work's scope, the engineering of this rocket will not be explained, but the design can be seen on Figure 8.1. This design consists of three sections, that will be called stages.

#### Propulsion stage

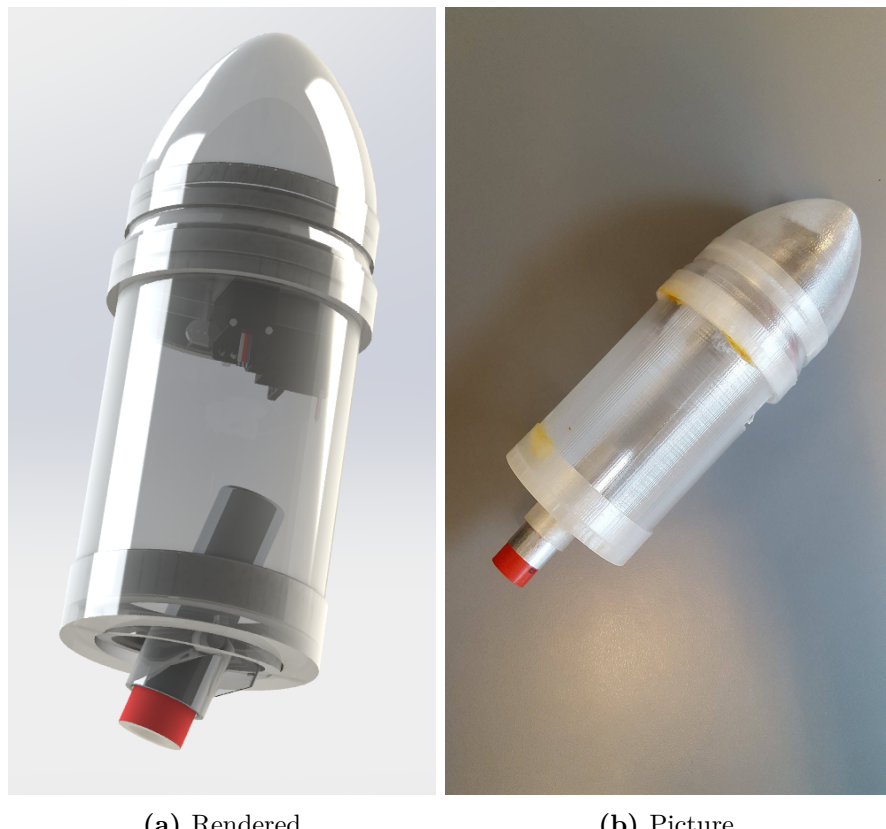
- A thruster / Solid Rocket Booster (SRB).
- A gimbal with two degrees of freedom.

#### Interstage

- An empty fairing separating the propulsion stage from the electronics.

#### Control stage

- A frame to contain the electronics.
- A power supply, logic board, battery and microcontroller.
- A plastic separator with anti-vibration bearings.
- An attitude sensor.
- A nose fairing.
- Two servomotors for actuating the gimbal



(a) Rendered

(b) Picture

**Figure 8.1:** Picture and render of the rocket design.

### 8.1.1 Choice of Thrusters for the Rocket

A thruster is a central component in all types of rocket. In the project the thruster will be chosen based on availability and lift force. The maximum weight of the rocket can not exceed 300 grams and the thruster should be able to lift this. The average thrust of the thruster should be have at least a average thrust of 3 Newton. The choice is limited to the thrusters which can be acquired within the European regulations. Through superficial research it is found that Klima 18 mm rocket motors is legal in all of Europe, and will be chosen for the thruster. The chosen thruster is the version D3-P with the specifications in Table 8.1.

**Table 8.1:** DP-3 thruster specifications.

Parameter	Value	Unit
Total impulse	17,4	[N]
Average thrust	$\approx 3$	[N]
Maximum thrust	$\approx 9$	[N]
Burn duration	$\approx 5,5$	[s]
Weight	0,105	[kg]
Length	0,07	[m]

### 8.1.2 Physical Parameters of the Rocket

The important factors for controlling the rocket is the physical parameters. These will effect how the rocket would transfer a input to its output. The force of the thruster will not be controlled and is considered a constant.

**Table 8.2:** Parameters of the rocket.

Piece	Parameter	Value	Unit
Rocket <sub>overall</sub>	Height	0.297	[m]
Rocket <sub>overall</sub>	Weight	0.28	[kg]
Interstage	Diameter	0.067	[m]
Thrust vectoring system	Max. angle	$\frac{\pi}{9}$	[rad]
Thrust vectoring system	Response time	3.907	[rad/s]

### 8.1.3 Choice of Sensors for the Rocket

This section describes the sensors chosen for the implementation in the rocket. The microcontroller unit, MCU, used in the system will be an Arduino Nano. The Nano is chosen based on its low weight (7 grams) and small size (18 x 45 mm) which will be an advantage when fitting it in the rocket.

As described in Section 4.1, the rocket can be a system with instability problems. In the inverted pendulum these instabilities are detected through sampling sensors and corrected through a DC motor control system. The same parameters are considered when controlling the rocket. A sensor is needed to detect the orientation and position of the rocket, and a control system is needed to counteract changes from the initial trajectory.

Choosing sensors for the rocket will be weighted based on following parameters:

- Compatibility.
- Power consumption.
- Availability.
- Physical dimensions and weight.

A sensor is needed for measuring:

- Orientation.
- Acceleration.

Determining the altitude, orientation and acceleration of the rocket can be done with different types of sensor. Two types of sensors can be considered when involving rockets; reference sensors and inertial sensors. Reference sensors have an external reference to measure from, whereas inertial sensors measures changes in its physical state from its inertial state. The sensors that will be used are:

- Gyroscope
- Accelerometer

An accelerometer measures acceleration in one to three axis(x,y,z). The reference for measuring is the gravitational force. A single axis accelerometer can measure the acceleration in the direction it is oriented, and can for example be used to determine the velocity of an upwards flying rocket. This can also be used to determine the distance travelled based on knowing acceleration and time. In the case of flying a rocket, a three-axis accelerometer will be implemented, as the rocket can move both laterally and vertically.

A gyroscope is, on the other hand, measuring the angular velocity changes in three dimensions. The difference between the accelerometer and gyroscope is that the gyroscope is capable of measuring the rate of rotation around an axis. It does not rely on a fixed reference and is commonly used in applications like drones and other flying objects. In the rocket it can be used to determine the orientation and rotation of the rocket based on measuring the rate of changes in any direction.

Combining these gives an Inertial Measurement Unit (IMU), which is commonly used in model planes and quad-copters. The application of this is to obtain the objects position through measuring velocity, orientation, rotation with the gyroscope and accelerometer.

Some performance factors must be considered when choosing an IMU. For example the g-force range of the IMU is important. If the maximum ratings is lower than the acceleration of the rocket, then the sensor would not be able to give sufficient data at maximum acceleration. The sensitivity of the accelerometer is also important. The rocket is a system with a high amplitude g-force when launching, and therefore a accelerometer with low sensitivity is preferable.

### Inertial Measurement Unit - GY-87

GY-87[4] is an IMU made available for use. It includes an MPU6050, which combines a 3-axis accelerometer and a 3-axis gyroscope, a BMP180 thermometer/barometer, and a HMC5883 3-axis magnetometer. It is chosen based on its combination of components and low power consumption of  $\approx 6.5$  mA in measurement mode. It is designed so it can be implemented with the Arduino Nano through I2C communication. All components on the GY-87 are convenient to implement with the Arduino. With the sensor determined the controller can be designed.

## 8.2 Rocket Controller Design

The goal of the controller is to balance the rocket body in an upright position. The system can be decomposed in a block diagram as shown in Figure 8.2.



**Figure 8.2:** Block diagram of the rocket system.

As seen in the modeling of the rocket and on Equation (8.1a), the system presents two poles in the origin of the pole-zero plot.

$$H = \frac{F_t \cdot L_{Cg} \cdot \frac{1}{M_r \cdot L_{Es}^2}}{s^2} \quad (8.1a)$$

$$H = \frac{3 \cdot 0.10 \cdot \frac{1}{0.180 \cdot 0.03^2}}{s^2} \quad (8.1b)$$

The root locus of the system on Figure 8.3 shows that the poles goes to infinity on the imaginary axis. This means that any oscillations or noise will never be damped solely by adding a gain.

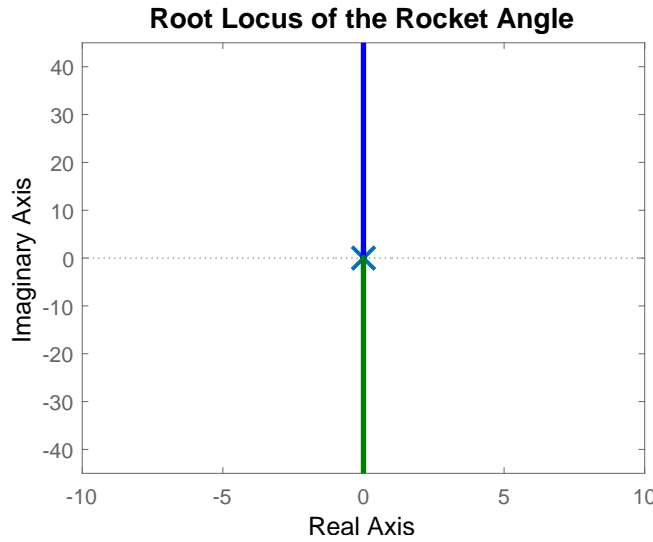


**Figure 8.3:** Root locus of the rocket angle transfer function.

However the real system is also influenced by the servomotors. The transfer function of the servomotors is shown on Equation (8.2b) cf. Appendix F.

$$H_s = \frac{1}{\tau s + 1} \quad (8.2a)$$

$$H_s = \frac{1}{0.04s + 1} \quad (8.2b)$$

Where:

$\tau$  is the time constant of the servomotors [s]

This function then adds a pole to the initial transfer function, resulting in an unstable system. This is shown on Figure 8.4.

This system could be controlled similarly to the inverted pendulum by doing cascade control. By having an inner loop that controls the servomotors as fast as possible the pole added can be assumed to have no effect. This would make the rocket control design similar to the inverted pendulum by having an inner loop with a simple gain and an outer loop where a compensator in form of a zero needs to be added.

This is not an option as the rocket built does not have any sensors to measure the servomotors. If the rocket was built differently this would be the preferred way to control it.

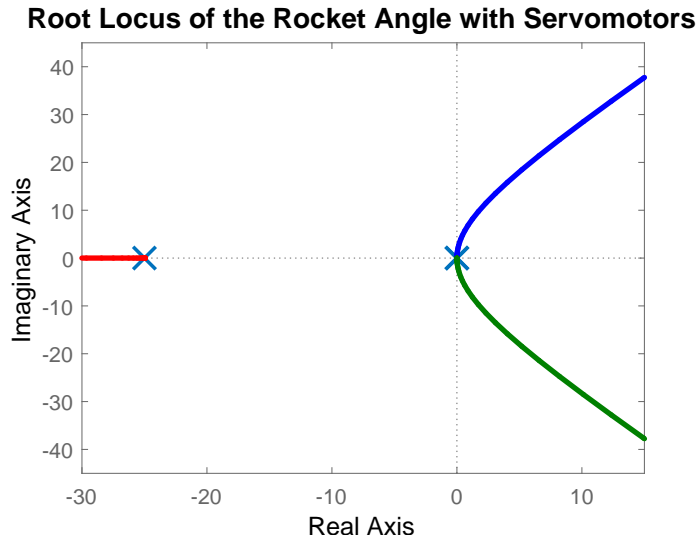


**Figure 8.4:** Root locus of the system with the pole from the servomotors.

### 8.2.1 Controlling the Rocket Angle without Cascade Control

To move the poles to the left half plane, a controller,  $D_{\text{rocket}}$ , adding a zero and a pole on the left side, is implemented to the rocket transfer function. If the zero is placed to close to the servo pole the loci will not be attracted to the real axis. Common practice recommends placing the pole at a location 20-40 times larger than the zero. The zero of the controller is chosen experimentally to be near origin in order to attract the poles. The pole of the controller is chosen to be 40 times larger than the zero. The controller  $D_{\text{rocket}}$  is shown in Equation (8.3) and its root locus can be seen on Figure 8.5.

$$D_{\text{rocket}} = \frac{s + 1.7}{s + 68} \quad (8.3)$$

The rocket requires a fast settling time and rise time in order to act as soon as possible and control the rocket's stability. Lead compensators enable the modulation of the rise time, but impact the overshoot.

According to the specification the settling time should be faster than 1.67 second.

The gain is selected to be 0.202 as this is where the poles hit the real axis. This should not give any overshoot but as seen on Figure 8.6 there's an overshoot of around 20%.

As there is an overshoot despite the poles being on the real axis, the gain will be doubled to get a faster rise and settling time. The final rocket controller then becomes

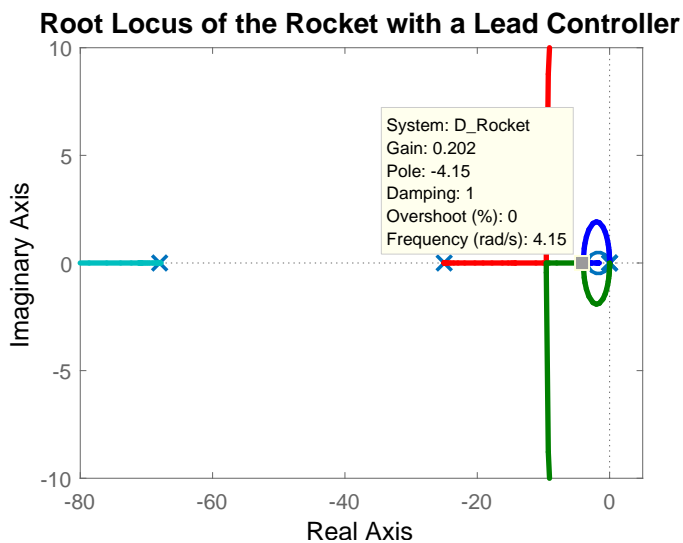


**Figure 8.5:** Root locus of the system with a lead controller,  $D_{\text{rocket}}$ , added.

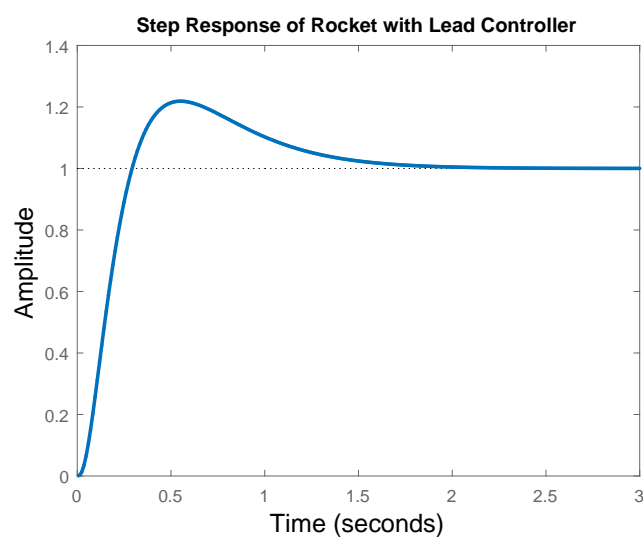


**Figure 8.6:** Step response of the rocket with a lead controller and a gain of 0.202.

Equation (8.4).

$$D_{\text{rocket}} = 0.404 \frac{s + 1.7}{s + 68} \quad (8.4)$$

The step response of this controller can be seen on Figure 8.7.

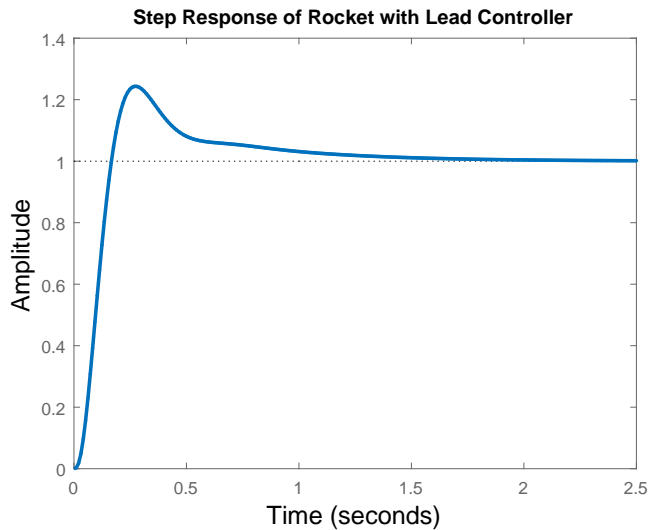


**Figure 8.7:** Step response of the rocket with a lead controller and a gain of 0.404.

The block diagram of the controlled rocket is shown on Figure 8.8.

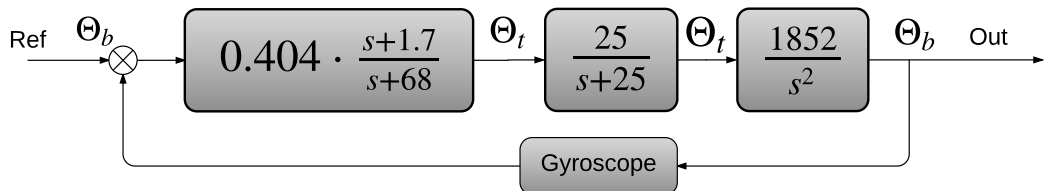


**Figure 8.8:** Block diagram of the rocket with a lead controller.



# Chapter 9

## Inverted Pendulum Implementation

This section describes the hardware and software implementation of the controllers designed Chapter 7. The goal is to determine if the designed controllers will balance the stick in the real world application. The section is separated into three different parts about sensors, hardware controller and software controller. The first part is to implement the feedback for the controllers which in the case is sensors.

### 9.1 Implementing Sensors

The following section describes the implementation of the sensors with an Arduino Uno and the inverted pendulum setup.

#### Potentiometer

The system consist of multiple sensors, as decribed in Section 3.1, where two of these are potentiometers. The potentiometers is tested in Appendix D. The appendix concluded with a first order approximation of both potentiometers. During the implementation it is realized that slight calibrations were needed because the potentiometer had moved in the setup. The approximation for  $\text{Pot}_{\text{arm}}$  is:

$$\theta_a = 63,11 \cdot V_{\text{Pot}_{\text{arm}}} - 117,0 \quad (9.1)$$

Where:

$V_{\text{Pot}_{\text{arm}}}$  is the output voltage of the arms potentiometer [V]  
 $\theta_a$  is the angle of the arm [°]

The approximation for Pot<sub>stick</sub> is:

$$\theta_s = 66,66 \cdot VPot_{stick} - 163,9 \quad (9.2)$$

Where:

$V_{Pot_{stick}}$  is the output voltage of the stick potentiometer. [V]

$\theta_s$  is the angle of the stick, but where zero degrees is when the stick has a zero degree deviation from the arm [°]

An example of implementing this is done through a pseudo-code which converts the analogue value to radians. The linear approximations of the potentiometers are used.

---

```

1 void loop() {
2     // read the input on A0 and A1:
3     int PotArm = analogRead(A0);
4     int PotStick = analogRead(A1);
5
6     double VPotarm = PotArm / 204.8; //Analog2Voltage
7     double ThetaA = 66.66 * VPotarm - 170.46; // Voltage2Degree
8     double ThetaARad = ThetaA * (31.415926 / 1800.0); //Degree2Radians
9     double VPotstick = PotStick / 204.8;
10    double ThetaS = 63.64 * VPotstick - 117.77;
11    double ThetaSRad = ThetaS * (31.415926 / 1800.0);
12 }
```

---

The sampling time of the sensors is an important aspect when ensuring stability of the control system. The sensor sampling can not be too slow because then the control loops will be slow and not update fast enough. Considering that the sensor is a potentiometer which does not have any active components, then the only limit is the Arduino. Arduino specifies that calling an analogRead() takes approximately 100 µs which corresponds to a sampling frequency of 10 kHz. This is considered fast enough for the system and is therefore not a problem.

## Tachometer

The tachometer and its precision has been tested in Appendix C. The test concluded that the internal tachometer's precision is within the limit of what can be implemented. The tachometer outputs a voltage which is close to linear with the number of revolutions per minute.

The test concluded with a transfer function for the tachometer, that gives the relation between the tachometer voltage and motor velocity:

$$\frac{1000 \text{ RPM}}{\frac{3.130 \text{ V}}{60 \text{ s}} \cdot 2 \cdot \pi} \cdot T_{Voltage}[\text{V}] = M_{Velocity} [\text{rad/s}] \quad (9.3)$$

The function can not directly be implemented with the Arduino. The tachometer will generate a negative and a positive voltage corresponding to the direction of the motor. Negative voltage can not be directly input to the Arduino without short circuiting it, and the positive voltage would be too high considering that the motor can go up to 8500 RPM. Interfacing is therefore needed between tachometer and Arduino. This interfacing is done through the ESCON motor controller included in the inverted pendulum setup. The two outputs of the tachometer are put into the motor controller via two analogue inputs. One acts as the positive connection and the other as the negative. How the motor controller is reacting to an input is configured through the ESCON studio included. In this case it is set with the conversion ratio from voltage to RPM on 3.130 V/1000 RPM, which was determined by external calibration from another tachometer and implemented in the software. The motor controller is set with a output that converts this RPM down between 1 and 4 V to the Arduino. Where 1 V is corresponding to -3000 RPM and 4 V corresponding to +3000 RPM. This gives the possibility to convert these values back to RPM in Arduino. How the motor controller converts the voltages is considered a black box. The wiring for the tachometer can be seen on Figure 9.1.

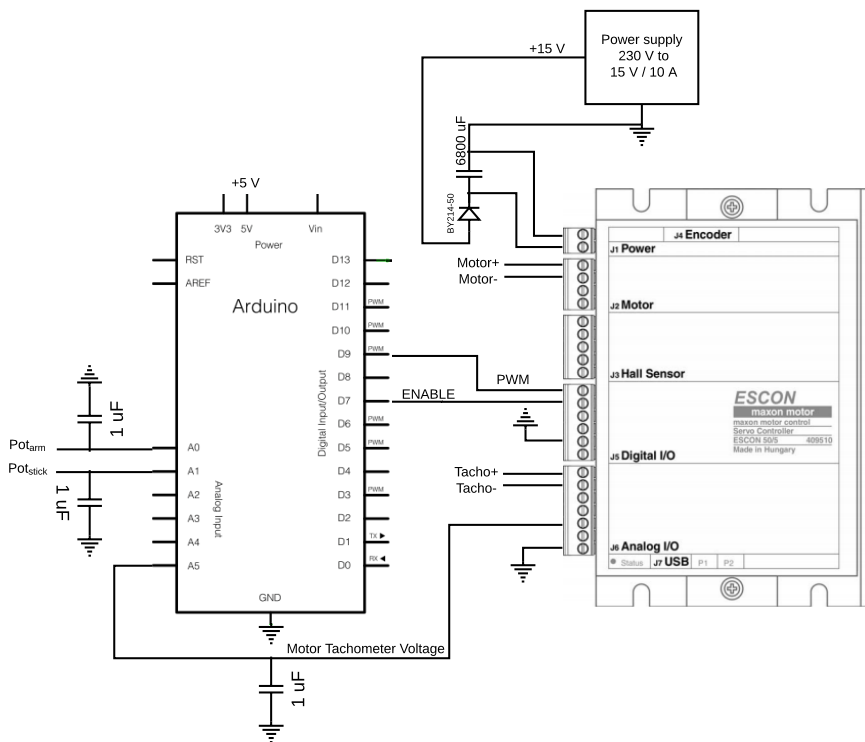


**Figure 9.1:** Circuit diagram of the wiring for the control setup.

## 9.2 Implementing ESCON Motor Controller

The following sections describes the implementation of the hardware motor controller with the Arduino. The motor controller in the setup is a Maxon Escon 50/5.

The Maxon ESCON 50/5 is a PWM servo controller, that can be used to control DC and EC motors. The application is to amplify signals and control systems through different control operations. It can also be used with a PWM input signal that can be outputted as an amplified and higher frequency PWM signal to a motor. The servo controller can be used in three different modes which can be configured through the included Maxon ESCON studio. It can be configured in two modes for speed control with open and closed loops with feedback from sensors through the board, and one mode for motor current control through inputs from other modules such as an Arduino. In the setup the Escon controller is set to current control.

It is set up through the ESCON studio with current control, and with an external controlled PWM signal. It then gives the possibility to input a PWM signal from the Arduino, which will be amplified so that 90% duty cycle equals 11 A and 10% equals -11 A. This means that 50% will give 0 A.

The Arduino uses a 8-bit timer for PWM as standard. To get a better resolution the TimerOne library is implemented. TimerOne is a 16-bit hardware timer which can be downscaled to give the possibility to have a 10-bit resolution on the PWM signal. A better resolution gives a higher number of duty cycle values which makes the control more precise than with 8-bit.

The configuration file for the ESCON studio is included in the attachment files under "/Attachment/Implementation/Motor Controller/Motor Controller Configuration File". It can be imported into the ESCON studio and loaded onto any 50/5 controller.

The main specifications of the ESCON is listed in Table 9.1.

**Table 9.1:** Maxon Escon 50/5 specifications[7].

Parameter	Value	Unit
Supply voltage $V_{cc}$	10-50 V	[V]
Output voltage (max.)	$0,98 \cdot V_{cc}$	[kg]
Nominal output current	5	[A]
Maximum output current (<20 s)	15	[A]
Current control PWM frequency	53,6	[kHz]

The wiring for the setup can also be seen on Figure 9.1.

The control PWM signal from the Arduino is set with a frequency of 5 kHz because that it is the maximum input frequency the motor controller will accept. It is set to 5 kHz so that the PWM avoids interference with the sampling frequency for the system. The input PWM signal is then amplified and made faster. The output PWM frequency of the motor controller is 53.6 kHz with a duty cycle from 10 - 90% which can not be changed in the ESCON studio. The switching frequency of the ESCON is considered close to optimal as the PWM frequencies are within the limit of the datasheet specifications. The main concern of a switching frequency of 53.6 kHz on the motor is heat dissipation. Therefore the minimum PWM frequency for the motor is calculated to see if the motor controllers PWM frequency fits the motor.

### 9.2.1 Calculating Minimum PWM Frequency

The only PWM frequency considered is the minimum switching frequency for the motor. This is done by considering the motor resistance and inductance versus the maximum amount of current ripple wanted on the motor. The values for the resistance and the inductance of the motor are calculated in Appendix A.4. The formula is seen on Equation (9.4).

$$f_{\text{switch}} \geq \frac{-1}{2 \cdot \ln(1 - \frac{p}{100})} \cdot \frac{R_m}{L_m} \quad (9.4)$$

Where:

$$\begin{aligned} p &\text{ is the maximum \% current ripple in the motor.} & [1] \\ R_m/L_m &\text{ is the inverse electrical time constant of the motor.} & [\text{Hz}] \end{aligned}$$

Replacing with the numerical values of the resistance and the inductance and choosing a max ripple percentage of 5%, the minimum switching frequency determined to be:

$$f_{\text{switch}} \geq \frac{-1}{2 \cdot \ln(1 - \frac{5}{100})} \cdot \frac{0.82 \Omega}{156 \cdot 10^{-6} \cdot \text{H}} \approx 51.2 \text{ kHz} \quad (9.5)$$

The maximum ripple in the motor is determined by making the ripple the unknown factor  $P_{\text{ripple}}$  and setting the PWM frequency to the implemented 53.6 kHz.

$$53.6 \text{ kHz} = \frac{-1}{2 \cdot \ln(1 - \frac{P_{\text{ripple}}}{100})} \cdot \frac{0.82 \Omega}{156 \cdot 10^{-6} \cdot \text{H}} = P_{\text{ripple}} = 4.785\% \quad (9.6)$$

This gives that the maximum current ripple is 4.785% if considering a PWM frequency on 53.6 kHz. A general rule is that the ripple should be less than 10% of the current, so considering that it is less than 5% is acceptable.

### 9.2.2 Implementing Controllers on Arduino

As the Arduino is a microprocessor, the continuous controller found in Chapter 7 needs to be transformed into a discrete controller. This also means a sample time needs to be determined. The sample time needs to be faster than the settling time of the fastest subsystem i.e. the motor loop. The motor loop has a settling time of 0.0137 seconds. The sample time is selected to be 0.002 seconds as it is faster than the motor loop. This gives a sampling frequency of Equation (9.7).

$$F_s = 500 \text{ Hz} \quad (9.7)$$

With the sampling time determined the continuous controller needs to be transformed to a discrete controller. For the two P-controllers it is as simple as multiplying the sampled input with the gain to get the discrete output. For the outer loop controller it is not as simple and is done by using the Z-transform. There are a couple of different options for performing the Z-transform each with their own nuances, but the differences won't be discussed and the bilinear transform will be used. For the bilinear transform, the  $s$  in Equation (7.15b) will be substituted with Equation (9.8).

$$s = 2F_s \frac{z - 1}{z + 1} \quad (9.8)$$

Equation (7.15b) then becomes Equation (9.9).

$$D_x = 8.8 \frac{2F_s \frac{z-1}{z+1} + 4.29}{2F_s \frac{z-1}{z+1} + 9.19} \quad (9.9a)$$

$$D_x = 8.8 \frac{2F_s(z-1) + 4.29(z+1)}{2F_s(z-1) + 9.19(z+1)} \quad (9.9b)$$

$$D_x = 8.8 \frac{(2F_s + 4.29)z + 4.29 - 2F_S}{(2F_s + 9.19)z + 9.19 - 2F_s} \quad (9.9c)$$

$$D_x = \frac{Y(z)}{X(z)} = 8.8 \frac{2F_s + 4.29 + (4.29 - 2F_S)z^{-1}}{2F_s + 9.19 + (9.19 - 2F_s)z^{-1}} \quad (9.9d)$$

$$Y(z) (2F_s + 9.19 + (9.19 - 2F_s)z^{-1}) = 8.8X(z) (2F_s + 4.29 + (4.29 - 2F_S)z^{-1}) \quad (9.9e)$$

The Z-transformed controller can then be made discrete by substituting  $aY(z)z^m$  with  $ay[k+m]$  and similarly for  $X(z)$ . This gives the discrete controller ready to be implemented in the Arduino in Equation (9.10b).

$$(2F_s + 9.19)y[k] + (9.19 - 2F_s)y[k - 1] = 8.8(2F_s + 4.29)x[k] + 8.8(4.29 - 2F_S)x[k - 1] \quad (9.10a)$$

$$y[k] = 8.8 \frac{2F_s + 4.29}{2F_s + 9.19} x[k] + 8.8 \frac{4.29 - 2F_S}{2F_s + 9.19} x[k - 1] - \frac{9.19 - 2F_s}{2F_s + 9.19} y[k - 1] \quad (9.10b)$$

### 9.2.3 Controller Software

This sections describes the software implemented on the Arduino. The software can be found in the attached materials under "Attachment/Implementation/Arduino Software/InvertedPendulumControlSoftware". The structure and processes is represented with a flowchart on Figure 9.2.

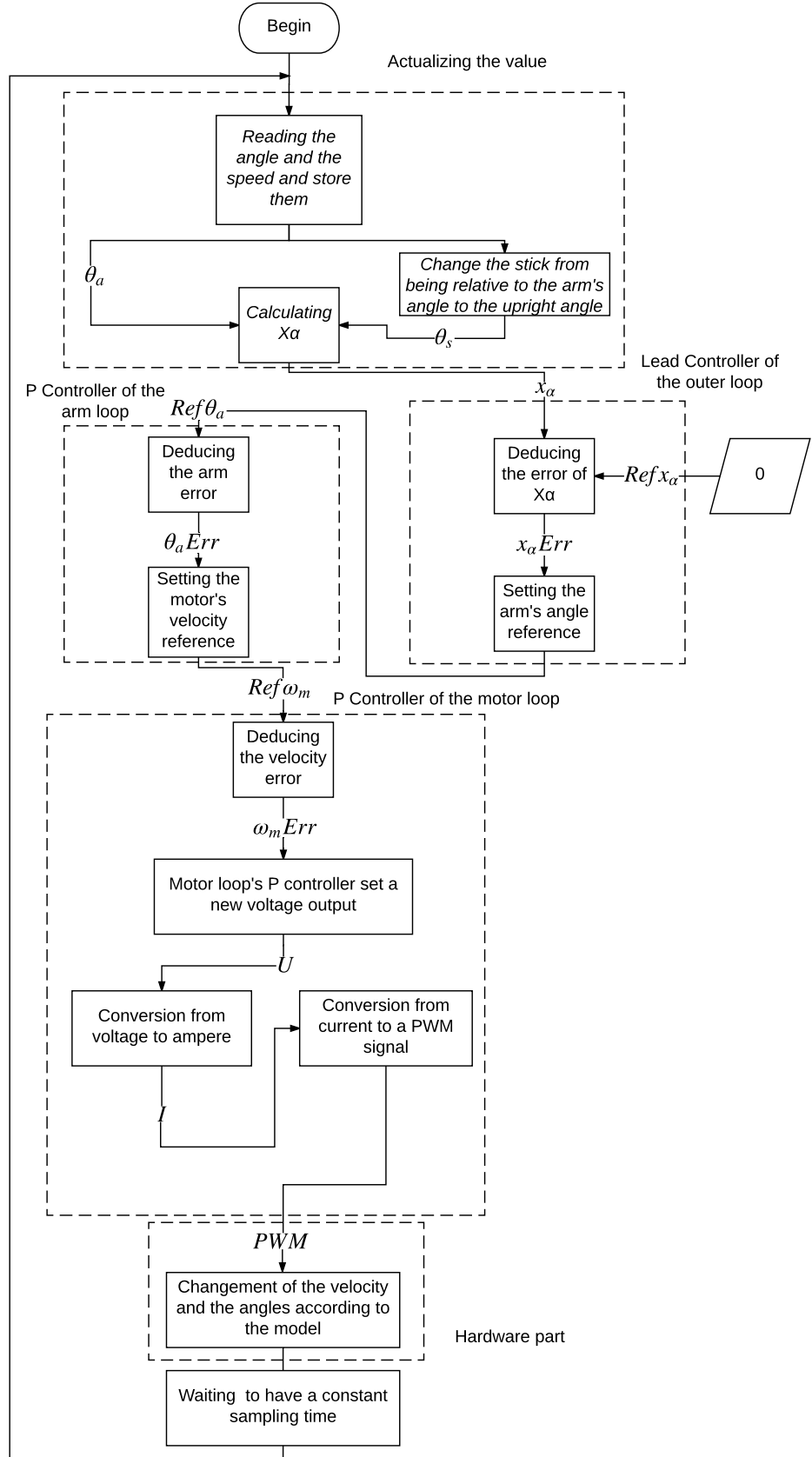


**Figure 9.2:** Flowchart for the implemented software on Arduino.

## 9.3 Implementation Evaluation

This following sections describes the different problems that occurred with the hardware and software through out the implementation. They will be explained to show the progress through out the implementation.

### 9.3.1 Filtering Sensors

During implementation of the arm loop, it was found that a shaking occurred through the motor, gear and out to the arm. From testing higher gains it was found that the shaking was amplified and became more unstable with the higher gains. Testing of the hardware and software was done to determine the source of the shaking. To start with, the sensors were checked for noise and floating. This was done to remove incorrect readings and unstable sensors. The sensors were read through an oscilloscope and it was found that the ESCON motor controllers PWM frequency was represented in the sensor signal. This can occur from incorrect ground or wires not correctly isolated. This problem was solved by adding a capacitor to the sensors as seen on Figure 9.1. The capacitor is connected from signal wires to ground to make a low pass filter.  $1 \mu\text{F}$  is chosen, one for each signal wire and considering that it is two  $10 \text{ k}\Omega$  potentiometers it will give a varying cut off frequency. The cut-off frequency is calculated to be:

$$\frac{1}{2 \cdot \pi \cdot 10000 \Omega \cdot 1 \cdot 10^{-6} \text{ F}} = 15.92 \text{ Hz} \quad (9.11a)$$

$$\frac{1}{2 \cdot \pi \cdot 2.97 \Omega \cdot 1 \cdot 10^{-6} \text{ F}} = 53.6 \text{ kHz} \quad (9.11b)$$

The resistance changes needs to go under  $\approx 2.97 \Omega$  before the cut-off frequency exceeds the frequency of the noise, and any resistance change higher will dampen with more than -3 dB. It is noticeable that the resistance values of the potentiometers are in between both limits of resistances and the noise is therefore damped. The conclusion of adding these filters, is that the high frequency noise that made the arm shake is reduced. There was still a small-amplitude shaking around the setpoint when the arm was at a position and kept there. This could due to non-optimal range and bad optimization of bits in the software. The software is made with scaling from analogue values to radians, which means that reading the arm potentiometer and having an analogue value from 235 to 527 and converting it to -0,785 to 0,785 radians means that that first two bits are not used. This gives that the 10-bit resolution of the PWM is not used optimally when two are static, but it is still better than having 8-bit with two static.

This can be optimized by changing the range of the potentiometers so the maximum angles the arm reaches correspond to the full 10-bit range. It could also be solved by

changing the model and with the conversion throughout the software. The analogue value would thus not be converted which would give a better resolution for the PWM output. They can also be combined for the best resolution. It is chosen to only implement the resolution optimization if and only if the acceptance test show that the system does not fulfil the set requirements.

### 9.3.2 PWM Frequency Problems

The stick control loop was implemented with an interrupt attached to the TimerOne to get the desired sampling rate. The simulations gave gains and results that could be implemented on the system. When implemented it was found that the arm did not control correctly when the stick moved. Repetitive test gave the conclusions that the speed of the arm was too slow. Higher gains were implemented but did not give the wanted result and the gains were set back to the simulated. An oscilloscope test was made on the Arduino PWM frequency by measuring the input frequency on the motor controller. The test showed that the frequency was 100 Hz and not 5 kHz as expected.

The software was revised and determined that attaching the interrupt to TimerOne overwrote the PWM switching frequency. The interrupt was removed and changed to a wait so that the sampling time was kept constant. The PWM frequency was then measured to be 5 kHz and the arm then behaved as wanted with the simulated gains.

### 9.3.3 I2T Limitation

Another problem observed where a run time limit on the control system. The system would slow down after approximately a minute but it was easily observed through the ESCON studio that an I2T limit was reached on the motor controller. An I2T limit is an algorithm that is described by the nominal current, the motor peak current in RMS, and the motor peak current in seconds. It is used to secure the motor and driver from damage and over heating. The parameters for the algorithm were set through the ESCON studio, with a nominal current on 5 A, a peak current on 11 A, and a thermal time constant on 200 seconds. When the limit is reached, the motor current only goes to 5 A so the motor controller is shut off to cool down before it can then be used again.

### 9.3.4 Controller tuning

An initial test showed that the controller designed could balance the stick but it was balanced when the arm was closer to 30° than 0°. This is likely caused by a steady state error somewhere in the system. As the motor loop controller had a steady state

error the gain was increased to reduce the error. This made the stick balance closer to the upright position. The new motor loop controller becomes Equation (9.12).

$$D_{\text{motor}} = 10 \quad (9.12)$$



# Chapter 10

## Rocket Implementation

### 10.1 Implementing Inertial Measurement Unit

The system consists of a thrust vectoring rocket with an Inertial measurement Unit (IMU) GY-87. Multiple physical and software constraints have to be taken into account when implementing the designed controller. For the software part, the controller is implemented in same manor as the inverted pendulum, with the variables values changed to fit the rocket controller.

### 10.2 Implementing Sensors and Servomotors

The response time of the sensors are an important feature when ensuring the stability of the rocket. It can not be too slow, otherwise the system will react to late to angle variation. The servomotors system dynamics are described in Appendix F. The implementation was done by implementing the Servo library in Arduino, and the position is set by a writing a position between -180 and 180 degrees trough the Servo.Write(); function.

I<sup>2</sup>C or Inter-Integrated Circuit, which is the protocol used to link the Arduino and the IMU. The I<sup>2</sup>C as working on the hardware wires for operation.

- SDA (Serial Data Line): Bidirectional data line
- SCL (Serial Clock Line): Bidirectional clock synchronization line

They are connected to the dedicated I<sup>2</sup>C pins on the Arduino. The gyroscope/angle sensor needs to write 14 bytes into the Arduino register. The code to use the MPU 6050 was done by Brainergizer [3]. Since the gyroscope has an internal clock of 1MHz [5], the sampling time for the angle sensor is  $\frac{14.8}{1 \cdot 10^6} = 1,12 \cdot 10^{-4}$  seconds giving a sampling rate of approximatively 8,9 KHz. The processing time of the 16 MHz

micro-controller is considered insignificant, since there is no time-intensive sensor processing tasks in the code.

The Arduino produces a PWM signal to control the servo angle. The servomotor standard integrated controller interprets the angle command based on the duty cycle. 0% is - 180° and 100% is + 180°. These PWM signals needs to be passed to the PSU board where the servo connector are seen cf. section 10.2.2.

To control the rocket and to fire it safely, 3 different PCB (Printed Circuit Boards) were designed. A logic board, a Power Supply Unit (PSU) and an electric igniter. The logic board and the PSU are stacked on top of each other and the battery is inserted between the two cards to optimize space. All cards schematics are available in the included in folder "/Attachment/Implementation/Rocket/Rocket PCB schematics".

### 10.2.1 Logic Board

The logic board hosts the Arduino Nano micro-controller, the battery connector, the servo output, the IMU and four indicator LEDs.



**Figure 10.1:** PCB stack assembled with the logic board on the top.

The battery voltage is directed towards an analogue input on the Arduino. This is to enable a batteri check for seeing the charge state, and light a LED when the battery

is below a threshold voltage.

The 3 other remaining LED indicators are provided for debugging purposes only. The battery input is then passed by a connector to the PSU below, that provides the 5 V rail to power the Arduino and the IMU.

### 10.2.2 Power supply

The rocket is electrically powered by a single cell 3,7 V, 680 mAh LiPo battery. These batteries are lightweight, rechargeable and available in small form factors that fitted perfectly the rocket's size.

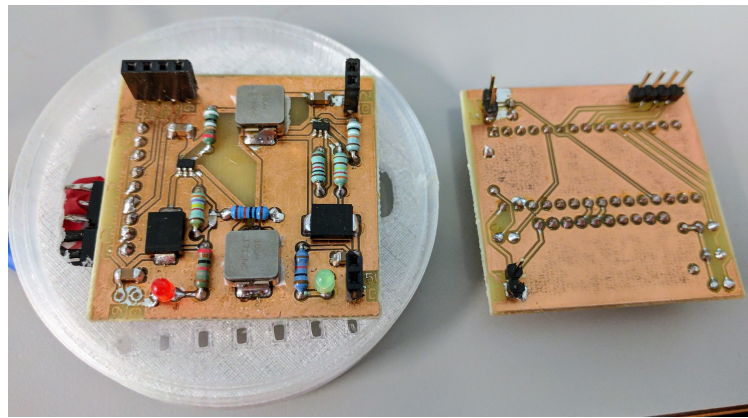


**Figure 10.2:** PCB stack disassembled, with PSU on the left.

The logic components and the actuators must be very well separated since if they are not, a current draw spike on the actuator side could take all available power and shut down the logic components for a brief amount of time. This would cause them to reset, and the rocket to go out of control.

Since the logic and actuator parts of the power supply needs to be separated, two different power supplies were created on the same board (with common ground).

The logic side needs a 5 V rail to function. The components are all powered by their Vin pin, which mean that they had a voltage stabilizer included. The 5 V output was set to 5,2 V to compensate for the losses in the stabilizing circuit.

The actuators, namely the pitch and roll servos is nano servos, which implies a small size and light weight. As most standard servo can operate from 4.8V to 6V, they will be faster and have more torque at higher voltage. The second power supply output was set to 6V to give the maximum torque. The servo test in Appendix F determined these supply conditions, based on testing the speed at different voltages. The servo connectors have 3 pins, a PWM input was connected to the PWM output from the arduino, Vin was the 6V from the PSU, and the last pin is ground.

The PSU 5 V rail was found to work at an input voltage as low as 3,6 V. The LED low battery indicator threshold was set to 3,65 V.

### 10.2.3 Igniter

The igniter plugs that were implemented needed a 6V to 9V supply to ignite. 3-cell LiPo batteries are very common in the university, so the power was taken from a LiPo balancing plug, thus only using 2 cells to get 7,4 V nominal voltage. The board is a switch mechanism, the ignition needs to be armed first by flipping a switch before pushing the "fire" button. The PCB also features a protection capacitor, a buzzer and LEDs for user feedback.



**Figure 10.3:** Lighting an igniter with the PCB.

The hardware implementation was completed and gave the possibility to implement the controller through Arduino software.

## 10.3 Rocket Software

The software implemented can be seen in the Arduino Software attachment folder "/Attachment/Implementation/Rocket/Controller\_code\_rocket/Controller\_Rocket.ino". A software flowchart is obtained to give a structural overview, which can be seen on figure. The principle is to determine the pitch and roll trough the IMU and then control the servo motor to a opposite angular reaction to stabilize the rocket.

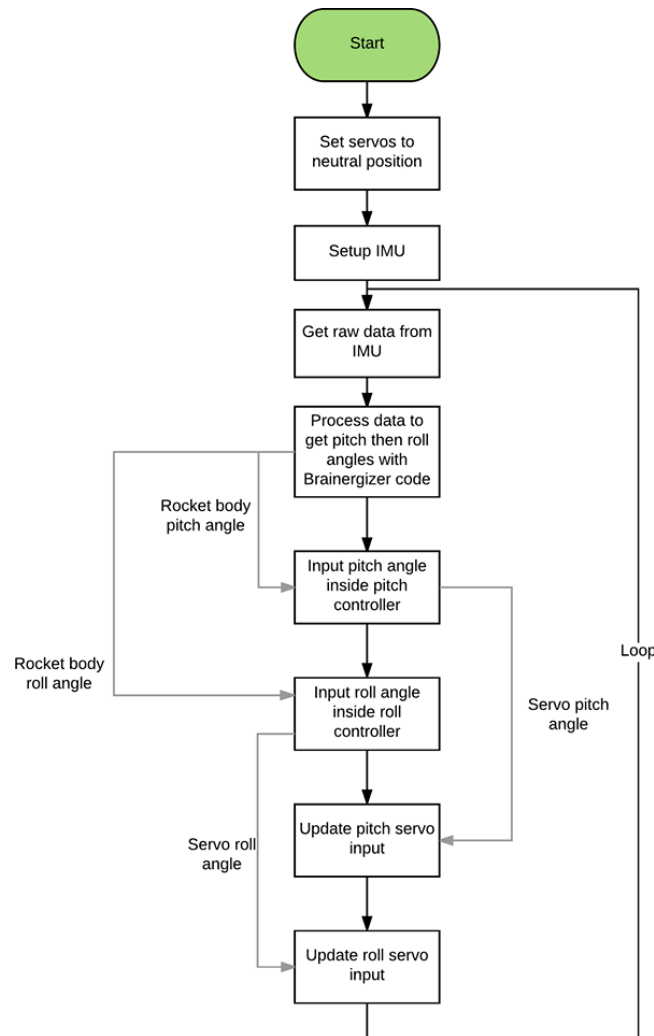


**Figure 10.4:** Flowchart of rocket software.

## 10.4 Flight test

The rocket was tested without the thruster to visually confirm if the system was behaving correctly. A video of this test is included in attachment folder "/Attachment/Implementation/Rocket/rocket\_controller\_check". The controller inclined the thruster in the correct direction according to the rocket's tilt. A flight test was planned but delays in the rocket's construction did not allow to make the test safely. Strings would have been attached radially to the center of gravity of the rocket, and wrapped around two sticks three meters apart. The wires would have been made long enough so the rocket would have been hovering slightly over the ground and then the thruster would be fired. Filming the flight and logging the angle data on the Arduinos memory could have shown the angle of the rocket during flight.

## **Part III**

### **Test & conclusion**



# Chapter 11

## Inverted Pendulum Acceptance Tests

In this section the tests to check whether the controllers designed for the inverted pendulum fit the requirements or not. As said in Section 6.1 the first acceptance test will not be documented as it is more an implementation requirement than a test.

### 11.1 Acceptance Test 1.

This test is there to verify the arm does indeed stop when it goes beyond  $\frac{\pi}{4}$ . To do so a large perturbation is applied to the stick such as the arm has to move beyond  $\frac{\pi}{4}$  to catch it. It is confirmed then that the arm indeed stops at  $\frac{\pi}{4}$ .

So the test is considered as a success.

### 11.2 Acceptance Test 2.

The goal of this test is to see if the inverted pendulum's stick and arm stay within the limits set in Requirement 2 and 3 described in Section 6.0.1. Figure 11.1 and 11.2 plot respectively the angles of the arm and the stick over a period of 30 s. The maximum and the minimum angles are put in evidence so that it is easy to compare them with the requirements.

From Figure 11.1 it can be seen that the arm is within the requirements by a large margin of 0.68 rad or 38.96°. This result is due to the transformation of the outer loop described in Section 7.2.1. Indeed the reference is not the upright angle of the stick anymore but the distance of a point on the stick compared with its position

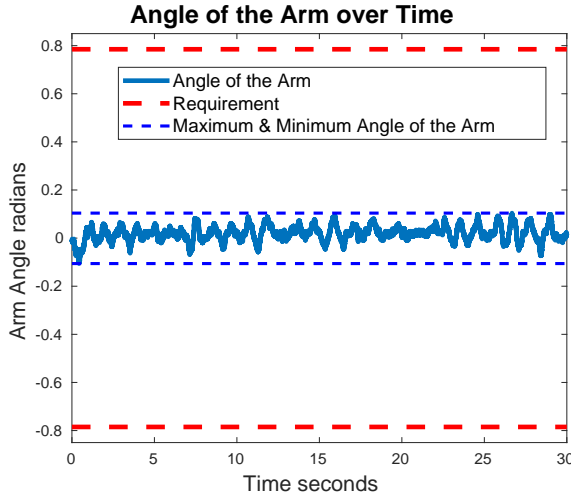


**Figure 11.1:** Plot of the angle of the arm over time with the limits set by the Requirement 1.

when both the arm and the stick are in upright position. Due to this, the controller will try to keep both the arm and the stick in the upright angle which explains the very low angle variation of the arm compared to the requirement.

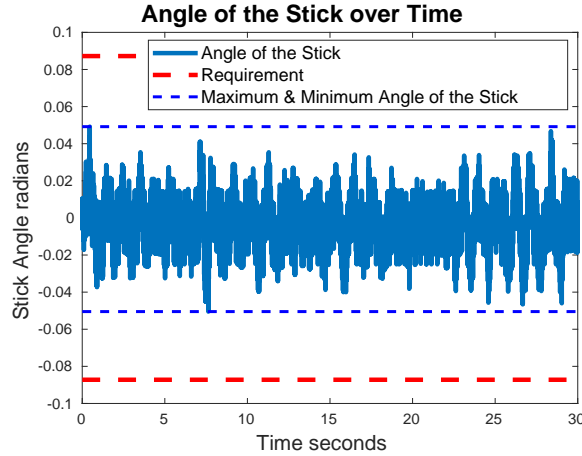


**Figure 11.2:** Plot of the angle of the Stick over time with the limits set by the Requirement 2.

In Figure 11.2, the largest angle the stick takes is 0.05 rad while Requirement 2 prescribes a limit of 0.9 rad. Again, the requirement is respected by a large margin.

From the tests results it can be concluded that the second acceptance test is a success.

### 11.3 Acceptance Test 3.

Unfortunately a method to precisely hold and release the stick was not found, therefore no precise data were able to be collected for this test. However, a video was taken during the test and will be joined with the report. This video in "Acceptance Test 3/Stick Control Acceptance Test 2" shows the reactions of the stick when different pushes are applied to it. The maximum angle for the stick set in the requirements are present and can be used as reference points. It can be noted that during the whole video the stick keeps its balance.

The results for the acceptance tests of the stick are a success.



# Chapter 12

## Discussion

### 12.1 Inverted Pendulum Possible Improvements

The inverted pendulum fulfills all requirements and the possible simple improvements such as the suppression of the shaking are already discussed in Chapter 9. What could have been done however, is to try other control design schemes such as state space equations or bode plots and test them to see which one performs the best. Unfortunately too much time was spent on fixing the setup to be able to do so.

### 12.2 Rocket

The rocket as it is has not been launched. Nevertheless the rocket could be improved in its physical design and on the controller chosen. As explained in Section 8.2 a controller similar to the Inverted Pendulum controller would be found by having an inner loop controlling the servomotors. The inertia model used was very simplified, a more complex one, e.g adding the rocket's lighter parts in the equations, could improve the performance of the controller. Similarly to the Inverted Pendulum improvements, other control design schemes, such as space equations or bode plot, could be implemented. It is to be noted that a lot time was spent on the rocket design and construction. On future implementations a ready-made rocket could be used to spare time.

### 12.3 Differences between the Rocket and the Inverted Pendulum

As explained in Section 4.4 the models are slightly different. First of all, opposite angles were chosen in the beginning of the modeling process. Moreover, the inverted pendulum is fixed to the gears and motor, while the rocket is floating in the air, and thus canceling the gravity. The inverted pendulum has two more zeros in 0 and two real poles equidistant from zero, whereas the rocket has two poles in 0. The difference in poles is due to the absence of gravity into the rocket modeling, while the difference in zeros might be due to the fact that the arm is rigidly attached compared to the thruster.

Unfortunately even if the systems are close, an identical model could not be found. This difference might come from the setup and its extra arm, which introduce a rotational force instead of a horizontal force e.g an inverted pendulum with a cart.

# Chapter 13

## Conclusion

An analysis was made to determine whether the inverted pendulum and rocket models could be controlled by the same controller. The mathematical models were not similar and a different controller for each system is thus necessary.

A controller was made for the inverted pendulum using cascade control to simplify the setup along with redefining the model to simplify it further. A lead controller was made to achieve a stable system and all controllers were implemented on an Arduino. The acceptance tests showed that the combination of cascade control and a lead controller could balance the stick in a satisfactory fashion despite not controlling the angle of the stick directly. This showed that it is not only important to design a precise controller but also important to choose the feedback wisely.

The rocket was not made readily available by the university and needed to be built. A controller was designed with the same procedure as the inverted pendulum and it could theoretically control the rocket's trajectory. It was, however, ultimately not tested as the rocket design and implementation was not ready in time for a test in flight. A video was taken, showcasing the principle of the small scale rocket using the controller designed by tilting the rocket manually. Given more time a test, with the thruster attached and the rocket tethered to the ground, would be made to check if the design satisfy the requirements.



# Bibliography

- [1] 2007 Group 631. Studentthesis, 2007. URL [http://projekter.aau.dk/projekter/da/studentthesis/balancing-stick\(9fa49107-ec90-436e-919d-e407eaac6b08\).html](http://projekter.aau.dk/projekter/da/studentthesis/balancing-stick(9fa49107-ec90-436e-919d-e407eaac6b08).html).
- [2] Tom Benson. rocket, 2014. URL <https://spaceflightsystems.grc.nasa.gov/education/rocket/rktstabc.html>.
- [3] Brainergiser. Brainergizer implementation of angle calculation with gyroscope (in description), 2016. URL [https://www.youtube.com/watch?v=U7lf\\_E79j7Q](https://www.youtube.com/watch?v=U7lf_E79j7Q).
- [4] GY-80 IMU. Imu gy-80, 2015. URL <http://selfbuilt.net/shop/gy-80-inertial-management-unit>.
- [5] invensence. *MPU-6050 IMU*, 2013. URL <https://www.invensense.com/wp-content/uploads/2015/02/MPU-6000-Datasheet1.pdf>.
- [6] Taylor W. Barton Kent H. Lundberg. History of inverted-pendulum systems. *IFAC*, 42:131 to 135, 2010. URL <http://www.sciencedirect.com/science/article/pii/S1474667015316049>.
- [7] MaxonMotor. *Maxon Escon 50/5 Servocontroller*. URL <http://www.maxonmotor.com/maxon/view/product/control/4-Q-Servokontroller/409510>.
- [8] Nasa. Center of gravity, 2016. URL <https://www.grc.nasa.gov/www/k-12/airplane/cg>.
- [9] C. R. Nave. Moment of inertia of a rod, 2016. URL <http://hyperphysics.phy-astr.gsu.edu/hbase/mi2.html>.
- [10] C. R. Nave. Natural frequency of pendulum, 2016. URL <http://hyperphysics.phy-astr.gsu.edu/hbase/pend.html>.
- [11] C. R. Nave. Moment of inertia examples, 2016. URL <http://hyperphysics.phy-astr.gsu.edu/hbase/mi.html>.

- [12] R Nave. Moment of inertia: Hollow cylinder, 2015. URL <http://hyperphysics.phy-astr.gsu.edu/hbase/icyl.html>.
- [13] NIST. Standard gravitational acceleration, 2016. URL <http://physics.nist.gov/cgi-bin/cuu/Value?gn>.
- [14] Parvex. Axem disc dc servo motor manual, 2003. URL <https://inverterdrive.com/file/Axem-Disc-DC-Servo-Motor-Manual>.

# Appendix A

## Test Journal: Gear Train System

**Test participants:** Maxime & Geoffroy

**Date:** 28/2/2017

### Purpose

The objective of this test is to determine all the characteristics of the gear train system composed of the DC motor and the gear train.

#### A.1 Electronics characteristics

##### A.1.1 Internal Resistance of the DC Motor $R_m$

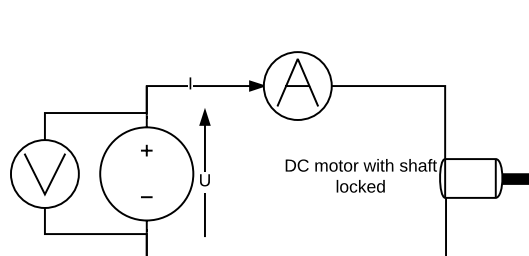
**Table A.1:** List of measurement equipment and components

Name	Brand	Model	AAU-number
Oscilloscope	Agilent	54621D	33941
Powersupply	Agilent	E3631A	78577
DC motor	Alsthom BBC	F9M2	08339

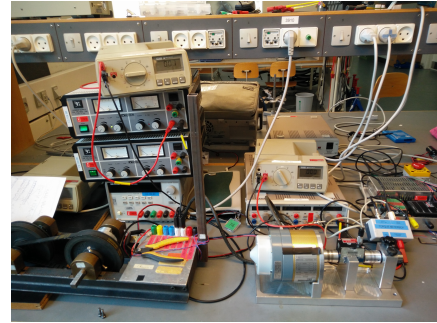
The first parameter to be tested is the internal resistance of the motor  $R_m$ . This resistance is needed in the motor's transfer function and will be used to determine the other parameters of the motor.

## Setup

Figure A.1 shows a diagram and photo of the measurement set up



(a) Diagram of the setup.



(b) Picture of the setup.

**Figure A.1:** The measurement setup.

## Method

This test consists of having the motor shaft locked while the voltage is increased by 0.5 V between each measurements.

## Raw data

Table A.2 is the plotted evolution of the voltage of the circuit according to the current.

## Data Processing

In order to find the motor's resistance  $R_m$ , the electrical equations of the motor will be used:

$$U_m = R_m \cdot i + L_m \frac{di}{dt} + K_e \omega_m \quad (\text{A.1})$$

With the motor shaft locked,  $\omega_m = 0$ . Moreover, the measurements are made a couple seconds after the change in voltage is made. The current is then constant, canceling its derivative.

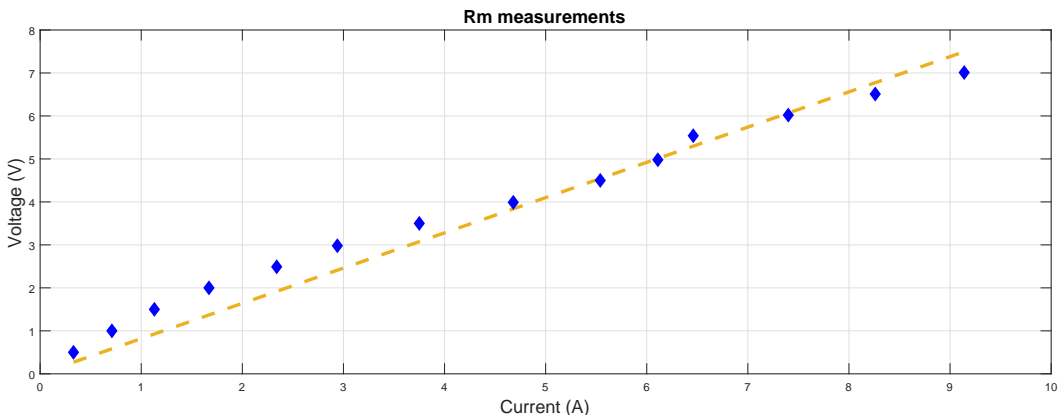
The resulting equation is Ohm's law:

$$U_m = R_m \cdot i \quad (\text{A.2})$$

**Table A.2:** Raw data used to determine  $R_m$ 

Voltage (V)	Current (A)
0.50	0.33
1.00	0.71
1.50	1.13
2.00	1.67
2.49	2.34
2.98	2.94
3.50	3.75
3.99	4.68
4.50	5.54
4.98	6.11
5.54	6.46
6.02	7.40
6.51	8.26
7.01	9.14

The measurement of voltage according to the current is presented in Figure A.2.

**Figure A.2:** Measurement of voltage according to the current

$R_m$  is the slope of the linear approximation (in dashed yellow) of the voltage over the current:

$$U_m = R_m \cdot i \quad (\text{A.3a})$$

$$R_m \approx 0.82 \Omega \quad (\text{A.3b})$$

### A.1.2 Internal Inductance of the DC Motor $L_m$

**Table A.3:** List of measurement equipment and components

Name	Brand	Model	AAU-number
Oscilloscope	Agilent	54621D	33941
Powersupply	Agilent	E3631A	78577
DC motor	Alsthom BBC	F9M2	08339

#### Setup

Figure A.3 shows a diagram and photo of the measurement set up.

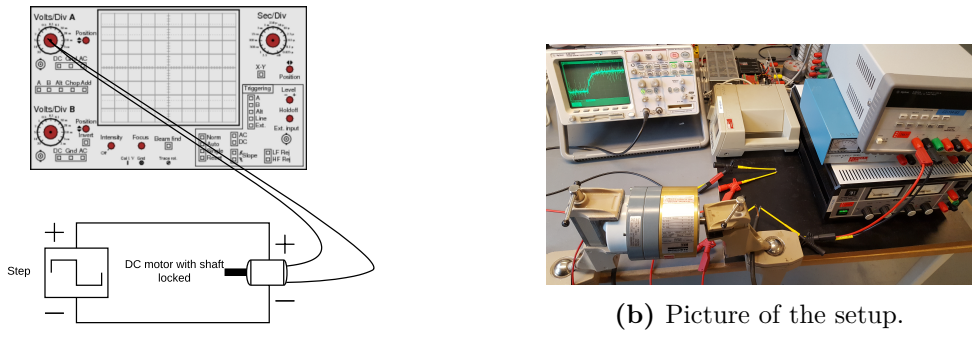


**Figure A.3:**  $L_m$  measurement setup.

#### Method

This test consists of having the motor shaft locked while a step is applied. The current is measured through the circuit. With the current step response, the inductance of the motor can be found.

#### Raw data

Figure A.4 is the plotted evolution of the current of the circuit in respect to time.

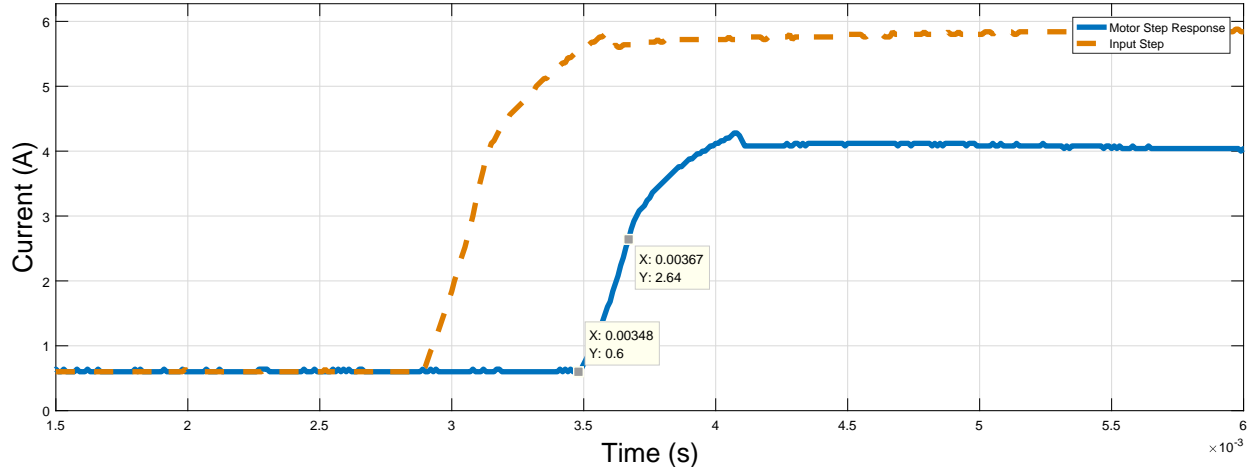


**Figure A.4:** Plot of the current step response in respect to time

### Data processing

When the shaft is locked and a step is applied the DC motor's electric equation can be resumed as in Equation (A.4).

$$F(s) = \frac{I(s)}{U(s)} = \frac{\frac{1}{R_m}}{\frac{L_m}{R_m}s + 1} \quad [1] \quad (\text{A.4})$$

Where:

$I(s)$ is the current in Laplace domain	[1]
$U(s)$ is the body's acceleration	[1]
$R_m$ is the internal resistance of the motor	[ $\Omega$ ]
$L_m$ is the internal inductance of the motor	[H]

When a unit step response is applied to the system Equation (A.4) becomes Equation (A.5).

$$F(s) = \frac{\frac{1}{R_m}}{\frac{L_m}{R_m}s + 1} \frac{1}{s} = \frac{-\frac{1}{R_m}}{s + \frac{R_m}{L_m}} + \frac{1}{R_m s} \quad [1] \quad (\text{A.5})$$

Equation (A.5) is then put in the continuous time domain to get Equation (A.6).

$$f(t) = \frac{1}{R_m} \left( 1 - e^{-\frac{R_m}{L_m}t} \right) \quad [1] \quad (\text{A.6})$$

Equation (A.6) means that at  $t = \frac{L_m}{R_m}$  the function would give  $1 - e^{-1} \approx 63.2\%$  of its settling value given that the step starts at 0 seconds. Therefore, at 63.2% of the

settling value  $t = \frac{L_m}{R_m}$ .

Since  $R_m = 0.82 \Omega$  is known, finding  $L_m$  becomes trivial. Here, the step starts at 0.00348 s.

### Conclusion

Since the settling value of the output current is 4.04 A. Then Equation (A.7) gives the value of  $L_m$ .

$$\frac{1}{R_m} \left( 1 - e^{-\frac{R_m}{L_m} t} \right) = 4.04 \cdot 0.63212055882 \quad [\text{s}] \quad (\text{A.7a})$$

$$t \approx 0.00367 - 0.00348 \approx 0.00019 \text{ s} \quad (\text{A.7b})$$

$$L_m = t R_m \quad (\text{A.7c})$$

$$L_m \approx 156 \mu\text{H} \quad (\text{A.7d})$$

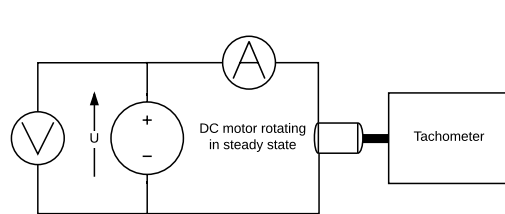
### A.1.3 The DC Motor velocity constant $K_e$

**Table A.4:** List of measurement equipment and components

Name	Brand	Model	AAU-number
Oscilloscope	Agilent	54621D	33941
Powersupply	Agilent	E3631A	78577
DC motor	Alsthom BBC	F9M2	08339

### Setup

Figure A.5 shows a diagram and photo of the measurement set up



(a) Diagram of the set up.



(b) Picture of the set up.

**Figure A.5:** The measurement set up for  $K_e$ .

## Method

This test consists of having the motor shaft rotating in steady state while the voltage  $U$  of the generator, the angular velocity  $\omega$  of the shaft and the current  $I$  are measured.

## Raw data

Table A.5 has all the measurements done.

**Table A.5:** Raw data used to determine  $K_e$

Voltage (V)	Current (A)	$\omega$ (rad/s)
3.0	0.72	52.36
3.5	0.75	67.54
4.0	0.77	83.15
4.5	0.79	98.75
5.0	0.83	113.10
5.5	0.85	126.71
6.0	0.88	140.95
6.5	0.90	156.03
7.0	0.93	170.38
7.5	0.94	185.35
8.0	0.95	198.97
8.5	0.96	214.68
9.0	0.99	229.34
9.5	1.00	244.31
10.0	1.02	258.66
10.5	1.03	274.05
11.0	1.06	289.03
11.5	1.06	304.73
12.0	1.05	321.49

## Data processing

When the shaft is rotating in steady state as shown in Figure A.5a, Equation (A.8) can be derived.

$$U = K_e \omega + R_m I \quad [\text{V}] \quad (\text{A.8})$$

Where:

$I$ is the current in the circuit	[A]
$U$ is the generator's voltage	[V]
$K_e$ is the velocity constant of the motor	[V rad <sup>-1</sup> s]
$R_m$ is the internal resistance of the motor	[Ω]

From Equation (A.8) Equation (A.9) is obtained by isolating  $K_e$ .

$$K_e = \frac{U - R_m I}{\omega} \quad [\text{V rad}^{-1} \text{ s}] \quad (\text{A.9})$$

### Conclusion

Figure A.6 plot the  $K_e$  found for each measurement. The  $K_e$  used in the model is average of these points. This gives  $K_e = 0.0343 \text{ V rad}^{-1} \text{ s}$

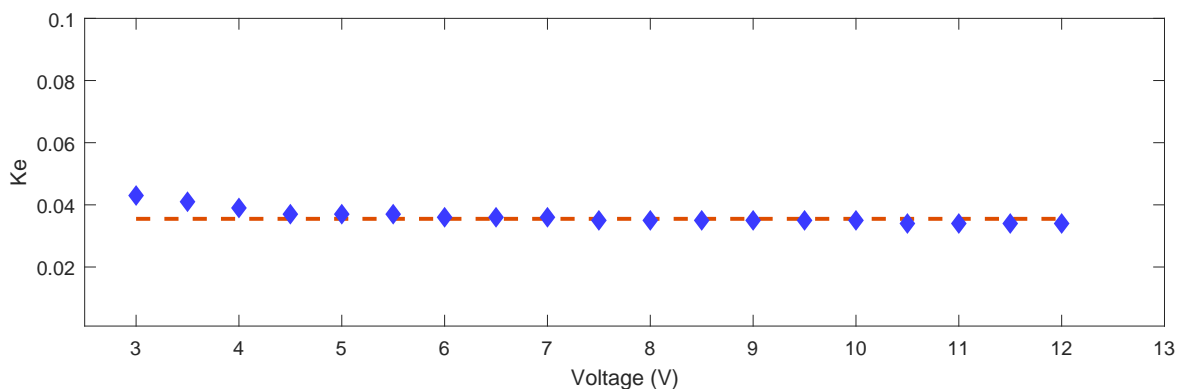


**Figure A.6:** Plot of  $K_e$  found for each measures

#### A.1.4 The DC Motor torque constant $K_t$

**Table A.6:** List of measurement equipment and components

Name	Brand	Model	AAU-number
Oscilloscope	Agilent	54621D	33941
Powersupply	Agilent	E3631A	78577
DC motor	Alsthom BBC	F9M2	08339

## Setup

Figure A.7 shows a diagram and photo of the measurement set up

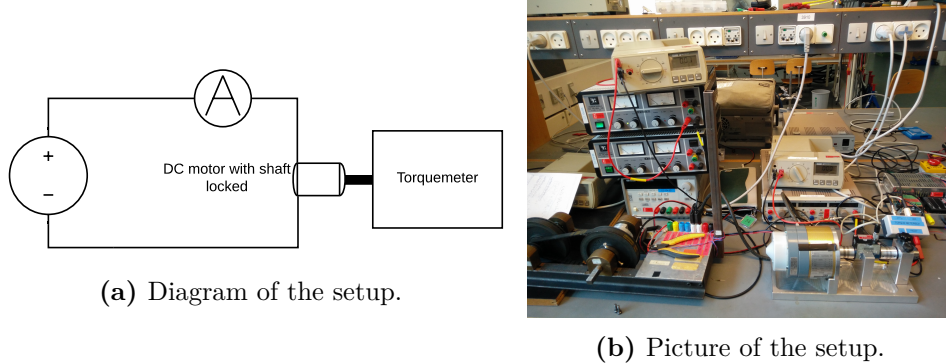


**Figure A.7:** The measurement setup.

## Method

This test consists of having the motor shaft locked while the torque  $\tau_m$  and the current  $I$  are measured.

## Raw data

Table A.7 has all the measurements done.

**Table A.7:** Raw data used to determine  $K_t$

Current (A)	$\tau_m$
4.0	0.1164
4.5	0.1314
5.0	0.1498
5.5	0.1606
6.0	0.1824
6.5	0.1896
7.0	0.2050
7.5	0.2192
8.0	0.2332
8.5	0.2478
9.0	0.2604
9.5	0.2750
10.0	0.2900

### Data processing

When the motor is in steady state and the shaft locked as shown in Figure A.7a, Equation (A.10) is found from Equation (3.33a).

$$K_t = \frac{\tau_m}{I} \quad [\text{N m A}^{-1}] \quad (\text{A.10})$$

Where:

$I$ is the current in the circuit	[A]
$\tau_m$ is the torque of the motor	[N m]
$K_t$ is the motor's torque constant	[N m A <sup>-1</sup> ]

### Conclusion

Figure A.8 plot the  $K_t$  found for each measurement. The  $K_t$  used in the model is average of these points. This gives  $K_t = 0.0293 \text{ N m A}^{-1}$

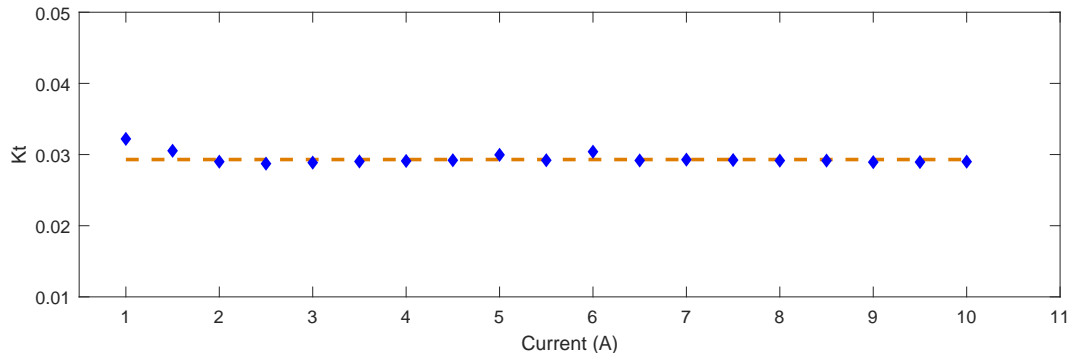


**Figure A.8:** Plot of  $K_t$  found for each measures

It should be noticed that  $K_e$  and  $K_t$  values are close, which comforts the results of the tests since they are theoretically equal.

## A.2 Mechanical Characteristics

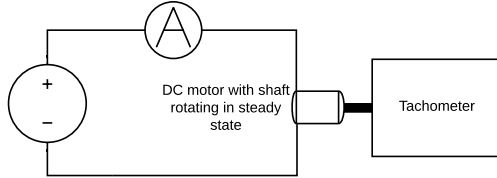
### A.2.1 Frictions $B_m$

**Table A.8:** List of measurement equipment and components

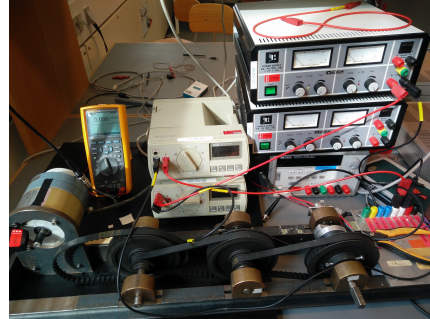
Name	Brand	Model	AAU-number
Oscilloscope	Agilent	54621D	33941
Powersupply	Agilent	E3631A	78577
DC motor	Alsthom BBC	F9M2	08339

### Setup

Figure A.9 shows a diagram and photo of the measurement set up.



(a) Diagram of the set up.



(b) Picture of the setup.

**Figure A.9:** The measurement set up for .

### Method

This test consists of having the motor shaft running in steady state while the torque  $\tau_m$ , the shaft angular velocity  $\omega$  and the current  $I$  are measured.

### Raw data

Figure A.10 has all the measurements done.

**Figure A.10:** Raw data used to determine  $B_m$ 

Current (A)	$\omega$ (rad/s)
0.74	89.0
0.76	96.9
0.78	106.8
0.80	116.2
0.82	128.8
0.84	144.5
0.86	150.8
0.88	165.5
0.90	184.3
0.92	204.2
0.94	216.8
0.96	232.5
0.98	252.4
1.00	289.0
1.03	321.5

### Data processing

The motor and the shaft are in steady state so  $\tau_m = \tau_{fm}$  which combined with Equation (3.33b) gives Equation (A.11).

$$B_m = \frac{K_t I}{\omega} \quad [\text{N rad}^{-1} \text{s}] \quad (\text{A.11})$$

Where:

$I$ is the current in the circuit	[A]
$K_t$ is the motor's torque constant	[\text{N m A}^{-1}]
$\omega$ is the shaft's angular velocity	[\text{rad s}^{-1}]
$B_m$ is the viscous friction constant	[\text{N m rad}^{-1} \text{s}]

### Conclusion

Figure A.11 plots the  $B_m$  found for each measurement. The  $B_m$  used in the model is the average of these points. This gives  $B_m = 120 \mu\text{N m rad}^{-1} \text{s}$ .

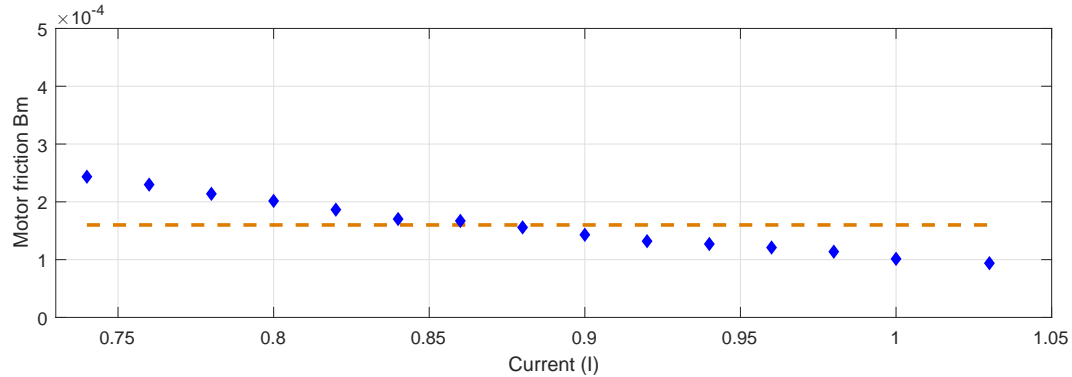


**Figure A.11:** Plot of  $B_m$  found for each measures

### A.2.2 Moment of Inertia of the Gears $J_{\text{gear}}$

The moment of inertia of the gear train was thoroughly calculated in a previous report and will be used here.

#### Method

The gear train can be divided in three parts: the large wheels, the small wheels and the axles. The latter is a solid cylinder whereas the wheels are considered as multiple hollowed cylinders. The moment of inertia about a symmetry axis through the center of mass for a hollow cylinder is described in Equation (A.12) [12]:

$$J_{\text{hc}} = \frac{1}{2}M(R_1^2 + R_2^2) \quad (\text{A.12})$$

Where:

$J_{\text{hc}}$ is the moment of inertia about a symmetry axis through the center of mass for a hollow cylinder	$[\text{kg m}^2]$
$M$ is the mass of the hollowed cylinder	$[\text{kg}]$
$R_1$ is the inner radius of the hollowed cylinder	$[\text{m}]$
$R_2$ is the outer radius of the hollowed cylinder	$[\text{m}]$

For the axles, the inner radius  $R_1$  is equal to zero, giving equation Equation (A.13) for the solid cylinder.

$$J_{\text{sc}} = \frac{1}{2}MR^2 \quad (\text{A.13})$$

Where:

$J_{sc}$  is the moment of inertia about a symmetry axis through the center of mass for a solid cylinder [kg m<sup>2</sup>]

$M$  is the mass of the solid cylinder [kg]

$R$  is the inner radius of the solid cylinder [m]

The mass of each wheels and axles are calculated using their volumes and the density of iron.

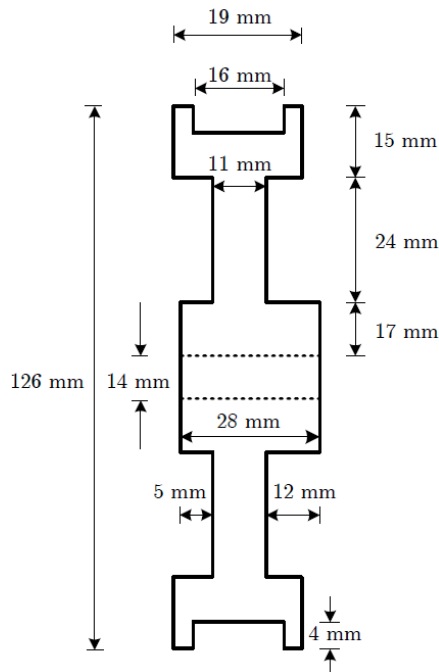


**Figure A.12:** Cross section of a large wheel [1].

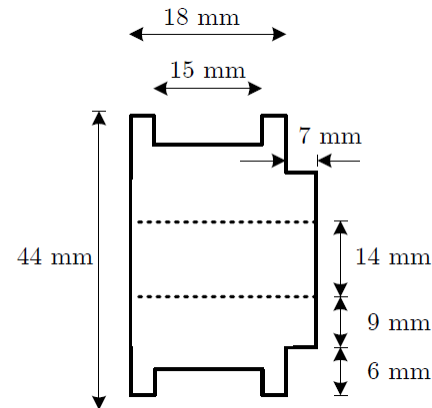


**Figure A.13:** Cross section of a small wheel [1].

## Conclusion

The moment of inertia for each part of the gear system [1]:

$$\text{Large Wheel: } J_{\text{Large}} = 1.433 \cdot 10^{-3} \text{ kg m}^2 \quad (\text{A.14a})$$

$$\text{Small Wheel: } J_{\text{Small}} = 0.037 \cdot 10^{-3} \text{ kg m}^2 \quad (\text{A.14b})$$

$$\text{Axe 1: } J_{A1} = 0.083 \cdot 10^{-3} \text{ kg m}^2 \quad (\text{A.14c})$$

$$\text{Axe 2: } J_{A2} = 0.078 \cdot 10^{-3} \text{ kg m}^2 \quad (\text{A.14d})$$

$$\text{Axe 3: } J_{A3} = 0.092 \cdot 10^{-3} \text{ kg m}^2 \quad (\text{A.14e})$$

The total moment of inertia of the gear system can be calculated from Equation (3.29b) in Section 3.3.

$$J_{\text{gear}} = N^2 J_1 + N^4 J_2 + N^6 J_3 \quad (\text{A.15})$$

With:

$$J_1 = J_{\text{Large}} + J_{\text{Small}} + J_{A1} = 1.553 \cdot 10^{-3} \text{ kg m}^2 \quad (\text{A.16a})$$

$$J_2 = J_{\text{Large}} + J_{\text{Small}} + J_{A2} = 1.548 \cdot 10^{-3} \text{ kg m}^2 \quad (\text{A.16b})$$

$$J_3 = J_{\text{Large}} + J_{\text{Small}} + J_{A3} = 1.562 \cdot 10^{-3} \text{ kg m}^2 \quad (\text{A.16c})$$

Finally,  $J_{\text{gear}}$  is calculated to be

$$J_{\text{gear}} = 0.153 \cdot 10^{-3} \text{ kg m}^2 \quad (\text{A.17})$$



## Appendix B

# Linearization of the Arm and Stick Model

This appendix will linearize Equation (B.1)

$$J_s \ddot{\theta}_s = \frac{l_s}{2} M_s \left( -l_a \ddot{\theta}_a \cos(\theta_a - \theta_s) + l_a \dot{\theta}_a^2 \sin(\theta_a - \theta_s) - \frac{l_s}{2} \ddot{\theta}_s - g \sin(\theta_s) \right) - b_{as} \dot{\theta}_{as} \quad (\text{B.1})$$

The linearization is made with a 1st order Taylor approximation. The linearization is done at the equilibrium point where the arm is in an upright position i.e.  $\theta_s = 0$ . In the equilibrium point the derivatives of all the inputs and outputs are 0. In this case the inputs and outputs are  $\theta_a$  and  $\theta_s$  and the operating point is  $\bar{\theta}_a = 0$  and  $\bar{\theta}_s = 0$ . The nonlinear model is expressed as a function of the inputs and outputs as seen in Equation (B.2).

$$f(\theta_a, \dot{\theta}_a, \ddot{\theta}_a, \theta_s, \dot{\theta}_s) = \frac{l_s}{2} M_s \left( -l_a \ddot{\theta}_a \cos(\theta_a - \theta_s) + l_a \dot{\theta}_a^2 \sin(\theta_a - \theta_s) - \frac{l_s}{2} \ddot{\theta}_s - g \sin(\theta_s) \right) - b_{as} \dot{\theta}_{as} - J_s \ddot{\theta}_s \quad (\text{B.2})$$

Generally all equilibriums can be found by setting Equation (B.2) equal to 0 and the derivatives to 0 and solving for  $\theta_a = \bar{\theta}_a$  and  $\theta_s = \bar{\theta}_s$ . For the pendulum it is easy to see the only two equilibriums are the stick pointing straight up and straight down.

The 1st order Taylor approximation of an equation with multiple variables is seen in Equation (B.3).

$$\begin{aligned} f(\theta_a, \dot{\theta}_a, \ddot{\theta}_a, \theta_s, \ddot{\theta}_s) &\approx f(\bar{\theta}_a, 0, 0, \bar{\theta}_s, 0) + \frac{\partial f}{\partial \theta_a}\Big|_{(\bar{\theta}_a, \bar{\theta}_s)} \hat{\theta}_a \\ &+ \frac{\partial f}{\partial \dot{\theta}_a}\Big|_{(\bar{\theta}_a, \bar{\theta}_s)} \hat{\dot{\theta}}_a + \frac{\partial f}{\partial \ddot{\theta}_a}\Big|_{(\bar{\theta}_a, \bar{\theta}_s)} \hat{\ddot{\theta}}_a \\ &+ \frac{\partial f}{\partial \theta_s}\Big|_{(\bar{\theta}_a, \bar{\theta}_s)} \hat{\theta}_s + \frac{\partial f}{\partial \ddot{\theta}_s}\Big|_{(\bar{\theta}_a, \bar{\theta}_s)} \hat{\ddot{\theta}}_s \end{aligned} \quad (\text{B.3})$$

Where:

$$\begin{aligned} \bar{\theta} &\text{ denotes the angle in an operating point} & [\text{rad}] \\ \hat{\theta} &\text{ denotes the angle of the small signal variances} & [\text{rad}] \end{aligned}$$

The three terms with sin or cos in Equation (3.7) will be approximated individually using Equation (B.3), remembering that  $\bar{\theta} = \dot{\bar{\theta}} = \ddot{\bar{\theta}} = 0$  in the equilibrium.

$$\begin{aligned} -l_a \ddot{\theta}_a \cos(\theta_a - \theta_s) &\approx 0 + l_a \bar{\dot{\theta}}_a \sin(\bar{\theta}_a - \bar{\theta}_s) \hat{\theta}_a \\ &- l_a \cos(\bar{\theta}_a - \bar{\theta}_s) \hat{\dot{\theta}}_a - l_a \bar{\ddot{\theta}}_a \sin(\bar{\theta}_a - \bar{\theta}_s) \hat{\theta}_s \end{aligned} \quad (\text{B.4a})$$

$$-l_a \ddot{\theta}_a \cos(\theta_a - \theta_s) \approx -l_a \hat{\dot{\theta}}_a \quad (\text{B.4b})$$

$$\begin{aligned} l_a \dot{\theta}_a^2 \sin(\theta_a - \theta_s) &\approx 0 + l_a \bar{\dot{\theta}}_a^2 \cos(\bar{\theta}_a - \bar{\theta}_s) \hat{\theta}_a \\ &+ 2l_a \bar{\dot{\theta}}_a \sin(\bar{\theta}_a - \bar{\theta}_s) \hat{\dot{\theta}}_a - l_a \bar{\dot{\theta}}_a^2 \cos(\bar{\theta}_a - \bar{\theta}_s) \hat{\theta}_s \end{aligned} \quad (\text{B.5a})$$

$$l_a \dot{\theta}_a^2 \sin(\bar{\theta}_a - \bar{\theta}_s) \approx 0 \quad (\text{B.5b})$$

$$g \sin(\theta_s) \approx g \sin(\bar{\theta}_s) + g \cos(\bar{\theta}_s) \hat{\theta}_s \quad (\text{B.6a})$$

$$g \sin(\theta_s) \approx g \hat{\theta}_s \quad (\text{B.6b})$$

The linearized model then becomes Equation (B.7).

$$J_s \hat{\ddot{\theta}}_s = \frac{l_s}{2} M_s \left( -l_a \hat{\dot{\theta}}_a - \frac{l_s}{2} \hat{\dot{\theta}}_s - g \hat{\theta}_s \right) - b_{as} \hat{\dot{\theta}}_{as} \quad (\text{B.7})$$

## Appendix C

# Test Journal: Tachometer

**Test participants:** Mathias  
**Date:** 10/04-2017

### Purpose

The purpose of the test is to determine the linearity and precision of the tachometer used in the system.

### Test equipment and components

**Table C.1:** List of measurement equipment and components

Name	Brand	Model	AAU-number
Oscilloscope	Agilent	54621D	33941
Power supply	Agilent	E3631A	78577
DC motor	Alsthom BBC	F9M2	08339
Tachometer	Compact Instruments	A2108	77087
Tachometer	Internal in motor	-	-

## Setup

The powersupply is connected to the motor directly. Both tachometers are connected to the oscilloscope to read output voltages. The internal tachometer functions as a generator, and will give a voltage depending on the motors RPM.

## Method

Step by step of test, maybe in enumerate

1. Connect motor directly to the power supply.
2. Connect tachometers to the oscilloscope.
3. Place a reflective tape on the motor axle.
4. Set holder for external tachometer so it lights at the motor axle.
5. Set the power supply to 2 V.
6. Note external tachometers voltage from the oscilloscope, and times the voltage with 1000 to find the number of rotations per minute.
7. Note the internal tachometers voltage from the oscilloscope, and times the voltage with 333,33 RPM/V to get numbers of rotations per minute.
8. Change the voltage with 1 V increments from 2 V - 10 V.
9. Note the Voltage and RPM with each increment.

## Raw data

**Table C.2:** Rotations Per Minute of the both tachometers.

Motor Voltage	Internal Tachometer (RPM)	A2108 (RPM)	Difference (RPM)
2 V	204	202	2
3 V	506	502	4
4 V	763	760	3
5 V	1023	1024	1
6 V	1324	1322	2
7 V	1641	1640	1
8 V	1912	1913	1
9 V	2218	2214	4
10 V	2460	2456	4

## Data processing

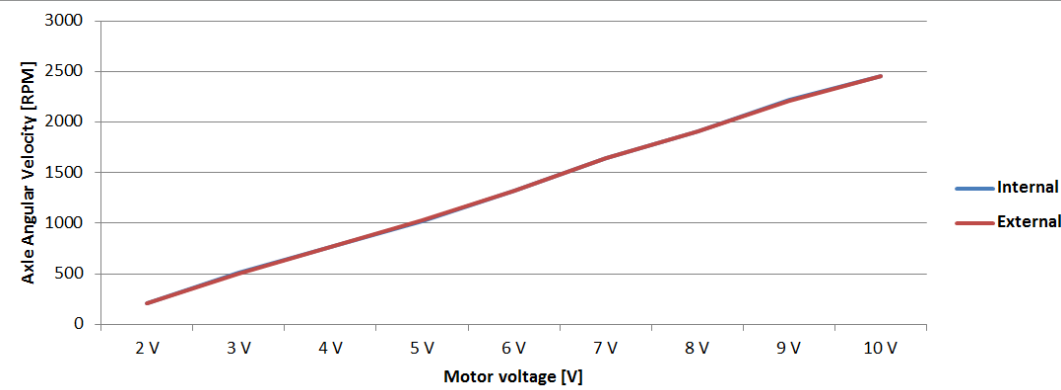


**Figure C.1:** Plot of RPM found for both tachometers

Which based on the know conversions gives a transfer function for the tachometer that is a relation between the tachometer voltage and motor velocity:

$$\frac{\frac{1000 \text{ RPM}}{3.130 \text{ V}} \cdot 2 \cdot \pi}{60 \text{ s}} \cdot T_{\text{Voltage}} = M_{\text{Velocity}} \text{ rad/s} \quad (\text{C.1})$$

## Conclusion

It its seen cf. figure C.1 that the difference between the tachometers is so little, that the lines is on top of each other. The precision do not change with higher velocities and the internal tachometer is chosen, as it changes voltage faster due to the generator principle. The external optical tachometer needs some rotations to determine the RPM, and is not optimal when direction change is needed.



## Appendix D

# Test Journal: Potentiometer

**Test participants:** Mathias  
**Date:** 20/04-2017

### Purpose

The purpose of the test is to find the angle which corresponds to the voltages of the potentiometers. This will be done for both the arm potentiometer and stick potentiometer.

### Test equipment and components

**Table D.1:** List of measurement equipment and components

Name	Brand	Model	AAU-number
Multimeter	Fluke	37	08181
Oscilloscope	Agilent	54621D	33941
Power supply	Agilent	E3631A	78577
DC motor	Alsthom BBC	F9M2	08339
Potentiometer	Bourns	Linear 10 kΩ 0,5% linearity	
Potentiometer	Bourns	Linear 10 kΩ 1% linearity	
Protractor			
Spirit level			

## Setup

Measurement setup is seen on Figure D.1

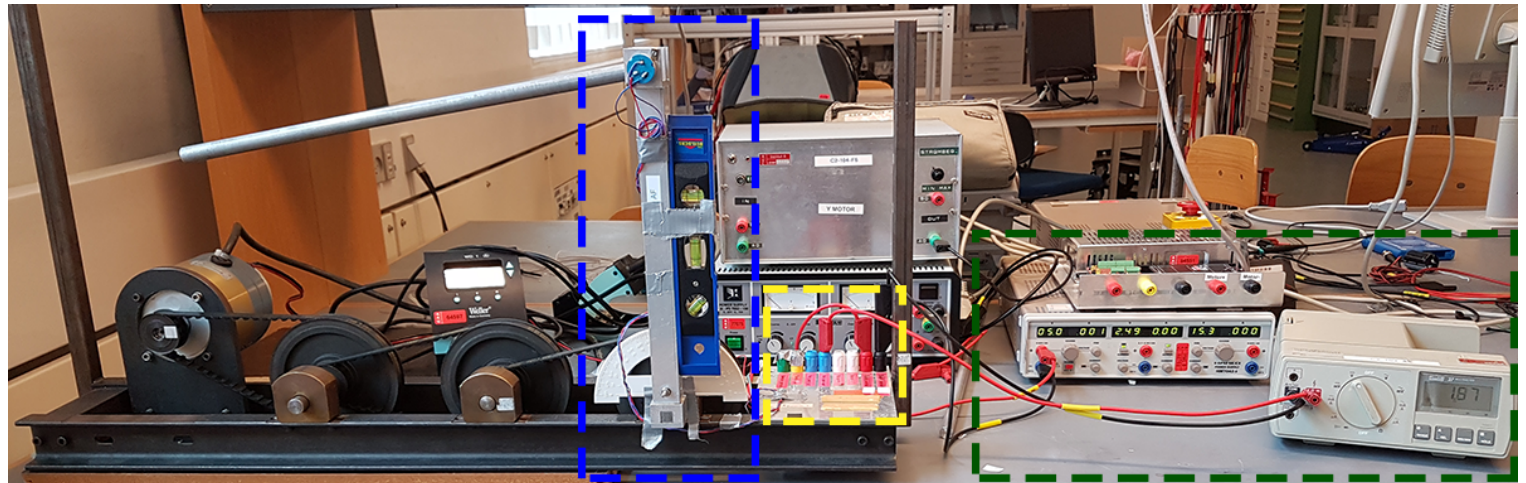


**Figure D.1:** Measurement setup.

Where:

**Blue box** contains the arm, with protractor and spirit level tool. [1]

The potentiometer is placed on the back of the opposite site of the arm axis.

**Green box** contains the power supply and voltmeter. [1]

**Yellow box** contains the power inputs and sensor outputs. [1]

## Method

The procedure for the test is as following:

1. Supply the sensor with 5 V and ground through the input and output connection board in the yellow box.
2. Attach the potentiometer of the arm to the voltmeter, the stick is not considered during measurement of the arm.
3. Use the spirit level to place the arm in vertical position which is the system's  $0^\circ$ .
4. Note the voltage.
5. Use the spirit level and protractor to place the arm in anti clockwise  $-45^\circ$  from vertical.

6. Note the voltage, and repeat earlier with  $-90^\circ$ ,  $45^\circ$  and  $90^\circ$
7. Place the arm in  $0^\circ$  and lock it.
8. Change the voltmeter to read the output from the stick potentiometer.

## Raw data

Voltages from each potentiometer are not expected to be the same. This is based on that the initial orientation of the potentiometers is not the same.

Position ( $^\circ$ )	Voltage Pot <sub>arm</sub> (V)	Voltage Pot <sub>stick</sub> (V)
$-90^\circ$	0,437 V	1,200 V
$-45^\circ$	1,146 V	1,89 V
$0^\circ$	1,860 V	2,558 V
$45^\circ$	2,573 V	3,23 V
$90^\circ$	3,270 V	3,90 V

**Table D.2:** Angle position and corresponding voltage.

## Data processing

The main objective is to determine its outer limits and how much 1 V corresponds to in angle change. This can give the possibility to convert the analogue input on an Arduino back to the corresponding angle.

It is shown that the linearity is acceptable and the proportional angle to voltage conversion is considered linear. The conversion must be separated into two parts. This is done because the angle to voltage is different between the potentiometers. To obtain a first order function the voltages and angles are plotted and approximated for both potentiometers.

Equation (D.1) corresponds to a relation between the voltage to angle of the arm on figure D.2.

$$\theta_a = 63,64 \cdot VPot_{arm} - 117,77 \quad [\text{rad}] \quad (\text{D.1})$$

The plot is repeated for the potentiometer on the stick.

Equation (D.2) that corresponds to a relation between the voltage to angle of the stick on figure D.3.

$$\theta_s = 66,66 \cdot VPot_{stick} - 170,46 \quad [\text{rad}] \quad (\text{D.2})$$

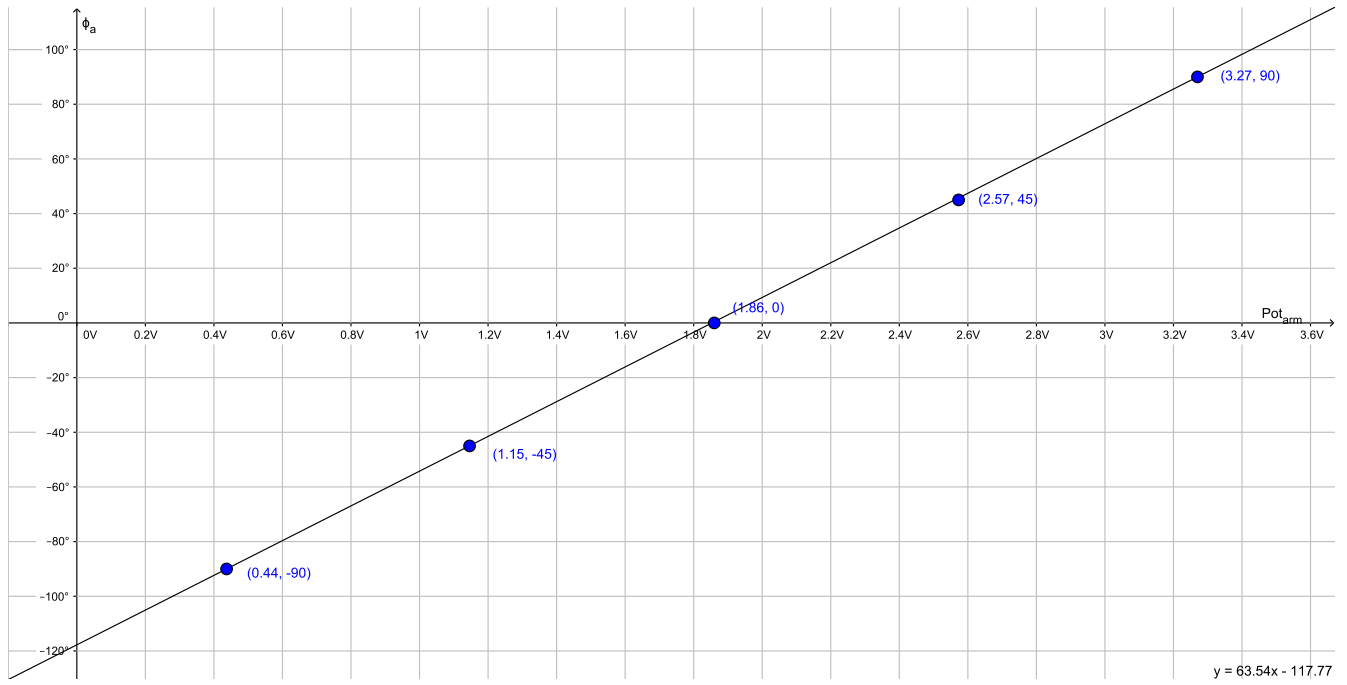


**Figure D.2:** First order approximation of the arm potentiometer.

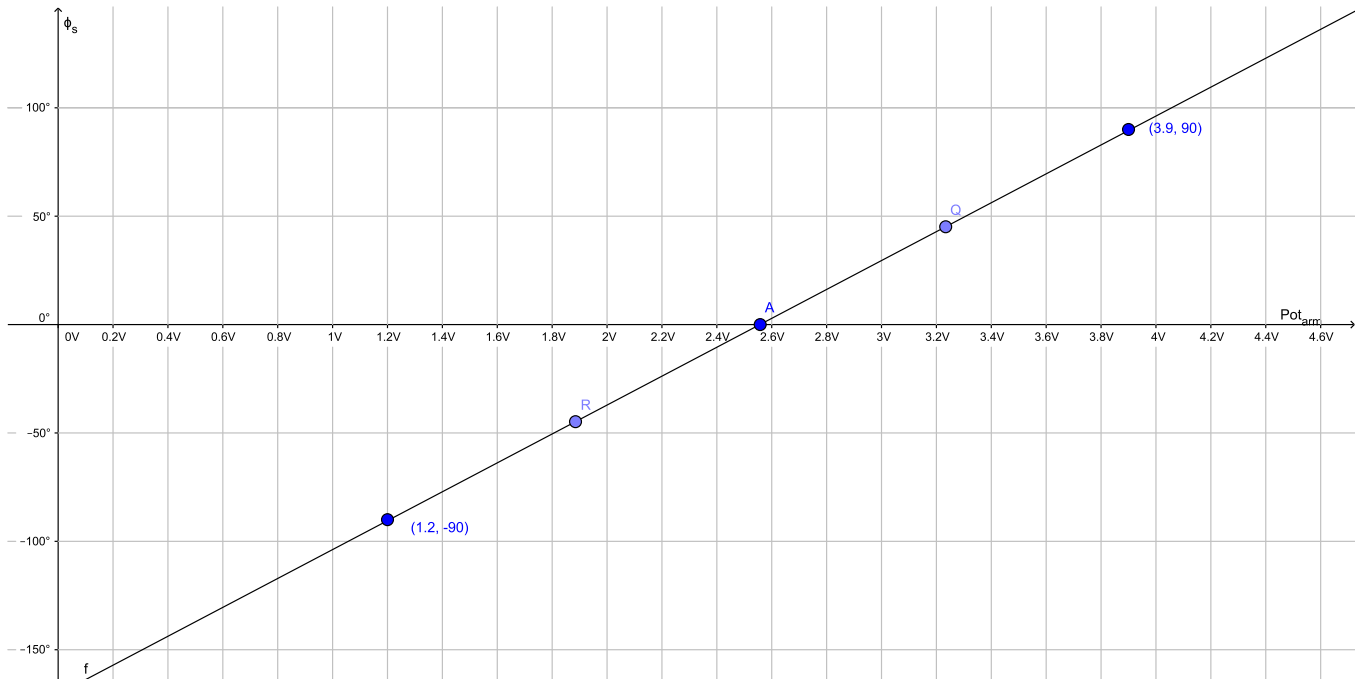


**Figure D.3:** First order approximation of the stick potentiometer.

Sampling the sensor with an Arduino will be done through reading the voltage on an input. The voltage will corresponds to a proportional analog value from 0-1023, where 0 V = 0 and 5 V = 1023. Translating the voltages into angles can give us the backwards conversion. Considering that the value can take 1024 values then:

$$\frac{1024 \text{ units}}{5 \text{ V}} = 204,8 \text{ units/V} \quad (\text{D.3})$$

Considering that the precision of the measurements and using an Arduino, all values would be rounded to the nearest integer. The linear approximations might be calibrated during implementation to minimize offsets. Further implementation is proceeded cf. section 9.1.

## Conclusion

The test concludes that it is possible to convert the voltage to values that can be used with an Arduino. The test also concludes that is able to keep the linearity of both potentiometers during conversions. The precision of the measurements shall be considered though.



## Appendix E

# Test Journal: rocket motor test

**Test participants:** Raphaël  
**Date:** 31/03-2017

### Purpose

The purpose of this test is to characterize the thrust of the Klima D3-P rocket motor.

### Test equipment and components

**Table E.1:** List of measurement equipment and components

Name	Brand	Model	AAU-number
Torsion scale	Made in AAU	N/A	N/A
Rocket motor	Klima	D3-P	N/A
3D printed adapter	N/A	N/A	N/A

### Setup

Measurement setup is seen on Figure D.1



**Figure E.1:** Measurement setup.

The torsion scale was lent by Jens Frederik Dalsgaard Nielsen, and the Arduino code was improved to filter the data. This code is available in the attached files.

## Method

The scale was calibrated using a known weight before the experiments.

1. The motor is placed inside the adapter, facing the ground
2. The scale is clamped strongly on the table. The clamping should be the same as during the calibration.
3. Scale turned on, a standard quick fuse and a lighter was used to start the motor.
4. After the motor had burned, the scale was shut off and the files on its SD card copied to a computer.
5. The operation was repeated with two motors from two different boxes.
6. Using Matlab, the data was plotted and put to scale according to the calibration.

## Raw data

The raw data from the scale is in the attached files.

## Data processing

Using the calibration weight, the data was put to scale using the Matlab code "scale\_reader.m" attached. It produced the graph displayed here. The force in Newton was translated in equivalent gram of lift for easier interpretation.

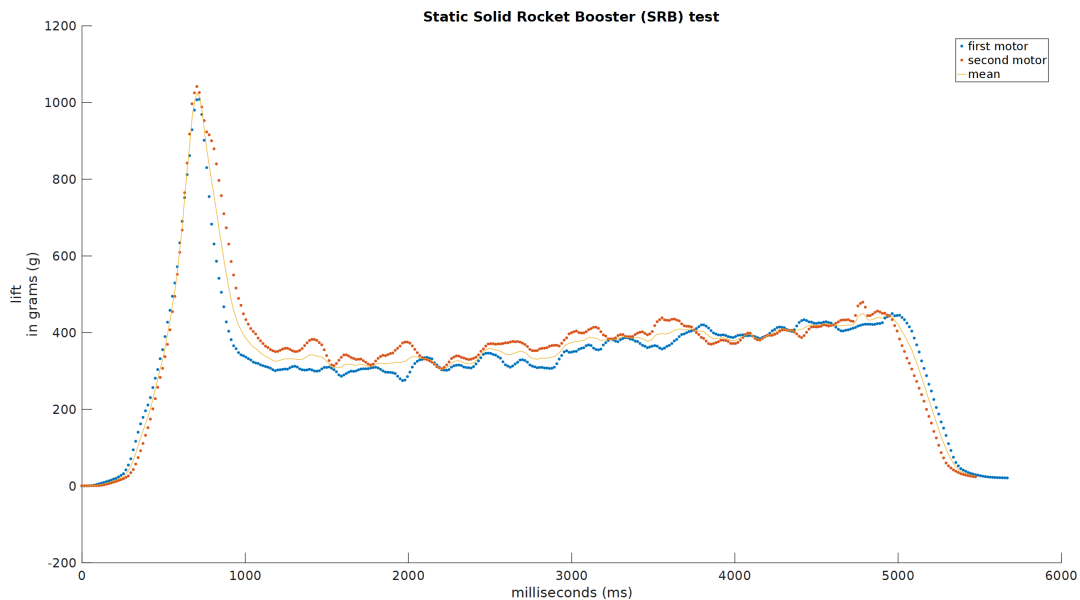


**Figure E.2:** Processed thrust data

## Conclusion

It can be seen that the two motors are very similar. The thrust builds up quickly producing a force peak of around 10 Newtons, or 1 Kg equivalent lift, for less than 400 ms. It then goes down and stabilizes to 330 grams of lift, slowly going up to 410g (taking in account the 20g mass loss of the motor during the thrust). Since the rocket is less than 300 grams, the motor should be able to lift it.



## Appendix F

# Test Journal: Servomotors

**Test participants:** Romain & Raphael

**Date:** 01/05-2017

## Purpose

The purpose of the test is to verify the proper functioning of the servomotors, and calculate the time constant of the servomotors' required tasks.

## Test equipment and components

**Table F.1:** List of measurement equipment and components

Name	Brand	Model
Servomotors	SpringRc	SM-s2309s
Controller	Arduino	Arduino Nano
Camera	LG	Nexus 6P
Media Player Classic	Gabest	Home Cinema

## Setup

The servomotors are controlled and powered by an Arduino Uno. Three different positions of the servomotors sticks are set up with code found in the attachments. The measurement setup is seen on the photos of the three different positions.

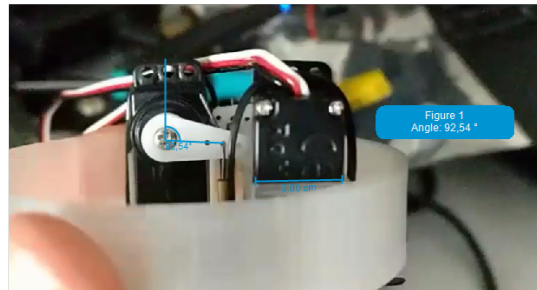


**Figure F.1:** Photograph of the servomotor at the medium position.

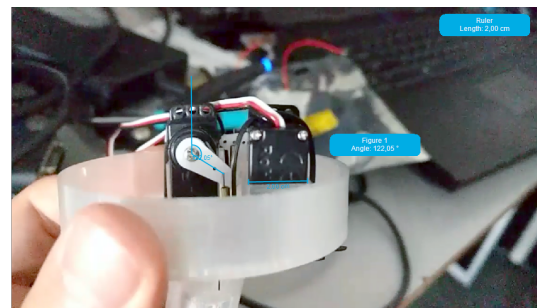


**Figure F.2:** Photograph of the servomotor at the lower position.

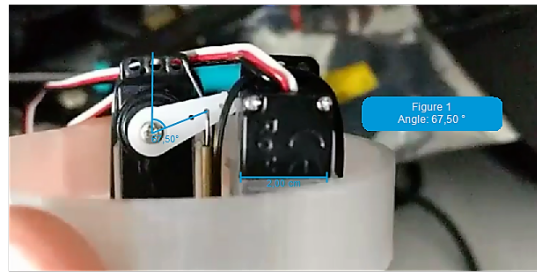


**Figure F.3:** Photograph of the servomotor at the higher position.

## Method

The servomotors' arms are controlled to go from one position to another one. The process is filmed in slow motion in order to analyse it. An x/y basis is used with the base set at the rotation center.

### Angle variation

The angle variation is found by measuring the angle difference between the horizontal axis and the stick direction. The servomotors function properly if the angles desired correspond to the real angles.

### Time constant

In order to find the time constant, the time to go from one position to another is measured using the video software. The time constant is equal to 63 % of the total time from one position to another.

## Raw data

### Angle variation

**Table F.2:** Measurement time of different set points.

Position	Angle(°)
Lowest	122.05
Middle	92.54
Highest	67.50

### Time constant

**Table F.3:** Measurment time of different set points.

Test	Time of departure (s)	Time of arrival(s)	total time (s)
1	2.507	2.641	0.134
2	2.508	2.642	0.134
3	60.066	61.133	0.133
4	60.033	61.082	0.131

## Data processing

### Angle variation

The angle variation is found by measuring the angle difference between the horizontal axis and the stick direction. The desired angle difference between the different positions is  $30^\circ$ . The servomotors function properly if the desired angles correspond to the measured angles.

$$a_{mh} = 29.51^\circ \quad (F.1a)$$

$$a_{ml} = 25.04^\circ \quad (F.1b)$$

Where:

$a_{mh}$  is the angle difference between the middle to highest position [°] of the servomotor's arm

$a_{ml}$  is the angle difference between the middle to lowest position [°] of the servomotor's arm

The error comes from measure errors and from the fact the servomotors need to lift a weight.

### Time constant

In order to find the time constant, the time to go from one position to another is measured using the video software. The time constant is equal to 63 % of the mean value of the total time from one position to another :

$$t_{\text{constant}} = \frac{63}{100} \cdot t_{\text{mean}} \quad (F.2a)$$

$$t_{\text{constant}} = \frac{63}{100} \cdot 0.133 = 0.084 \quad (F.2b)$$

Where:

$t_{\text{constant}}$  is the time constant of the servomotors [s]

$t_{\text{mean}}$  is the mean value of the total time from one position to another [s]

## Conclusion

The image analysis presents errors. In flight the desired range of angle movement of the servomotors is inferior to  $-30$  to  $30$  degrees. The servomotors are considered precise enough for the project. The time constant of the servomotors is  $0.084$ .